A Study of Defibrillator Waveforms, Vectors, and Therapies

Kevin Anthony Michael MBChB MPhil

Submitted in accordance with the requirements for the degree of Doctor of Medicine

The University of Cape Town
School of Medicine
October 2012

The candidate confirms that the work submitted is his own and that appropriate credit has been given where reference has been made to the work of others.

(MCHKEV003) **Kevin A Michael**

October 2012

Abstract

Introduction:

Implantable cardioverter- defibrillators (ICDs) have become widely applied in both ischaemic and non-ischaemic aetiologies to reduce the incidence of sudden cardiac death (SCD). The challenge has been to improve defibrillation efficacy, prolong battery longevity, and to minimise the device footprint. The pursuit of a painless therapy has motivated the development of anti-tachycardia pacing (ATP). Both defibrillation and ATP are the mainstays of ICD therapy.

Objectives:

To explore novel applications for both modes of ICD therapy:

1. To evaluate measures that enhance the efficacy of defibrillation using an animal based model.
2. To assess the usefulness of painless ATP therapy as a means of pacing for Supraventricular Tachycardia - Ventricular Tachycardia (SVT-VT) discrimination and to assess the burden of inappropriate therapies (ITS) in a clinical context where this data may be useful.

Methods:

The defibrillation studies were performed in a porcine model given its resemblance to the human heart and its resilience to repeated ventricular fibrillation inductions (VF) and defibrillations. A novel sequential preshock waveform was assessed in a prototype serial capacitance device. Single and multi-electrode defibrillation vectors were evaluated in intra-cardiac, subcutaneous (SQ), and intra-pericardial configurations. The burden of ITS and the factors improving detection were assessed. Anti-tachycardia pacing was used to evaluate therapies in this patient cohort. The diagnostic utility of the post pacing interval (PPI) after failed ATP episodes was then investigated to help discriminate between atrial fibrillation/tachycardia (AF/AT) and VT.

Results

A monophasic preshock was found to be adjunctive together with a standard biphasic waveform; presumably because of the prolongation of the post shock iso-electric window. A multi-site Right Ventricle (RV) defibrillation strategy was shown to improve measures of defibrillation outcome. A single antero-posterior SQ defibrillation vector was as efficacious as a multiple SQ array configuration; however, an additional parasternal anode was less effective. Percutaneous delivery of an intra-pericardial defibrillation electrode is technically feasible and is effective for both a pace/sense and defibrillation strategy. Despite advances in ICD development, ITS occurred in 15% of cases studied. Failed ATP resulted in PPIs that could be used to discriminate AF/AT from VT in this population.

Conclusions

Defibrillation efficacy may be enhanced by the addition of a monophasic preshock. Marginal benefit was demonstrated with the addition of a second RV defibrillation electrode. An SQ antero-posterior transthoracic shock vector was optimal in a transthoracic defibrillation strategy and an intra-pericardial defibrillation electrode could be percutaneously positioned and used effectively to defibrillate.

The PPI after failed ATP is a useful discriminator of AF/AT from VT and has diagnostic potential in single chamber devices.
The burden of ITS is reduced with dual chamber ICDs, programming advanced discriminators, and higher detection intervals.

Table of Contents

List of Figures

List of Tables

Abbreviations

AF	Atrial Fibrillation
APD	Action Potential Duration
AT	Atrial Tachycardia
ATP	Anti-Tachycardia Pacing
AVN	Atrioventricular Node
BiV	Biventricular ICD
Can	The Active Housing of the ICD
CL	Cycle Length
DFT	Defibrillation Threshold
DR	Dual chamber ICD
ED	Energy Discharge
EDF	Endocardial Defibrillation
EGM	Electrogram
ICD	Implantable Cardioverter-Defibrillator
IPG	Implantable Pulse Generator
ISI	Inter-Shock Interval
ISW	Iso-Electric Window
ITS	Inappropriate Therapies
LV	Left Ventricle
MES	Multi Electrode Strategy
NPV	Negative Predictive Value
PPI	Post Pacing Interval

PPS	Posterior Pericardial Space
PPV	Positive Predictive Value
PVC	Premature Ventricular Complex
RA	Right Atrium
RV	Right Ventricle
RVA	Right Ventricle Apex
RVOT	Right Ventricle Outflow Tract
SQA	Subcutaneous Array
SVC	Superior Vena Cava
SVT	Supraventricular Tachycardia
TCL	Tachycardia Cycle Length
TDF	Transthoracic Defibrillation
TDI	Tachycardia Detection Interval
ULV	Upper Limit of Vulnerability
VF	Ventricular Fibrillation
VT	Ventricular Tachycardia

Publications and Presentations Arising from this Thesis

Alternative Strategies to Enhance Defibrillation Efficacy.
Michael KA, Paisey JR, Sunni NS, Allen S, Robinson S, Roberts PR, Morgan JM.
Poster presentation at Heart Rhythm UK, Birmingham 2006.

Does the Interval between a Preshock and Primary Biphasic Shock Affect Defibrillation Thresholds?
Michael KA, Paisey JR, Yue AM, Sunni N, Roberts PR, Morgan JM. Europace 2006:8, supplement 1:24/5.
Oral presentation at Cardiostim Nice 2006.

An Investigation of Weight Variation on Defibrillation Outcome Comparing an Endocardial vs. Subcutaneous Configuration in a Porcine Model.
Michael KA, Paisey JR, Bullens RWM, Smits KFAA, Robinson S, Allen S, Sunni N, Yue AM, Roberts PR, Morgan JM.
Poster presentation at the European Society of Cardiology Conference, Barcelona 2007.

The Use of Dual Defibrillator Coils in the Right Ventricle Lowers Shock Impedance but does not consistently Improve Defibrillation Efficacy.
Michael KA, Paisey JR, Bullens RWM, Smits KFAA, Robinson S, Allen S, Sunni NS, Yue AM, Roberts PR, Morgan JM. Heart Rhythm May 2007, Vol. 4(5) Supplement S209.
Poster presentation at Heart Rhythm, Denver 2007.

The Post Pacing Interval after Failed Anti-Tachycardia Pacing may be a Useful Diagnostic Tool in Differentiating Atrial Fibrillation/Atrial Tachycardia from Ventricular Tachycardia.

Michael KA, Redfearn DP, Fair S, Miranda R, Abdollah H, Simpson C, Baranchuk A. Canadian J of Cardiol. Oct 2010: Vol 26; S78D.

Oral presentation at the Canadian Cardiovascular Conference, Montreal 2010.

Slow Ventricular Tachycardia Zone Programming Increases the Risk of Inappropriate Therapies.

Michael KA, Baranchuk A, Miranda R, Simpson C, Abdollah H, Redfearn DP. JICE 2011: Mar 2011, Vol 30(2), Abs 19-10.

Moderated poster presentation at the European Cardiac Arrhythmia Society, Paris 2011.

The Post Pacing Interval Following Failed Anti-tachycardia Pacing can be used to Differentiate between Atrial and Ventricular Tachycardias in ICDs.

Michael KA, Fair S, Miranda R, Baranchuk A, Simpson C, Haley C, Abdollah H, Redfearn DP. HRJ May 2011: Vol 8(5); p.S1-S 576. Supplement.

Poster presentation at the Heart Rhythm Society meeting, San Francisco 2011.

Current Issues in ICD SVT-VT Discrimination: Pacing for SVT-VT Discrimination.

Oral presentation delivered at the Heart Rhythm Society Meeting as part of the core curriculum, Boston 2012.

Also prepared as a chapter for the Intech open access book entitled:

"**Cardiac Defibrillation**" ISBN 980-953-307-733-3.

Full Manuscripts in Preparation or Currently Under Review

Failed Anti-Tachycardia Pacing can be used to Differentiate Atrial Arrhythmias from Ventricular Tachycardia in Implantable Cardioverter-Defibrillators.

Michael,KA; Haley, C; Baranchuk, A; Simpson, C; Miranda, R; Abdollah, H; Redfearn, DP.

An Analysis of Inappropriate Therapies in Implantable Cardioverter-Defibrillators and Measures to Reduce this Deleterious Effect.

Michael, KA; Haley, C; Baranchuk, A; Simpson, C; Miranda, R; Abdollah,H; Mayosi,B; Redfearn, D.

A Transvenous Multi-Electrode Defibrillator Lead Strategy within the Right Ventricle in a Porcine Model Improves Defibrillation Outcome.

Michael, KA; Paisey, JR; Mayosi, B; Roberts, PR; Morgan, JM.

Assessment of the Optimal Placement of Subcutaneous Arrays in a Transthoracic Defibrillation Strategy in a Porcine Model.

Michael, KA; Paisey, JR; Mayosi, B; Roberts, PR; Morgan, JM.

Acknowledgements

I wish to thank Prof. Bongani Mayosi for helping to bring this project to completion and for his constant support. I also thank Prof. Commerford, Prof. Okreglicki, Prof. Scott-Millar, Dr Stevens, and Dr Levetan at the Cardiac Clinic, University of Cape Town, South Africa.

I thank Prof. Mitha, Prof. Mathiva, Prof. Naidoo, and Prof. Motala at the Nelson R Mandela School of Medicine, University of Natal, South Africa.

I thank Dr John Morgan and Dr Paul Roberts, for supervising and guiding the biomedical component of this work, Dr Arthur Yue and Dr John Paisey for the invaluable advice and help they provided, and Jas Barley and her ever-willing staff at Southampton University Hospital's Biomedical unit, United Kingdom.

I thank Dr Damian Redfearn, Dr Adrian Baranchuk, Dr Chris Simpson and Dr Hoshiar Abdollah at the Heart Rhythm Service, Queen's University, Ontario, Canada for the clinical aspects of this thesis and for helping me piece the collage together.

1. Introduction

The first human implantation of a defibrillator was reported by Mirowski and colleagues in 1980[1]. Since then, there have been remarkable changes that have advanced the indications for implantable cardioverter-defibrillators (ICD).

Three major technological advances that have contributed to the enhanced clinical application of the ICD are the use of transvenous leads, an active Can (the active housing of the ICD electrode) and the biphasic defibrillation waveform[2].

Despite great advances with defibrillator design and development, the optimal defibrillation waveform to minimise energy drain on the battery and to achieve a painless shock remains elusive.

This thesis discusses the current understanding of the mechanisms and theories of ventricular fibrillation (VF) as well as the concepts of defibrillation and anti-tachycardia pacing (ATP). The experimental chapters that follow advance these concepts by expanding on waveform design and novel vectoral arrangement using a porcine model. The modality of ATP is explored in the clinical chapters.

The use of animal subjects for these experiments is required given that defibrillation threshold (DFT) testing requires multiple VF inductions and defibrillations that may result in neurological and cardiac injury[3;4].

The clinical trend is to avoid defibrillation testing as a routine but when it is performed, it is to insure a 10J safety margin rather than to determine the DFT.

However, DFT testing remains the only method to titrate the minimum level of energy required to defibrillate fibrillating myocardium successfully. Defibrillation threshold testing, therefore, still has relevance in a research capacity.

The development of 40J high-energy devices may seem to negate the need to find ways to reduce DFTs. However, deleterious effects have been identified with higher energy shocks. These include electroporation cell injury, altered action potential waveforms and duration, resting membrane potential disruption, increased pacing thresholds, loss of excitability, induction of after-depolarisations that may be pro-arrhythmic, myocardial stunning, haemodynamic alterations including progression to heart failure, and psychological trauma[5]. This validates further research into reducing defibrillation energies.

Anti-tachycardia pacing is an effective and painless component of therapy in modern ICDs. I have addressed ATP as a form of pacing for supraventricular tachycardia (SVT) and ventricular tachycardia (VT) discrimination and identified the post pacing interval (PPI) after ATP as having diagnostic potential .This thesis comprehensively addresses both forms of ICD therapies and takes a novel outlook on their roles and application[6].

Current device algorithms have a sensitivity approaching a 100% in identifying ventricular arrhythmias[7]. However, inappropriate therapies (ITS) remain a significant problem[8]. The burden of ITS is examined here in a typical clinical cohort as well as factors related to device programming that help ameliorate ITS. This provides a clinical context for further work into ICD discrimination algorithm

development and sets the tone for possible further investigation into the PPI as a programmable diagnostic parameter.

Our knowledge of the mechanisms of ventricular fibrillation and defibrillation is still incomplete. In the following introductory sections I will describe the current state of knowledge around concepts related to the basic science experiments in this manuscript. These experiments are intended to build on our current understanding of defibrillation waveforms, polarity, and cellular response to high voltage energy delivery.

Aspects of ICD structure and design will be elaborated on to encapsulate the challenges faced in order to minimise device volume while promoting battery longevity.

A basic description of high voltage lead design is also necessary as this is relevant to the several chapters related to lead position and manipulation of leads and arrays in order to alter defibrillation vectors in an attempt to enhance defibrillation efficacy.

The clinical studies relevant to ICD treatment is also briefly highlighted with relevance to landmark trials that demonstrate survival benefit and this brings into context the clinical aspect of the thesis.

Advancements in ICD therapy include the development of ATP, and the clinical trials that have led to this technology are also mentioned. A basic understanding of the concept of ATP is established before I embark on the experimental chapters related to its diagnostic relevance.

1.1 Concepts Related to Defibrillation and Defibrillation Testing

Theories about the Mechanisms of Defibrillation

Concepts of defibrillation have evolved from the Dudel model (1968), which called for complete myocardial paralysis, and Wiggers (1930s) who formulated a **Total Extinction Hypothesis.** Both implied that complete annihilation of fibrillating myocardial wavefronts was required to terminate VF[9].

Mower et al. and Zipes et al. contradicted these theories with a **Critical Mass Hypothesis** that suggested that in order to terminate VF a critical mass of myocardium was required to effect defibrillation. This was proven in a canine model by infusing a potassium solution into the coronary arteries in a sequential fashion until VF was terminated[10].

Chen et al. postulated that there is a vulnerable period during which VF is stopped but is re-initiated by sub-therapeutic shocks. Beyond a particular threshold, defibrillation does not re-initiate VF. This is referred to as the **Upper Limit of Vulnerability**[11;12].

The Iso-electric Window

An apparent period of electric quiescence has also been recognised to occur after delivery of a high voltage shock. This is referred to as the **iso-electric window** (ISW). This window lasts for a variable duration ranging between 40–100 ms before VF re-initiates[13]. This has been recognised from optical mapping

studies and therefore excludes artefact from blanking or post shock saturation of conventional electrical mapping systems as an explanation for this observation[14]. Sub-threshold propagated graded responses, as well as undetectable micro re-entry have been postulated to occur during this period with re-initiation shown to occur preferentially at epicardial locations and within the intra-myocardial layer of the left ventricle (LV)[15;16].

Supposedly, re-initiation of VF after the ISW may be on the basis of triggered activity in the form of early after depolarisation. Hyperpolarisation of the cellular membrane with a sequential and timely delivered shock into the ISW may possibly suppress the after depolarisation. This concept may explain why preshock delivery may lower DFTs and relates to the first experimental chapter in this thesis (Chapter 4).

Defibrillation Testing

Acute defibrillation testing at implantation has traditionally been employed to test the efficacy of the circuit. However given advancements in modern lead and device design, it has become apparent that such practices may be obsolete and a more selective approach to defibrillation threshold testing should be taken[17]. Protagonists for avoiding DFT testing argue that DFT testing increases patient morbidity and does little to benefit patient care with an already known high efficacy of modern ICDs[18]. This argument, however, is not relevant to the experiments in this thesis as performance of DFTs is the only reliable way of

determining the minimum defibrillation energy required. This was also carried out in an animal model, and not on human subjects, thereby eliminating the ethical factors relating to myocardial injury and psychological trauma. The defibrillation threshold is defined as the lowest energy that successfully terminates VF. The threshold plotted against probability of success translates into a sigmoidal graph. The DFT is reflected as the probability of success at a given energy and is quoted in terms of percentage; e.g. DFT50 indicates 50% of successful shocks for the given energy discharge (ED) and ED90 represents 90% successful shocks at this portion of the curve[10] (Figure 1.1.1).

Defibrillation Testing Algorithms

1. Binary search – this starts at an intermediate level of energy and employs an up/down strategy to derive the lowest energy of defibrillation.
2. Bayesian search – this closely resembles the binary search format but uses voltage output for defibrillation testing.
3. Step-down protocols – the first energy is set at 10 J below the maximum energy output of the device. If successful, the energy is sequentially reduced until a minimum point is reached which fails to defibrillate.
4. Single energy success – this method minimises the testing, reducing total duration in VF and is a favoured clinical option as it limits the number of inductions and shocks during testing. Typically, an output 10 J less than the maximal energy of the device is chosen for defibrillation. This may be repeated given the probabilistic nature of defibrillation. Thereafter, the device is programmed to a maximum output while assured of a 10J safety margin.

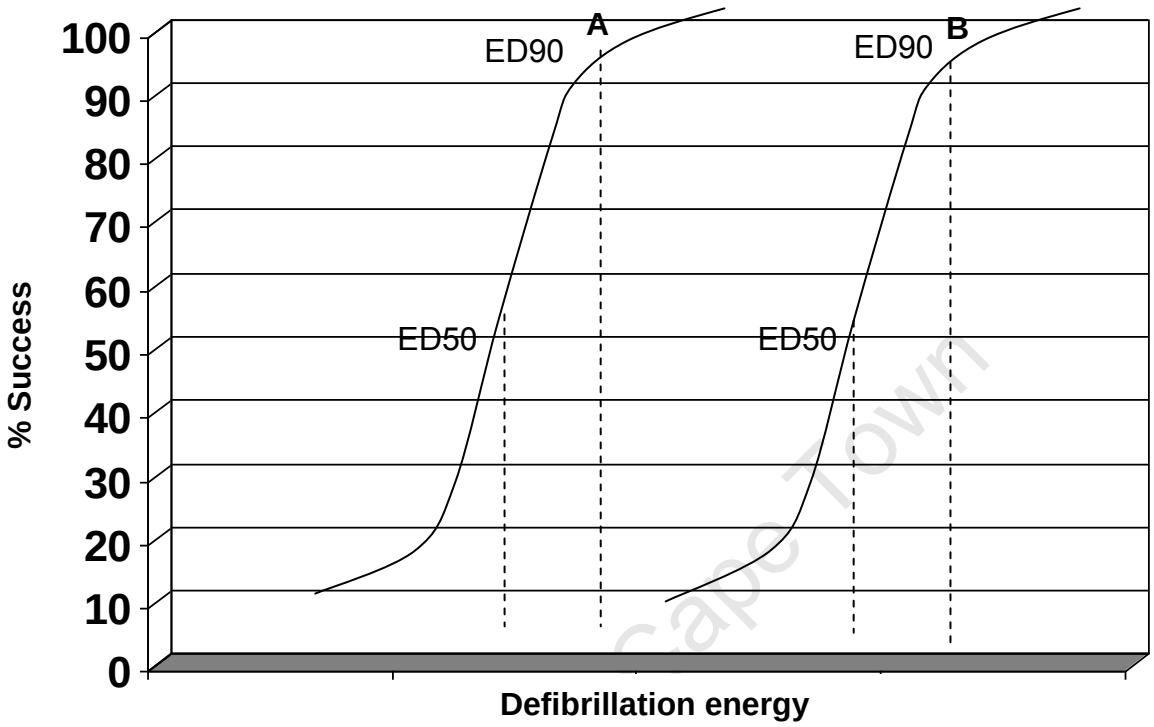

Figure 1.1.1

Graphic representation of shock energy against % of successful defibrillation attempts. Graph B represents a higher energy requirement for defibrillation success.

(Reproduced from *From Cell to Bedside* 5th ed. Zipes, 2009[10]).

Clinical Factors Affecting Defibrillation

Efficacy of defibrillation may be influenced by factors related to the substrate and then by the ICD system itself[19].

Substrate related factors include

1. Hypoxia
2. Ischaemia
3. Hyperkalaemia
4. Increased myocardial mass, either due to hypertrophy or dilatation[20]
5. Increased body mass index
6. Pneumothorax and pericardial effusions – these create parallel currents shunting energy away from the myocardium[21]
7. Antiarrhythmic drugs – Amiodarone has been recognised to increase DFTs, however, this was shown to be marginal and probably not clinically relevant in the OPTIC trial[22-24]
8. Multiple defibrillations
9. Prolonged VF duration

Factors Related to the ICD System

1. Poor lead position
2. Increased high voltage impedance
3. Poor current distribution (Low impedance from current shunting)
4. Current shunting from retained guide wires/leads (passive electrode effect[25])
5. Suboptimal waveform

Thus, in a clinical setting, recognition of factors that may impair defibrillation may then be the criteria to select patients for defibrillation testing in order to insure safety margins rather than opting for routine DFTs.

Measures Employed to Improve Defibrillation Thresholds

Reversing the polarity of the shock vector is usually the first adjunctive measure in a clinical setting, as it requires no further intervention, but is a programmable option in the ICD. Repositioning of the right ventricle (RV) endocardial lead and using the sensing and pacing parameters as a surrogate for optimal electrode and tissue contact is also a consideration. Thereafter, addition of extracardiac electrodes, either subcutaneously or transvenously, are relied upon to provide alteration in the shock vector and to increase the amount of muscle mass that is interposed within the defibrillation circuit, e.g. the addition of a separate transvene superior vena cava (SVC) coil placed within the azygous or left subclavian veins[26;27]. The proximal coil (integrated SVC coil) in dual coil defibrillator leads should also be optimally situated outside the right atrium (RA) at the left subclavian level and SVC junction. This SVC component of these dual coil leads can be programmed in or out of the circuit as can the active Can electrode of the ICD by some manufacturers.

Apart from altering the shock vector, varying the phase duration of waveforms has also been shown to improve DFTs[28;29].

The addition of subcutaneous arrays may also be considered in addition to the intravascular defibrillation electrodes but this does involve further surgical

intervention[30]. Still, it may be the preferred option if vascular access is obstructed by stenoses, or in order to avoid intravascular and intra cardiac lead placement in children.

In addition, manipulation of anti-arrhythmia agents may be a clinical consideration, such as removal of Amiodarone, which raises DFTs, or the addition of Sotalol and Dofetilide, which lower DFTs[31].

The initial measures derived from clinical practice mentioned here relate to waveform alteration and defibrillation vectoral changes. These provided the motivation and basis for the hypothesis generation behind the defibrillation-based studies contained in this thesis.

1.2 The Implantable Cardioverter-Defibrillator, Leads, and Implantation Techniques

Initial ICD designs were large, weighing 195–235 g, and required abdominal implantation under the rectus sheath and connection to epicardial defibrillator patches requiring transthoracic placement. These have now markedly reduced in size but have increased in functionality.

Complex algorithms are now commonplace to aid diagnostic differentiation of rhythms and to minimise the risk of ITS.

Ventricular tachyarrhythmia therapies include both high rate overdrive ATP of various permutations, as well as the programmable shock discharge.

Modern ICDs now may have a volume of 30–39 cm^3 and weigh merely 66–84 g. Implantation is either pre- or sub-pectoral with a transvenous closed-chest implantation technique that can be performed under local anaesthesia and conscious sedation.

Batteries

The majority of the bulk of the devices was contributed by the size of the battery and capacitors (Figure 1.2.1). Two batteries were used in the past; a Lithium-based composite (e.g. Li Iodide) required for the pacemaker function and internal circuitry, and a silver vanadium oxide (SVO) battery to charge the capacitors for a high voltage discharge (both are contributors to device volume).

Lithium silver manganese vanadium oxide is now used. Two batteries in series help prolong the device life, but increase overall size[32]. Current devices have been significantly reduced in size with hybrid single battery technology that provides greater longevity extending out from 2–8 years depending on usage.

The stored energy of original batteries was in the order of 8000J. Current batteries store a charge of 18000J. Two of these batteries are usually configured in series, although newer devices now employ a single hybrid battery. This single battery is required to support both the anti-tachycardia and bradycardia functions, telemetry and discriminator circuitry with an anticipated longevity of approximately 8 years.

A beginning of life charge of 3.2 V is typical and elective replacement indicator is reached at 2.6 V. This allows elective scheduling of pulse generator replacement whereas a 2.2 V charge indicates end of life and warrants urgent replacement.

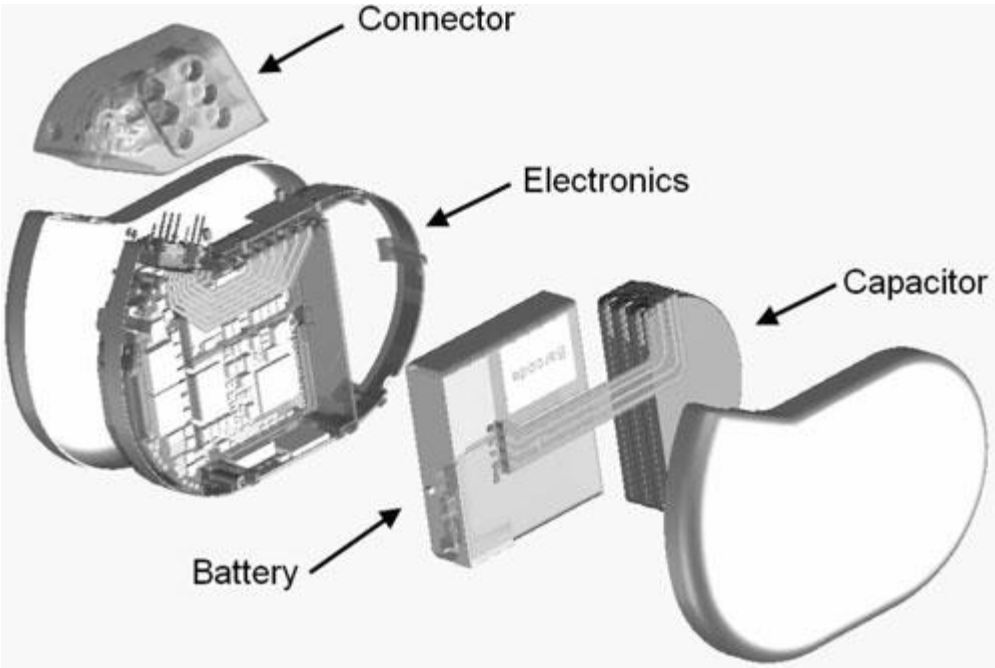

Figure 1.2.1

An internal view of the structure of a typical ICD

(Reproduced from *Improvements in 25 Years of Implantable Cardioverter Defibrillator Therapy*. *Neth Heart J* 2011[32]).

Capacitors

Since the battery alone cannot build up sufficient charge to deliver high energy shocks, capacitors are required to store and release a charge into myocardial tissue. Aluminium based electrolyte capacitors have been used because of their ability to charge to energies of 30–40 J from a total battery charge of 3.2–6.4 V over a rapid period of 10–30 seconds.

A reduction in capacitor size is advantageous since smaller ICDs allow ease of implantation and concealment at the implant site. However, smaller capacitors require a higher peak voltage improving defibrillation safety margins. Capacitors are now smaller in the 60–90 μF range, which parallels the time membrane constant for human cardiac cells, as opposed to the 140μF capacitors used previously in older ICDs. This has shown a modest reduction in DFTs.

Amplification of Signals

Sensed signals from the device are processed through high and low pass filters that help remove extraneous noise so that a mid-range of signal is made available to discriminatory algorithms. There is an overlap between atrial and ventricular events, as well as depolarisation and repolarisation phenomena, including sensed myopotentials or noise from the device system itself that make this prone to misdiagnosis, resulting in ITS.

Telemetry Circuits

Wireless communication with the ICD and its programmer is now available in a Real-time telemetry format. These signals are sent as radiofrequency signals or a pulsed magnetic field. The radiofrequency signal is pulsed and encoded at a particular frequency that is specific for each manufacturer[33]. This prevents error programming of other devices and eliminates the influence of environmental sources. It also makes manufacturer signals specific for device analysers.

Microprocessors

The microprocessor in an ICD or pacemaker has to be engineered to limit its battery usage, whereas a microcomputer has potentially endless power available from an AC source. The implantable pulse generator (IPG) may contain both ROM and RAM (read only and random access memory, respectively) although exclusive RAM based generators limit production costs and allow flexibility in terms of software upgrades or troubleshoot patches that may eventually arise.

ICD Lead Technology

Modern leads are multi-lumen, consisting of both a pace/sense as well as high voltage components for defibrillation. They may be dual coil or single coil and contain passive (tined ends) or active fixation mechanisms (a spiral screw at the lead tip). Leads may be integrated bipolar, where pacing and sensing utilises the

tip electrode and RV defibrillation coil, or true bipolar which uses the tip electrode and a proximally located, separate ring electrode.

The outer coating may consist of silicone, polyurethane or fluoropolymers, which are all biocompatible. More recently, a blend of polyurethane and silicone has been employed or a polyurethane outer coating which reduces friction, improves handling at implantation and apparently enhances lead durability as per manufacturer claims[34]. Fibrotic adhesions are also reduced and this is advantageous during ICD and lead revisions or replacements. It also potentially reduces the incidence of venous occlusion.

Implantation Techniques

Although a general anaesthetic is used by some centres, defibrillator implantation is also performed under conscious sedation. A transvenous technique is favoured from either a left or right pre-pectoral or sub-pectoral site. Both sites have been shown to be efficacious although right sided implants may have higher DFTs[33;35]. This facilitates rapid recovery and does not result in increased morbidity or discomfort to the patient. The defibrillator lead is implanted at an RV apical location with the SVC coil (in dual coil leads) positioned in the SVC to the right of the vertebrae, but superior to the right atrium.

Surgical transthoracic placement with epicardial patches or a hybrid technique with endocardial and epicardial leads is an option. Because of the size of previous ICDs, abdominal implantation was favoured in the past[32].

The use of a dual coil defibrillator lead has not been shown conclusively to be superior to a single defibrillator coil lead[36].

In the subsequent experimental chapters, I have performed studies in close chested pigs, primarily using a transvenous lead implantation technique except for transthoracic and intrapericardial lead placements. The RV apical electrode position was also used in the control experiments with the active Can electrode in a left chest, subcutaneous pocket to resemble a typical clinical implantation. The SVC coil was usually excluded from the circuit as this lead could not always be optimally placed in the pigs.

1.3 Shock Waveforms and Cellular Response.

Shock Waveforms

The shock waveforms can affect defibrillation efficacy as well influence the extent of cellular damage caused by the transmembrane potential induced by shock. This is referred to as electroporation and is explained in detail later in this introduction.

Several waveforms have been developed from the basic monophasic square wave and include: a damped sine wave, truncated descending waveform, and a truncated exponential ascending/ramp waveform (Figure 1.3.1)[10].

The shape of the waveform determines the peak voltage and the energy achieved which impacts on stimulation thresholds while the phase duration i.e. time constant also determines the efficacy of the waveform. A time constant of 2.8–4 ms has been determined to be optimal for internal defibrillation while 5 ms is optimal for external defibrillation.

The fast rise to peak voltage after a capacitor discharge results in a typical leading wavefront spike. If the rate of rise of this wavefront is slowed, this results in a rounding of the peak. This variation has been shown to result in improved defibrillation efficacy in biphasic and triphasic waveforms[37;38].

The effect of a shock discharge on myocardial tissue is both stimulatory and defibrillation. To defibrillate myocardium successfully, a shock has to alter the transmembrane potential of the majority of cells, whereas stimulation only has to

affect the transmembrane potential of a certain number of cells adjacent to the electrode.

The first phase of a biphasic waveform serves to alter transmembrane potential in order to minimise heterogeneity of charge across several cells while the second phase restores transmembrane potential and obliterates virtual electrodes[39].

Despite the evidence from prior studies, the options for manipulation of defibrillator waveforms remain limited to polarity reversal and pulse wave duration in modern ICDs. These remain largely non-programmable.

In the first two chapters of this thesis, I evaluated delivery of preshock as a programmable option in a serial capacitance prototype defibrillator. This prototype affords additional options for waveform manipulation and optimisation in an effort to improve defibrillation efficacy.

The Burping Theory[39;40]

The first phase of a biphasic shock extends the refractory period of ventricular myocytes, while the second phase removes excess charge from the remaining cells. This is beneficial for marginally stimulated cells that have a delayed potential. Myocardial cells in the vicinity of an electrode and in areas bordering “virtual electrodes” are temporarily damaged (electroporation) by the extreme current release[41;42].

Electroporation

This refers to the acute injury sustained by myocyte cell membranes from delivery of a high voltage electric field. The result causes increased permeability of the cell membrane to ionic efflux in a regional manner. This is a transient phenomenon and is reversed during the second phase of a biphasic shock. The polarity of shock delivery plays a role in the degree of cell membrane injury but this data is inconsistent in studies[43;44].

Virtual Electrode

The physical electrode charge induces a similar charge on the surrounding myocytes up to a variable diameter depending on the strength of the field. Therefore a virtual anode will surround the physical anodal electrode because of migration of the oppositely charged ions to cluster around the electrode at the tissue interface.

The virtual electrode effect produced during defibrillation on myocytes influences the efficacy of shocks and depolarised regions[41;42].

The Effect of Polarity

Previously, the RV electrode was programmed as the cathode (-) and this was regarded as normal polarity. This, however, has been shown to cause expanding wavefronts with delivery of shocks, dissipating into the surrounding fibrillating myocardium and is thus potentially arrhythmogenic. With programming of the distal electrode as the anode (+), these wavefronts implode around the electrode,

reducing their stimulatory effect. Kroll et al. demonstrated in their meta-analysis that anodal RV shocks for the first phase of a biphasic shock are superior[45].

The trend currently seems to be to reduce the need for defibrillation testing at implantation and therefore requiring that the optimal defibrillation waveform be empirically programmed at the outset[46;47].

The biphasic waveform typically consists of two monophasic pulses with leading edges greater than the trailing edge. The level of voltage decay between the leading and trailing edges may be set typically as 50%, at which point a polarity inversion occurs and a further 50% decay of voltage occurs to termination (Figure 1.3.2).

There are fixed tilt and phase duration systems such as the Medtronic ICD population (Medtronic Inc. MN. USA). This is typically set at 2.6 ms/2.8 ms (first and second phases, respectively). The optimal formation of this biphasic waveform has been contentious. Commercially available ICDs typically discharge a defibrillation waveform having a 50%/50% or 65%/65% tilt to each phase.

Evidence also suggests that pulse width programming or a “tuned” phase duration programming is more effective than fixed tilt programming[28;48]. Arguably, new generation devices may require more flexible defibrillation waveform programming to deal with high DFT situations.

This may be explained by understanding the relationship of membrane charge relative to capacitor dissipation. This is referred to as the time constant Tau[28].

The value of Tau may be influenced by myocardial fibre orientation and composition, which takes into account the scar content of the myocardium. It therefore seems that a fixed tilt waveform may be suboptimal.

This would suggest that the optimal biphasic waveform requires match between the time constant Tau of the defibrillation system and the cell membrane. The diagrammatic representation of a biphasic shock waveform against membrane response in Figure 1.3.3 shows that the first phase reduces the peak membrane response, and then the second phase returns the membrane potential to zero[40]. However, phase two persists beyond the zero point for a few milliseconds, which is wasteful and potentially detrimental.

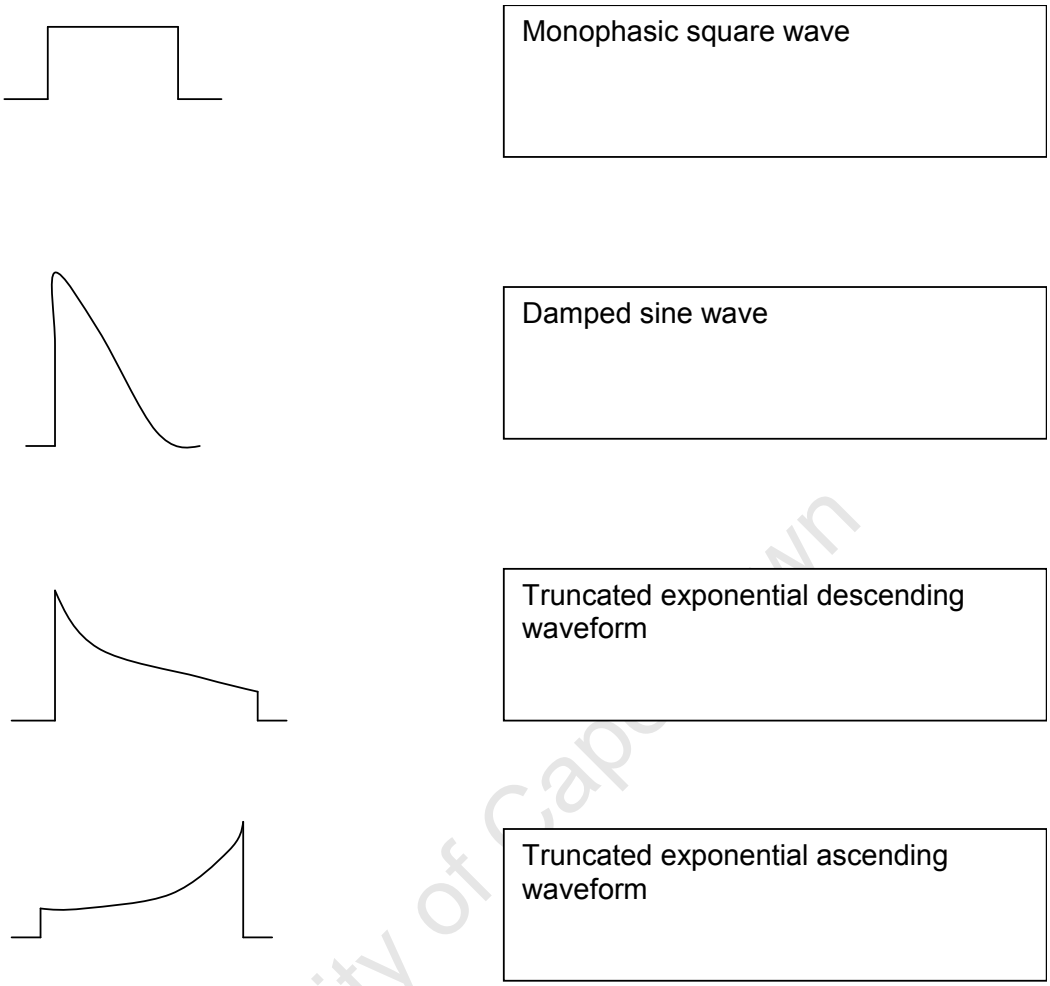

Figure 1.3.1

Diagrams of the monophasic components of defibrillation waveforms.

(Reproduced from *From Cell to Bedside* 5th ed. Zipes 2009[10]).

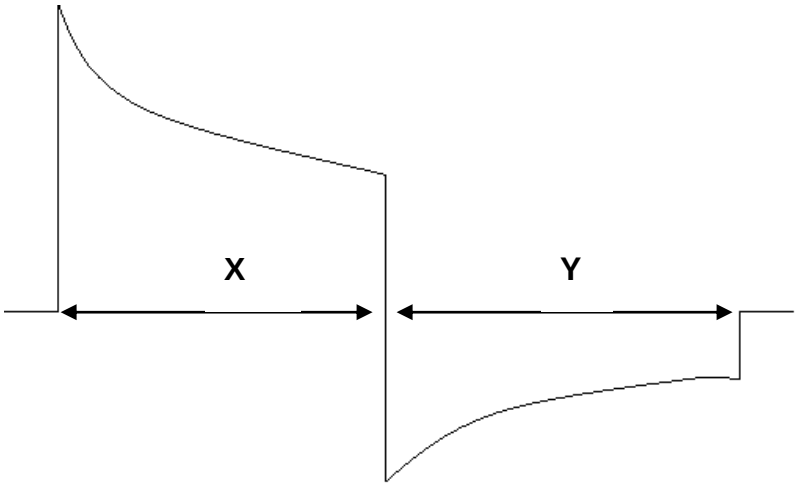

Figure 1.3.2

A biphasic truncated exponential descending waveform with 50% tilt of both phases. Polarity reversal occurs after the voltage has decayed to 50% from the leading edge in phase 1 then a decay of 50% from the leading edge in an inverted phase 2. Thereafter, the waveform is truncated.

The phase durations (X and Y) are programmable in some devices; alternatively this is determined by having a fixed or programmed tilt.

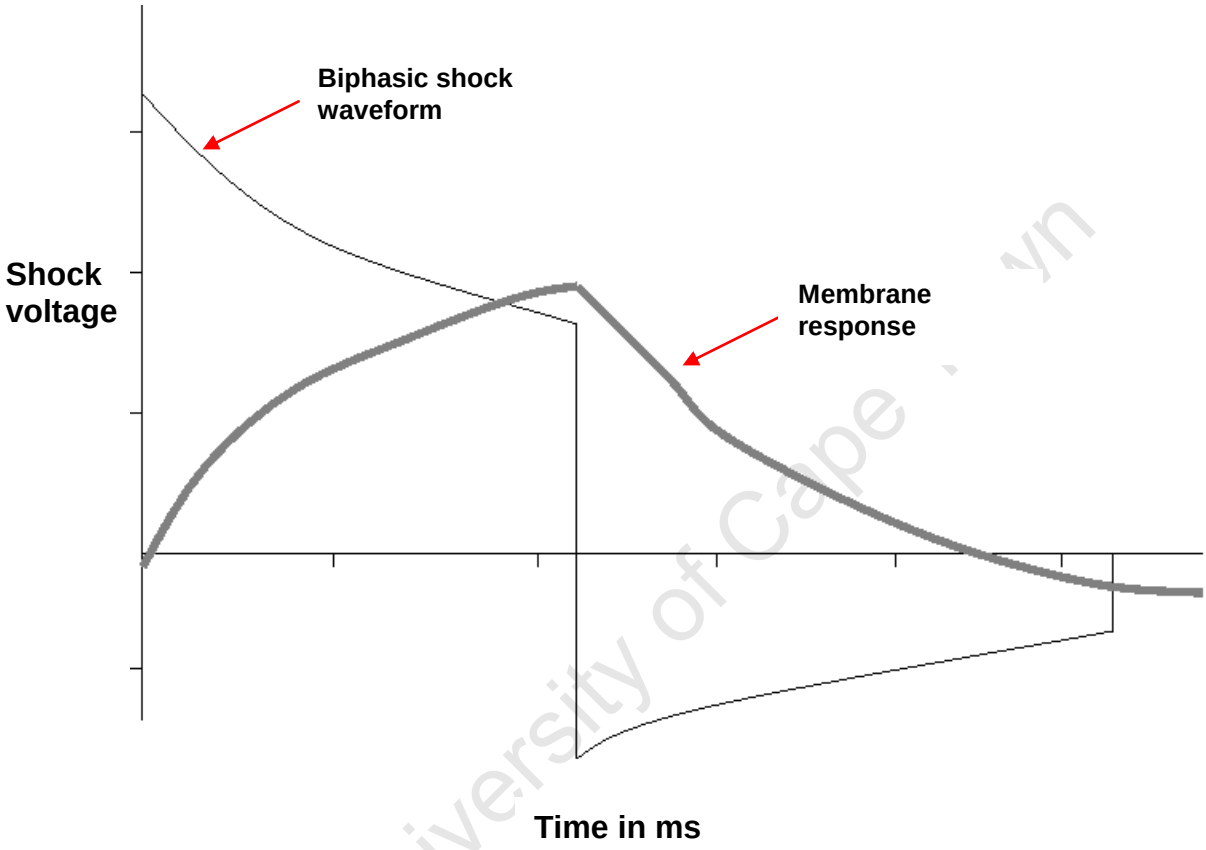

Figure 1.3.3

A theoretical biphasic waveform with equal tilt with a matched membrane response.

(Reproduced from *From Cell to Bedside* 5th ed. Zipes 2009[10]).

Upper Limit of Vulnerability

Sub-threshold shocks delivered within a vulnerable zone of repolarisation (during the T wave) may induce VF. However, with incremental shock energies VF becomes no longer inducible. This critical point is termed the upper limit of vulnerability (ULV), which interestingly corresponds to the DFT[40;49;50].

Cellular Manifestations of Shock Delivery

Optical mapping studies in cellular mono-layers indicate that changes in trans-membrane charge induced by shocks are non-linear. This is asymmetric and characterised by a greater negative polarity, presumably due to calcium leaking through the positive areas of the cell membrane. This links the concept of electroporation with the shift in cell membrane potential, in response to a strong shock[51;52].

Mechanisms of Initiation

Ventricular arrhythmias are initiated either by:

1. Macrore-entry
2. Early after depolarisations (occurring in phase 1 and 2 of the action potential) as in the case of Torsade de Pointes and Long QT syndromes.
3. Delayed after depolarisations (phase 4)
4. Abnormal automaticity

The initiating event is usually a premature ventricular complex (PVC) initiating VT/ VF.

In the case of acute ischaemia, the K_{ATP} channel is opened causing acidosis and anoxia in cardiac muscle. The result of K^+ efflux is a large dispersion of repolarisation across the border-zone of the ischaemic region. Tissue excitability increases resulting in spontaneous activations.

For re-entry to occur, two criteria must be met:

1. There must be a unidirectional block within the myocardial substrate
2. The cycle length of the tachycardia must exceed the longest refractory period of the myocardium.

The action potential duration (APD) in ventricular myocardium is heterogeneous. The duration is longer at the base of the heart than at the apex and longer in the endocardium than in the epicardium, but longest at the mid-myocardial layer (M-cell layer). This dispersion in APD may be the cause of VF generation in diseases such as Brugada Syndrome and the Long QT syndrome[53;54].

Ischaemic Ventricular Fibrillation

The border-zone areas of regional ischaemia leading to electrical heterogeneity have been identified as the substrate and site for the generation of triggers initiating VF[55]. Thrombotic occlusion of coronary arteries is more likely to be associated with VF than non-thrombotic occlusions. The rise in extracellular K^+ and Na^+ (due to Ca^{2+}-Na^+ exchange) contribute to the excitability of tissue. Norepinephrine levels become elevated within border-zones following ischaemia. These factors create a critical milieu that provides the catalyst for electrical instability leading to VF.

Effects of Repeated Defibrillation on Myocardium

The effects of direct current, electrical shock on myocardium have been studied in animals and there is anecdotal evidence from post-mortem human specimens. Focal areas of coagulation necrosis with haemorrhage occur in the subepicardium. At an ultra-structural level, there is disruption of the intercalated discs[56]. Modest elevations of the cardiac enzymes have been noted to occur[57]. The electrical shock also may alter the appearance of the ST segment and T waves on the surface ECG.

1.4 Ventricular Fibrillation Induction

Ventricular fibrillation is typically induced in a clinical setting using the following techniques:

1. Pacing using high frequency alternating current delivered from the ICD to the myocardium either through endocardial or epicardial electrodes at 60, 50, or 30 Hz as described by Kleiman et al.[58].
2. Delivery of a low energy shock (typically 1J) during the vulnerable part of the T wave after a short ventricular pacing train.
3. Application of direct current though the pace/sense electrodes. This is referred to as DC Fibber in ICDs manufactured by St. Jude Medical (St Paul's, MN, USA).
4. Delivery of sub-threshold shocks until the ULV threshold is reached[59].

The relevant induction protocol to each experiment has been elaborated on in the methods sections of this thesis.

1.5 Clinical Trials and the Impact on ICD Development

The ability of the ICD to save lives in survivors of cardiac arrest has been demonstrated in these landmark secondary prevention trials: Arrhythmia Versus Implantable Defibrillator (AVID) trial, Canadian Implantable Defibrillator Study (CIDS) and Cardiac Arrest Study Hamburg (CASH)[40;60-62] Factors that influenced the benefit of ICDs included an ejection fraction <35%, increased age, and heart failure.

The primary prevention trials include MADIT, MUSTT, MADIT II, which went on to demonstrate the benefit of ICDs implanted in patients with ischaemic cardiomyopathies as a primary prevention strategy[49;63].

The CABG-Patch trial, however, showed no benefit with prophylactic ICD implantation in patients receiving coronary artery bypass[40;64].

The DEFINITE and SCD HeFT extended the indication to include patients with non-ischaemic cardiomyopathies[64].

The indications for defibrillators are therefore expanding. This places a need for evolving technology including extended battery longevity, improved detection algorithms to minimise ITS, and to reduce morbidity from shock delivery.

1.6 Painless Anti-Tachycardia Therapy

Anti-tachycardia pacing has been shown to reduce pain and psychological trauma following defibrillation[49;65]. There is increasing data to suggest that shock delivery, whether appropriate or inappropriate, also portends a poor prognosis, predicting increased mortality from progressive LV dysfunction and heart failure[66].

The PAINFREE II Rx trial helped advance the idea of empiric ATP for an episode of VT, even though it is identified in the VF zone. The ATP will be discharged first as long as the rhythm remains stable[67]. This option is programmable and helps reduce the number of shock therapies, reducing morbidity, and conserving the ICD battery.

The ATP is programmable for the number of pulses and coupling intervals. A fixed set of equally spaced pulses is referred to as a “burst”. A “scan” refers to a decrement in the interval between successive burst sequences if the criteria for rhythm termination after ATP are not identified. The ATP may then be programmed to become more aggressive so that there is always an escalation of therapy in the case of an ongoing event and never a step down in therapies.

This may consist of a “ramp” where there is a decrement between each delivered pulse. Each pulse may also be programmed at individual coupling intervals and is referred to as a “ramp plus” by Medtronic (MN, USA).

At the same time, ATP can be deleterious. Overzealous ATP programming can result in eventual progression of shock delivery, which may result in a prolonged period of VT or VF.

Anti-tachycardia pacing can potentially be pro-arrhythmic if delivered inappropriately. On the other hand, ATP can be used as a diagnostic tool depending on the interaction it yields with the underlying tachycardia.

I explore the incidence of ITS from ICDs in a clinical context and explore the diagnostic applications of failed ATP and its potential for active/dynamic discrimination of SVTs and VT in the clinically applied chapters in this thesis.

2. Overview of Experimental Design and Methods for Animal Studies

2.1 Animal Selection and Characteristics Relevant to Ventricular Arrhythmia Induction and Defibrillation

Both canine and porcine models have been used in large animal defibrillation studies because of the ability to procure the animals as well as their comparable cardiac anatomy to humans[68;69]. The porcine heart bears closer resemblance to human cardiac structure. In contrast, the canine heart has greater myocardial bulk, presumably because of higher levels of activity[70].

Landrace pigs were chosen for these experiments, as they are commercially bred and easier to obtain than dogs for scientific procedures.

The following non-clinical experiments used pigs as test subjects:

- Assessment of a sequential defibrillation waveform in a prototype serial capacitance defibrillator (Chapter 4).
- An investigation of multi-site right ventricular endocardial electrode placement on measures of defibrillation outcome (Chapter 5).
- Transthoracic defibrillation studies (Chapter 6).
- A pilot project to assess defibrillation from an intra-pericardial location (Chapter 7).

Electrophysiological Comparisons between the Pig Model and Humans

The measured R wave from the pig`s electrocardiogram is in the order of 5.9–10.4 mV and for man this has a comparable range of 6.9–17.9 mV, whereas the R wave in the dog ranges between 24.0–30.0 mV reflecting its thicker myocardium. The QT interval in the pig is longer, hence the relative ease in inducing VF with T wave synchronous sub-threshold shocks[71].

The mean VF cycle length in humans is 200 ms compared to 95 ms in pigs.

Martin and colleagues compared the temporal characteristics of VF among seven patients with previously analysed swine data[72].

In the patients, VF frequency was 4.23 ± 0.93 Hz at onset, which then ebbed displaying bimodal peaks at 4.4 ± 1.01 Hz at 55 sec and 3.98 ± 0.5Hz at 5.47 ± 0.45 min (Figure 2.1.1 A).

In the pigs, the initial VF frequency was 13.5 ± 1.68 Hz at induction, which ebbed to 8.6 ± 0.87 Hz at 1.22 ± 0.19 min. This was followed by a single peak of 13.7 ± 1.79 Hz occurring at 3.55 ± 0.57 min (Figure 2.1.1 B).

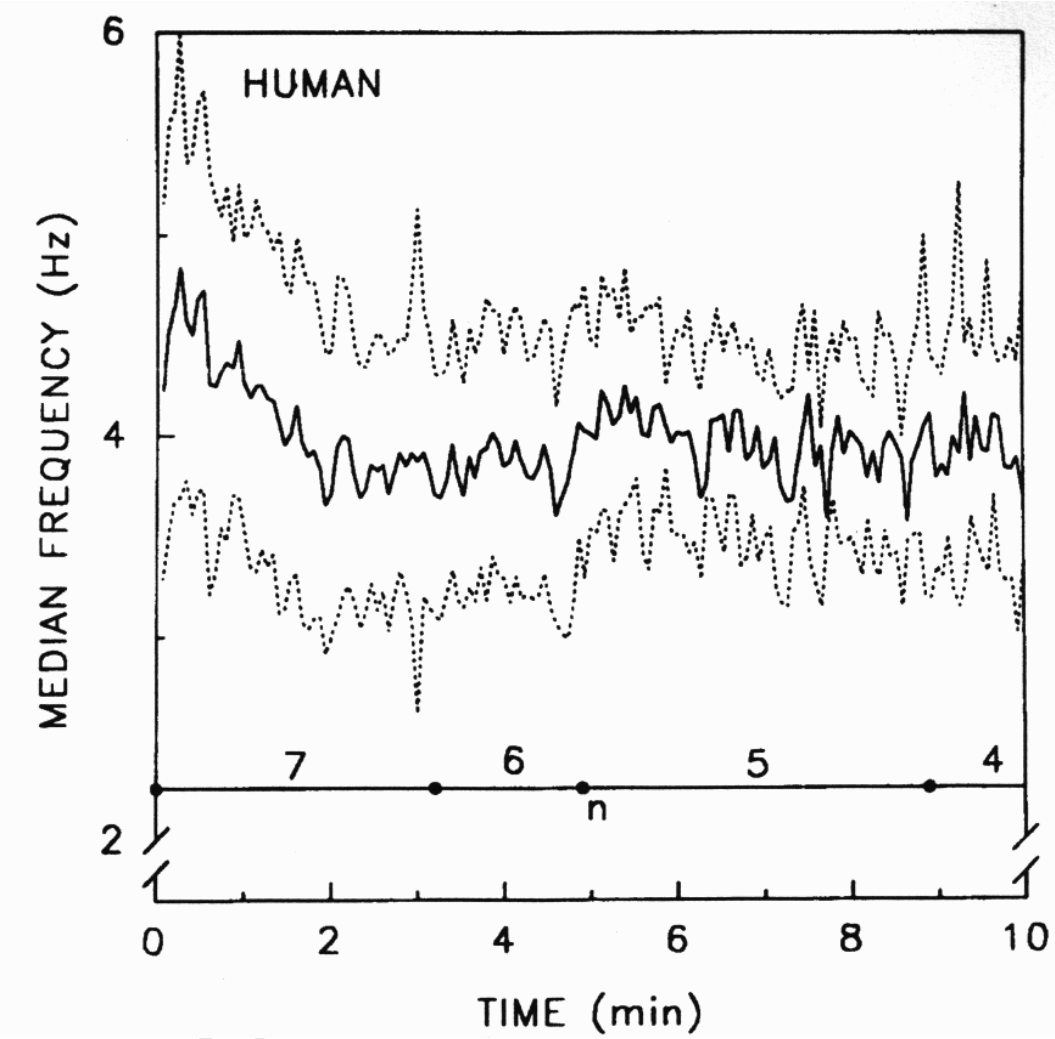

Figure 2.1.1A

Plot of the median frequency of VF in seven human subjects. The frequency is shown over time in minutes and the standard deviation is indicated by dotted lines.

(Reproduced from *Frequency analysis of the human and swine electrocardiogram during ventricular fibrillation*. *Resuscitation* 1991[72])

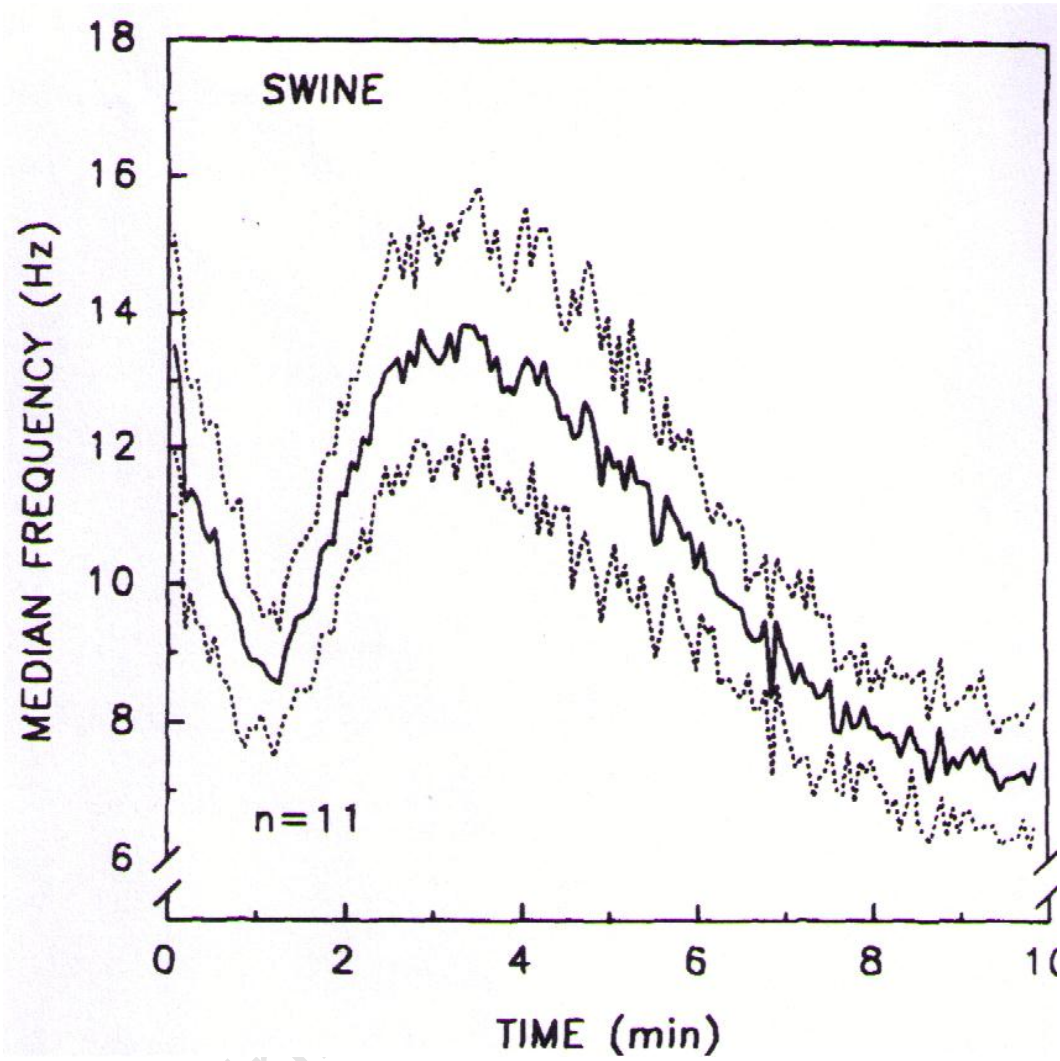

Figure 2.1.1B

Plot of the median frequency of VF in eleven pigs.

The frequency is shown over time in minutes with the standard deviation depicted by dotted lines.

(Reproduced from *Frequency analysis of the human and swine electrocardiogram during ventricular fibrillation*. *Resuscitation* 1991[72]).

2.2 Animal Preparation and Handling

Experiments were batched, with only one experiment per day and two to three per week. This was done to optimise the use of laboratory resources as well to allow sufficient time for the animals to acclimatise to their new surroundings. The pigs were also brought in five days prior to the scheduled experiments in order to reduce the stress levels of the animals prior to experiments. An additional challenge was to control the feeding and weight of the pigs prior to experiments to maintain uniformity between the study subjects since weight influenced defibrillation thresholds.

Premedication

On the day of each experiment, animals were sedated with an intramuscular injection of Azperone (Stresnil) at 2 mg/kg approximately 30 min prior to anaesthesia.

An intravenous cannula was inserted into an ear pinna vein. A bolus dose Alfaxalone/Alfadolone acetate (Saffan) was administered intravenously for rapid induction. The animal was then immediately transported to the operating table.

Intubation Technique

The epiglottis of the pig is longer than in humans and tends to obstruct vision of the cords and larynx. This was obviated by placing the pig in the left lateral position. A laryngoscope with an elongated straight blade was used to depress the tongue and forceps were used to gently manipulate the epiglottis in order to

expose the cords and larynx. The larynx and vocal cords were then sprayed with Xylocaine.

A cuffed endotracheal tube was then advanced over a trocar into the trachea and the cuff was inflated. The animal was ventilated with a mixture of Oxygen (100%) and Isofluorane (5% initially, then reduced to 2%) with flow rates of 2–3 L/min. The tidal volume was calculated at 10 mL/kg. A CapeWain Multipurpose ventilator (Cape, Warwickshire, UK) with a soda lime carbon dioxide extraction system was used. Additional Saffan boluses were administered intravenously if required to deepen anaesthesia.

Monitoring

All animals were monitored using cutaneous surface ECG recordings with a Hewlett Packard HP 78353B (Hewlett Packard, CA, USA) monitor.

Intracardiac electrogram recordings were monitored through the pace/sense component of a defibrillator lead after positioning within the RV using the respective ICD programmer (Symphony, Ela Medical, Sorin Group, France or Medtronic analyzer).

A cut down to a femoral artery was performed and an indwelling cannula was left in situ to maintain continuous intra-arterial blood pressure recordings. Femoral vein access was also established for administration of fluids (0.9% saline).

Animals were draped and core body temperature was monitored.

Euthanasia

All experiments were non-recovery. At the conclusion of each experiment animals were administered a lethal dose of sodium pentobarbital at 20 mg/kg. On cessation of cardiac activity, the ventilator was turned off. The animal was observed for absence of respiratory effort and cardiac function. The animals were disposed of by incineration. In some cases, an autopsy of the heart was performed before disposal to assess for macroscopic evidence of cardiac trauma from repeated defibrillation and to assess the position of the electrodes, particularly with intrapericardial placement.

2.3 Anaesthesia Choice and Anticipated Interactions

The intravenous preparation of Saffan is a mixture of 9 mg Alfaxalone and 3 mg Alfadolone acetate and was administered at 0.5–1.0 mL/kg/h. The effects of Saffan on the cardiovascular system were studied by Cox et al., who noted a progressive increase in heart rate with its use[73]. This was postulated to be due to a vagolytic mechanism at a suprapontine level.

Isofluorane was used as the inhalation agent for maintenance of anaesthesia and is preferred because of its cardiac stability.

3. Ethical Considerations and Safety Measures for Animal Usage.

All animal studies were carried out in a secure and managed biomedical facility attached to the Southampton Universities Hospital Medical School, UK.

The pigs used in these experiments were obtained from an approved and registered supplier to the University of Southampton.

Both the supplier and biomedical facility held a certificate of designation under the Animals Scientific Procedures Act of 1986 to perform regulated procedures on non-protected animals. Scheduled and unscheduled inspections were conducted by a delegate from the Home Office to ensure compliance with ethical standards for animal care. All animal technicians and handlers were employed by the University and held personal licenses regulating their level of involvement with animal experimentation after undertaking appropriate training and examinations conducted by the Home Office. All project and personal licenses required annual review and renewal.

The working conditions of all animal handlers, including surgeons were regulated under the Health and Safety Act in the UK. All animal handlers and surgeons wore surgical scrubs, protective overshoes, and gloves. The surgeon was required to wear a surgical cap, mask, and gloves during the procedures. Lead aprons were worn by all personnel present within the operating room whenever fluoroscopy was in use.

All lead aprons were routinely checked by Southampton General Hospital's radiology services for compliance and all primary operators wore TLD dosimeters on their torso, headgear, and a ring TLD for hand exposure monitoring.

A project licence (PPL: 30/2044) was granted to Dr John Morgan and Dr Paul Roberts, my senior supervisors in the UK, to conduct the animal experiments contained in this work.

I was granted a personal License by the Institute of Biology after attending an approved training course in order to undertake the specific procedures conducted on animals as detailed in this thesis.

The animal usage and number per study was chosen with adherence to concepts of replacement, reduction, and refinement.

4. Assessing A Sequential Optimised Defibrillation Waveform in a Prototype Serial Capacitance Defibrillator.

4.1 Does a Monophasic Preshock Improve the Defibrillation Efficacy of a Conventional Biphasic Waveform?

Introduction

In a previous study, Roberts et al. demonstrated that a nominal preshock delivered from a lead placed in the middle cardiac vein in a porcine model succeeded in reducing defibrillation energy requirements in all configurations incorporating the preshock[30]. This, however, was not evaluated as a sequential discharge from within the RV, which is the conventional transvenous lead location. Post-mortem analysis of the pigs used in that study showed evidence of contusions around the middle cardiac vein, even from these nominal preshocks, making the endocardial preshock delivery more desirable. Furthermore, in his thesis, Dr Paul Roberts ("An Examination of Pathways of Defibrillation", University of Leeds, School of Medicine, February, 2000) speculated about delivery of the preshock and a definitive shock from a single capacitor in order to minimise delay between the waveforms. This chapter expands on this work with the use of a prototype device.

In this study, a prototype defibrillator using two Alto2 defibrillator capacitors was constructed in close collaboration with the Ela Medical (Sorin Group, France) research and development team. Although consisting of two capacitors, as in Robert's study, the serial arrangement of the capacitors rendered that this device

function as a single capacitance unit. A custom software patch named elaterm was designed and uploaded to a laptop computer to program and configure waveforms and to activate the device via a header adapter used to establish telemetry between the computer and the non-implantable device.

The external prototype device was connected to an emulator Can and to a standard defibrillator lead which was implanted in the pig (detailed in the methods section below).

Objectives:

1. To assess the influence of a preshock delivered before a biphasic definitive shock, in a conventional RV endocardial configuration on DFTs.

2. To assess the functionality of a prototype serial capacitance device and its software (elaterm, Ela Medical, Sorin Group, France).

Methods

Animal Selection and Preparation

Six female Landrace pigs of 30–40 kg with normal hearts were anaesthetized using isofluorane and monitored using the method previously described. All experiments were non-recovery with euthanasia of the animals as previously described (Section 2.3).

A cut down to the left internal jugular vein was performed and a dual coil defibrillator lead (Medtronic 6931, MN, USA: 2.3 mm 7F, 62 mm RV electrode coil length, surface area = 513 cm^2) was inserted under fluoroscopic guidance into the right ventricular apex (RVA) (Figure 4.1.1 and Figure 4.1.2). The SVC electrode was excluded from the circuit.

The defibrillator lead used in this experiment was chosen prior to knowledge of the high incidence of 7F lead related failures[74].

The pace/sense component of the implanted defibrillator lead was inserted to the corresponding IS-1 port of an Alto VR 625 single chamber ICD (Ela Medical Sorin Group, France) and was not implanted into the animal. This device was used to conduct sensing and pacing threshold tests and to induce VF with 30Hz burst pacing through an ela Medical Symphony (Ela Medical, Sorin Group, France) programmer.

Figure 4.1.1

The dual coil 7F Medtronic 6931

This Medtronic (MN, USA) lead was implanted to the right ventricle of the pigs.

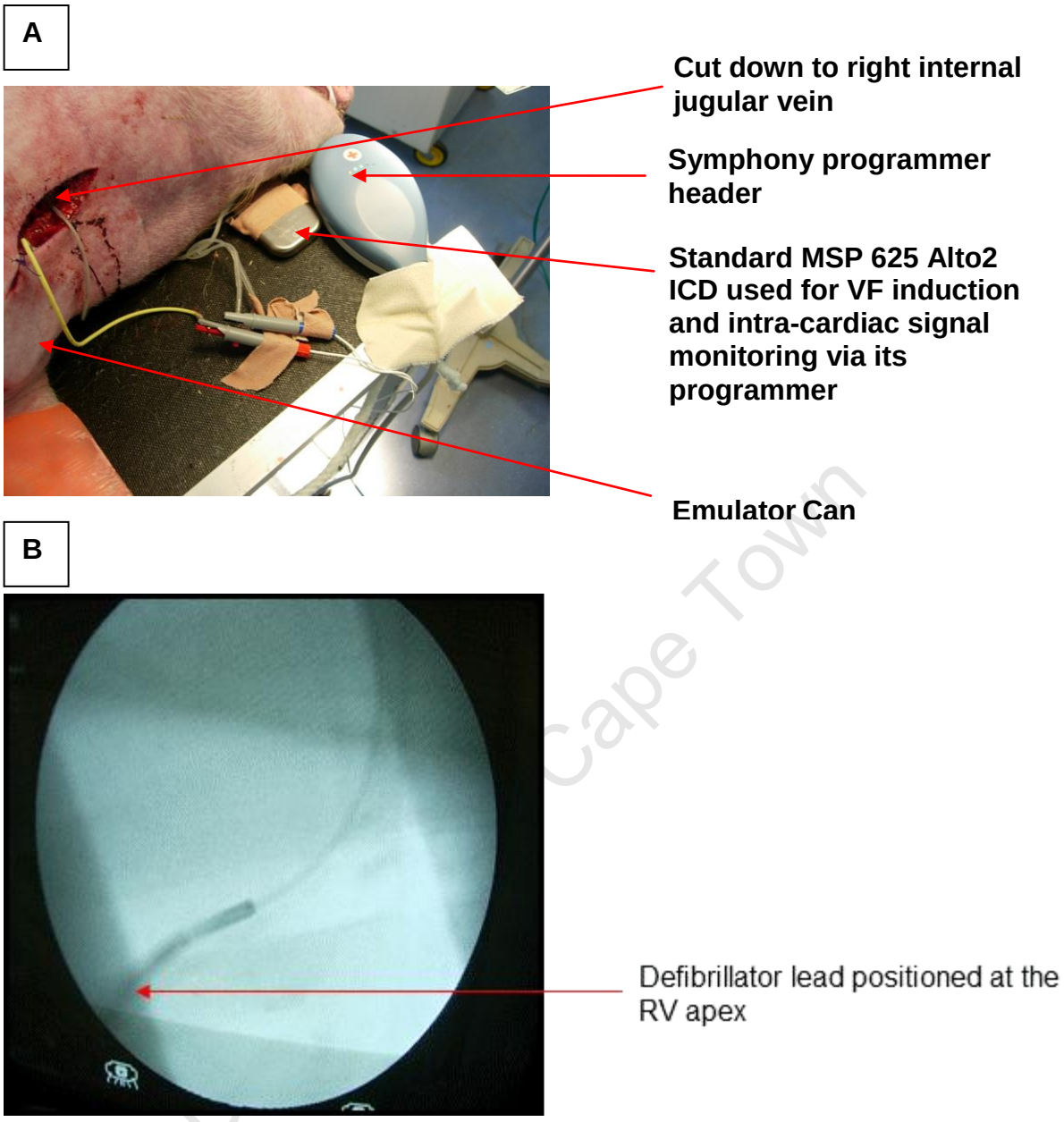

Figure 4.1.2

The dissection site and the defibrillator lead position.

A. With the pig in a left lateral position, the site of dissection to the left internal jugular vein is shown with the emulator Can implanted into a left pre-pectoral pocket.

B. The fluoroscopic position of the distal RV coil electrode at the apex of the right ventricle is shown in a left lateral view.

R wave sensing of ≥ 5.0 mV with a pacing threshold of ≤ 2.0 V at 0.5 ms was regarded as acceptable for a stable lead placement.
The RV high voltage component of the lead was attached to the external prototype defibrillator by crocodile clips to the DF-1 component of the lead. It could be programmed cathodal/anodal through the prototype ICD.

An emulator active housing based on the 9001 Defender ICD (surface area = 75 cm^2, 84.9 mm x 60 mm x 19 mm, Ela Medical Sorin Group, France) was implanted into the left pre-pectoral region to resemble clinical implantation and was then sutured into the pocket. This, in turn, was also connected by crocodile clips to the prototype ICD and therefore could have the designated polarity adjusted to +/- in the same way.

Defibrillation Protocol

Ventricular fibrillation induction was performed using three modalities in a sequential fashion if the preceding step failed to induce true VF.

30Hz Burst pacing from this externally connected ICD was delivered through the endocardial lead for 5 seconds duration. If this failed to induce VF, a T-wave shock was employed.

Custom software called **elaterm** (Ela Medical, Sorin Group, France) was uploaded to a dedicated laptop. The energy for defibrillation was programmed into the external prototype defibrillator using telemetry via a wand adapter connected to the computer.

Defibrillation testing was conducted using a binary up/down method with a 3-stage reversal pattern (Figure 4.1.3). Shock energies were programmed commencing at 13.9 J and delivered by the device in either a biphasic format alone (control) or with a preceding pre-shock (test) followed by a biphasic shock. The control or test shock DFT protocol was randomised. If this initial energy shock failed to defibrillate, the energy was increased in the next stage of the binary method to 19.8 J and the induction was repeated. If the 19.8J shock was ineffective, then the next step up would have been to 26.8 J and then to 28.7 J. This describes the sequential step up process.

If the 13.9 J shock was effective, the next induction and defibrillation was stepped down to 9.0 J.

Depending on the success or failure of this defibrillation, a step up or step down of energy was programmed.

The final energy for which defibrillation was successful was regarded as the DFT. The protocol was repeated and the average of the two DFTs was then taken as the final DFT for the protocol (control/test).

After each induction and shock delivery, a three minute recovery was observed or until haemodynamic stability (HR and blood pressure return to baseline) was achieved.

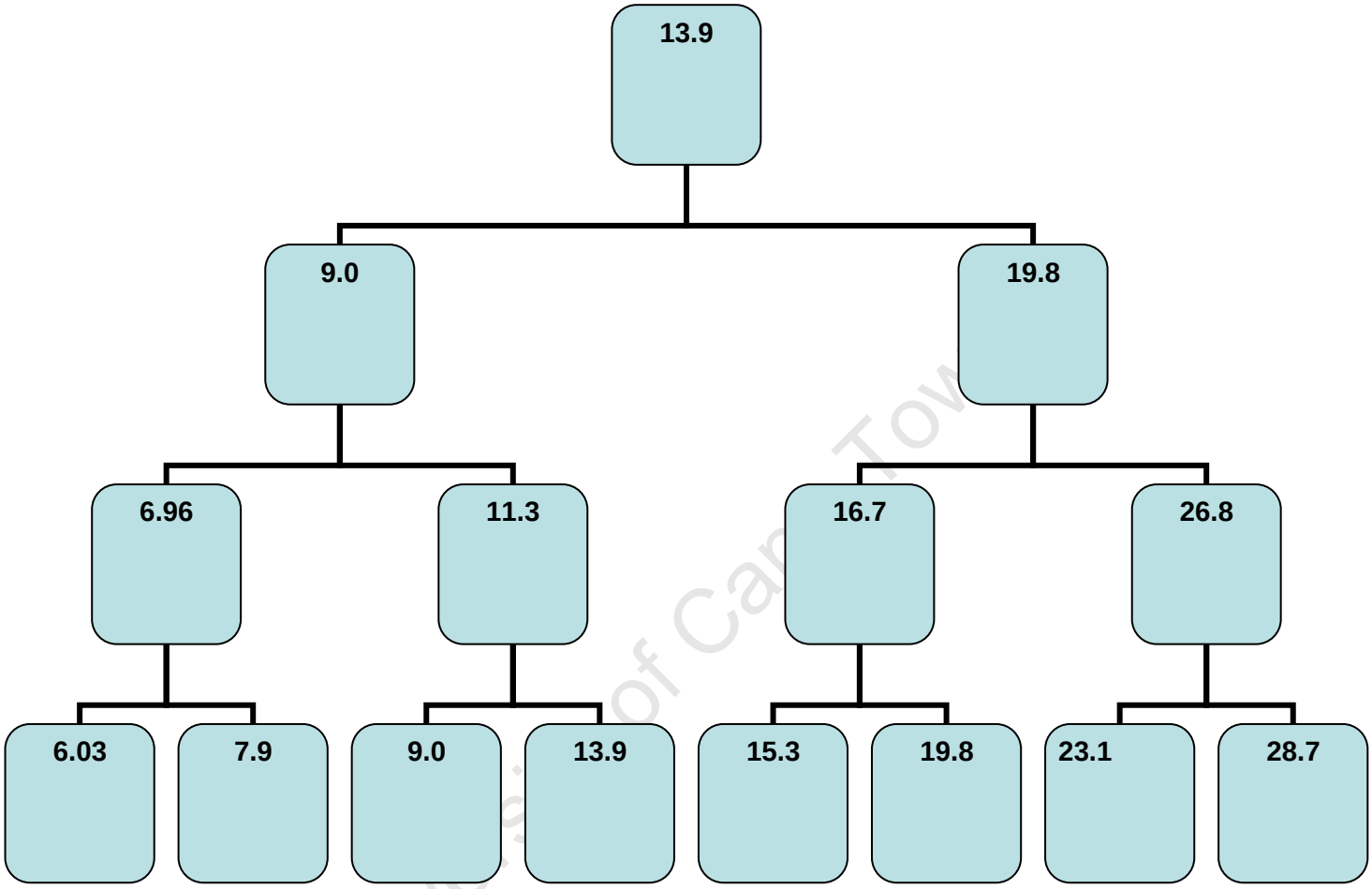

Figure 4.1.3

The binary up/down 3- reversal defibrillation protocol.

This schematic illustrates the protocol used to perform the defibrillation threshold test. This reflects delivered energies measured in joules (J).

Description of the Control and Test Shock Waveforms

A standard biphasic shock was delivered with an initial phase polarity of Can > RV coil (SVC coil was excluded) and a 50% tilt and 2.8 ms duration to both phases was regarded as the control waveform.

The preshock was a monophasic waveform with a RV (anode) > Can (cathode) orientation, tilt was automatically adjusted (non-programmable) in order to deliver a third of the total programmed capacitor discharge with a fixed 1ms phase duration.

The total energy dissipation in between preshock and the biphasic waveform was in a 1:2 ratio and is illustrated in Table 4.1.1.

Rescue Shock Delivery

Rescue shocks, in cases of a failed defibrillation, were delivered initially at a maximal discharge (30.1J) from the prototype device as a standard biphasic waveform with 50% tilt for both phases with a Can > RV coil initial polarity. If this failed, a transthoracic 200J external biphasic shock was used.

The concern after delivery of high-energy rescue shocks was the degree of electroporation cellular injury and the impact on subsequent DFTs. Thus, rescue shocks were first delivered endocardially before a transthoracic delivery and in a biphasic format so that the second phase was reparative from the initial electrical cellular insult induced in phase I of the shock waveform, as postulated by the "Burping theory"[75].

Total energy	Preshock	Definitive shock
6.0	2.0	4.0
7.0	2.3	4.6
7.9	2.6	5.3
9.0	3.0	6.0
11.3	3.8	7.5
13.9	4.6	9.3
15.3	5.1	10.2
16.7	5.6	11.1
19.8	6.6	13.2
23.1	7.7	15.4
26.8	8.9	17.9
28.7	9.6	19.1

Table 4.1.1

Stored energy (Joules) dissipated in a 1:2 ratio between preshock and biphasic components of the sequential test waveform.

Defibrillation Waveform Characteristics

The shock waveform consisted of an initial monophasic initial preshock followed by a randomised, adjustable inter-shock interval (ISI) preceding a conventional tilt dependent biphasic discharge (Figure 4.1.4).

Preshock: This was a monophasic discharge from the capacitor with the distal RV electrode denoted cathodal (-). The emulator Can and SVC coil (included in the circuit) were both anodal (+). The energy dissipated by the preshock was fixed as a third of the total discharge (including the definitive biphasic phase). This then determined the tilt of this auxiliary waveform as the phase duration remained 1 ms.

Definitive shock: Biphasic waveform delivered with the distal electrode (RV) being anodal for the first phase with 50% tilt from the lead edge and 15 ms phase duration. Thereafter, a reversal of polarity for the second phase was programmed with 50% decay from the leading edge as well.

Inter-Shock Intervals (ISIs): The inter-shock interval was defined as the interval between the monophasic discharge and the biphasic phase. These were programmable through a custom designed software patch (elaterm, Ela Medical, Sorin Group, France) that allowed interval increments up to 100 ms.

However, the ISIs chosen were limited to three, as having more permutations would have increased the number of defibrillation attempts.

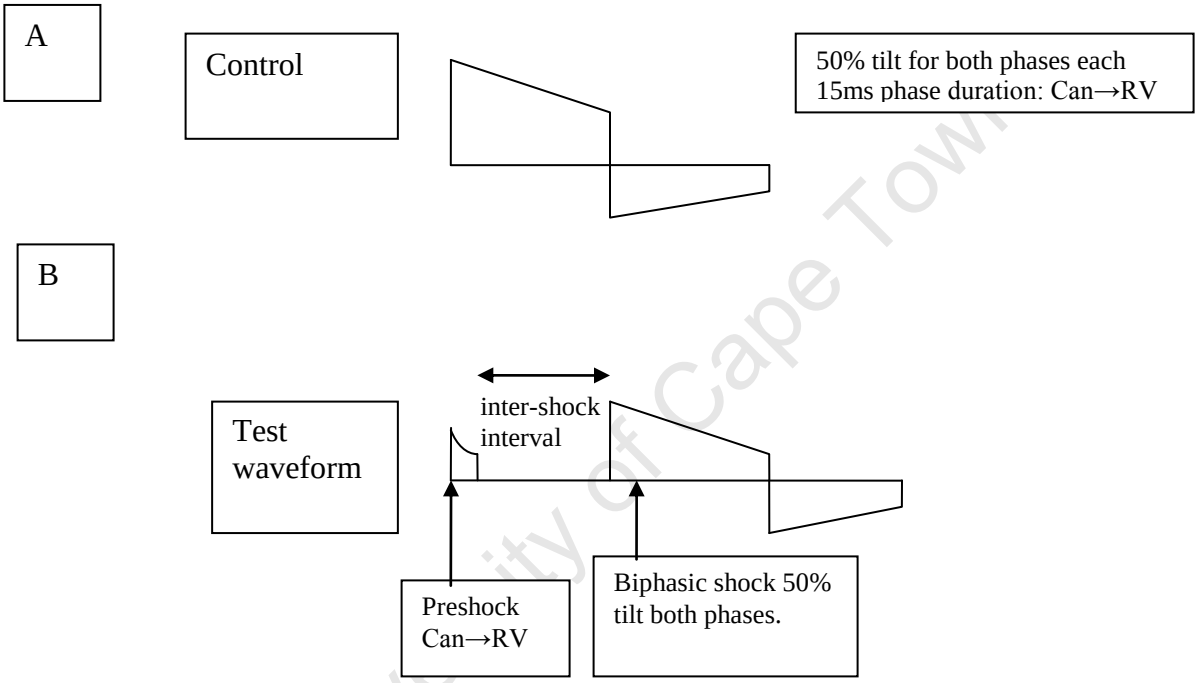

Figure 4.1.4

Control and test waveforms

A. The control shock waveform consisting of a single biphasic shock delivered at Can > RV, for the initial phase polarity.

B. The test waveform consisting of a preshock preceding the definitive biphasic shock.

This may not have been tolerated by the animal. Furthermore, the data derived later in the protocol would be made less reliable. The ISIs included 16, 31, and 47 ms (Table 4.1.2).

These were arbitrarily chosen but the selection was guided by the maximum duration of the ISW as measured by optical mapping means using voltage sensitive dye from previously established data[76].

The order of testing between control and each test interval was randomised.

The Prototype Serial Capacitor

The custom manufactured defibrillator was based on a commercially available ICD, the Alto 2 MSP 625 (Ela Medical, Sorin Group, France).

The prototype device was effectively a single capacitive defibrillator consisting of two serially arranged capacitors derived from the above mentioned ICD providing a combined capacitance of 105 μF.

Shocks are delivered by an H-Bridge composed of 4 switches (SW1–4) (Figure 4.1.5). These are activated sequentially and in pairs, in order to deliver a preshock. This also allowed the preshock to be delivered either as a monophasic or biphasic waveform if required.

The second definitive shock could likewise have been manipulated into a monophasic or biphasic basic format. The chosen waveform for the second shock was maintained as a biphasic waveform as discussed above.

	Preshock (polarity)	Primary shock (polarity)	Inter-shock interval (ms)
Permutation1		Can(+)→RVA(-)	0ms (control)
Permutation2	Can(+)→RVA(-)	Can(+)→RVA(-)	16ms
Permutation3	Can(+)→RVA(-)	Can(+)→RVA(-)	31ms
Permutation4	Can(+)→RVA(-)	Can(+)→RVA(-)	47ms

Table 4.1.2

Permutations of defibrillation testing.

Defibrillation testing was randomised between each of the above permutations and included the various inter-shock intervals listed.

The shock phases are either limited by the tilt with the amplitude of the leading edge determined by voltage in units of 25 V or by duration that was programmable in milliseconds. The ISIs were programmable to the following intervals only: 16, 32, and 47 ms. Both the non-implantable prototype ICD and the elaterm software patch to program its functions were constructed by the Research and Development team from Ela Medical, Sorin Group, France consisting of Marcel Lumisan (Head of R & D) in collaboration with Daniel Kroiss (Biomedical Engineering).

Statistical Analysis

All data were captured into an Excel spreadsheet and are represented as the mean ± standard deviation. Where relevant, statistical tests of significance were performed using a paired t-test.

Correlations were undertaken with a Spearman factor correlation for non-parametric data. These were processed using SPSS software.

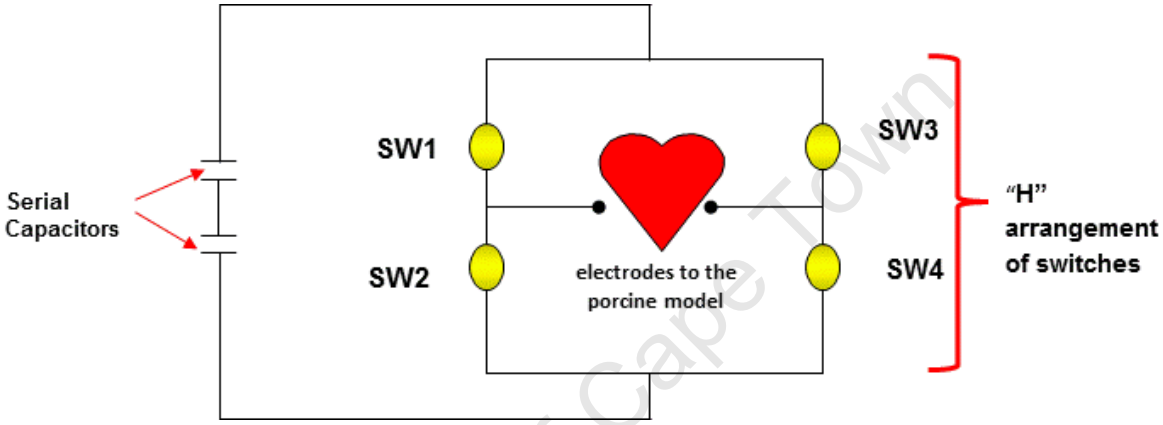

Figure 4.1.5

Diagrammatic structure of the prototype defibrillator.

This consists of serially arranged capacitors linked to an "H-Bridge" design comprised of four switches (SW). A shock entailed activation of SW1 & 4 for the first phase and then SW 2 & 3 for phase 2.

Delivery of a preshock required activation of a pair of switches before activation of the definitive biphasic shock.

Results

This study was conducted in 6 anaesthetised, close chested female pigs weighing 38.7 ± 7 kg.

There was no significant DFT reduction between a control of a standard biphasic shock and the test waveform of a nominal preshock ($p > 0.05$) for all permutations. The preshock alone never terminated VF.

Equivalent DFTs to the control were observed with the shortest ISI of 16 ms in the test waveform protocol ($p = 0.9$). Larger ISIs between a monophasic discharge and the biphasic definitive shock resulted in higher DFTs, but again these were not statistically significant (31 ms; $p = 0.1$ and 47 ms; $p = 0.2$) (Figures 4.1.6 and 4.1.7).

There was a linear correlation of the mean DFTs in each tested permutation (including control) with increasing ISIs, $r_s = 0.878$, $N = 4$, $p > 0.05$ (Figure 4.1.8).

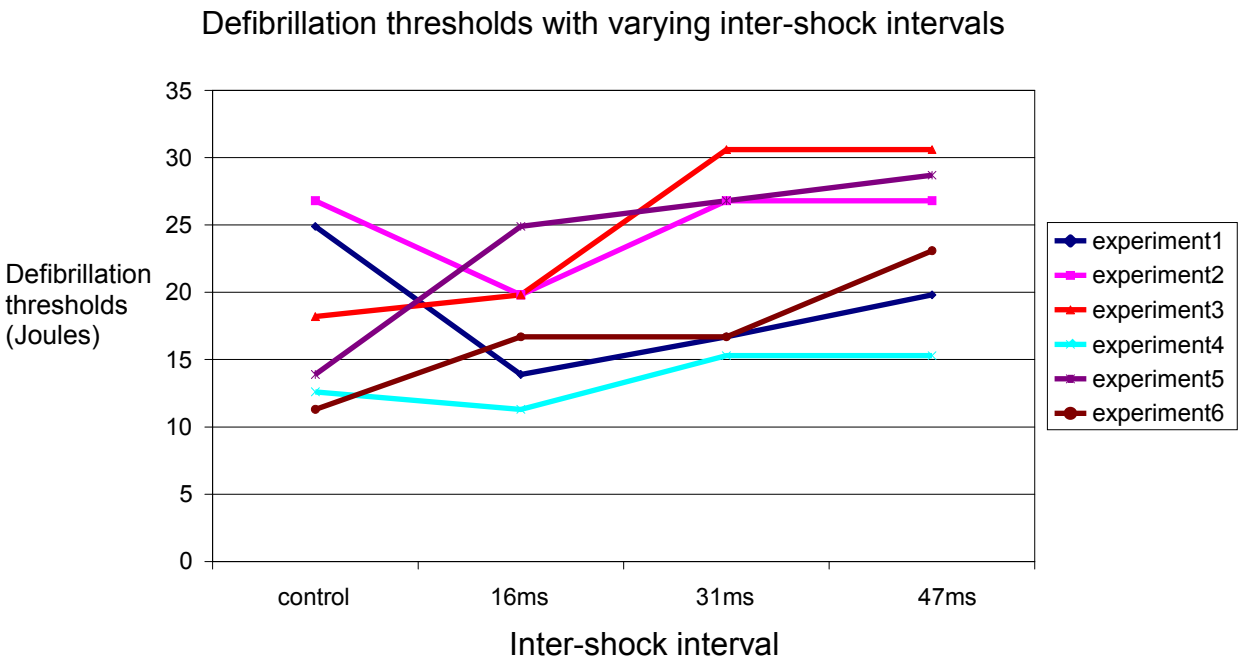

Figure 4.1.6

Linear graph depicting DFTs vs. ISIs.

	Intershock intervals			
Averages	**control**	**16ms**	**31ms**	**47ms**
DFT (joules)	17.8±5	18±3	22±5	23±5
Impedance (ohms)	48.7± 6	47.4±4	48.2±5	49.2±5
VF duration (seconds)	22±7	18±4	19±2	22±3

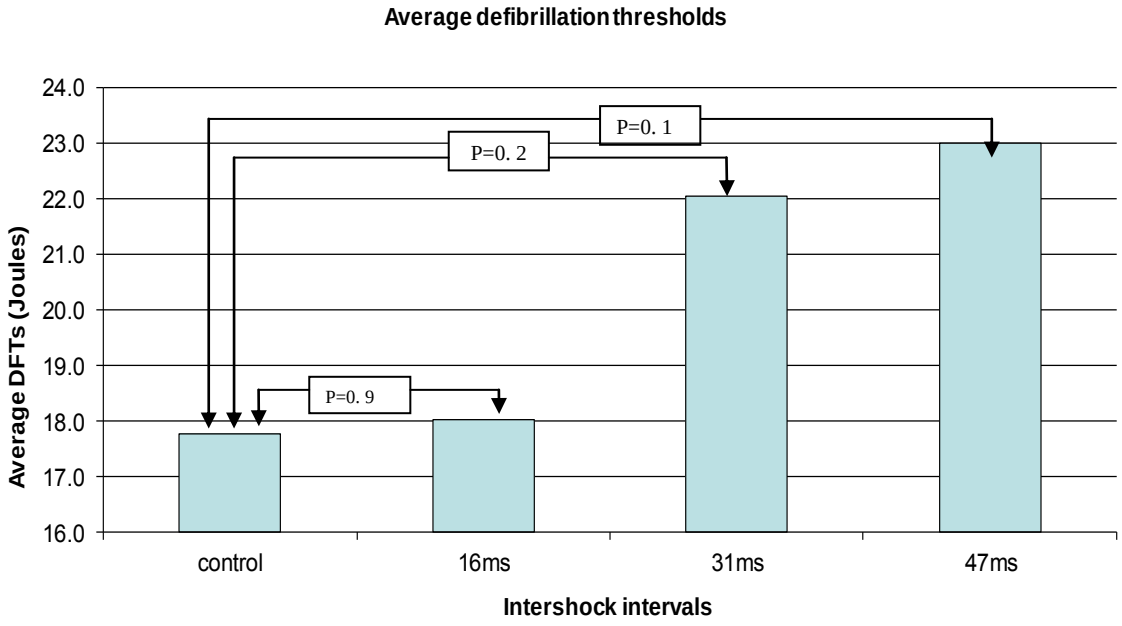

Figure 4.1.7

Summary of defibrillation outcomes at varied ISIs

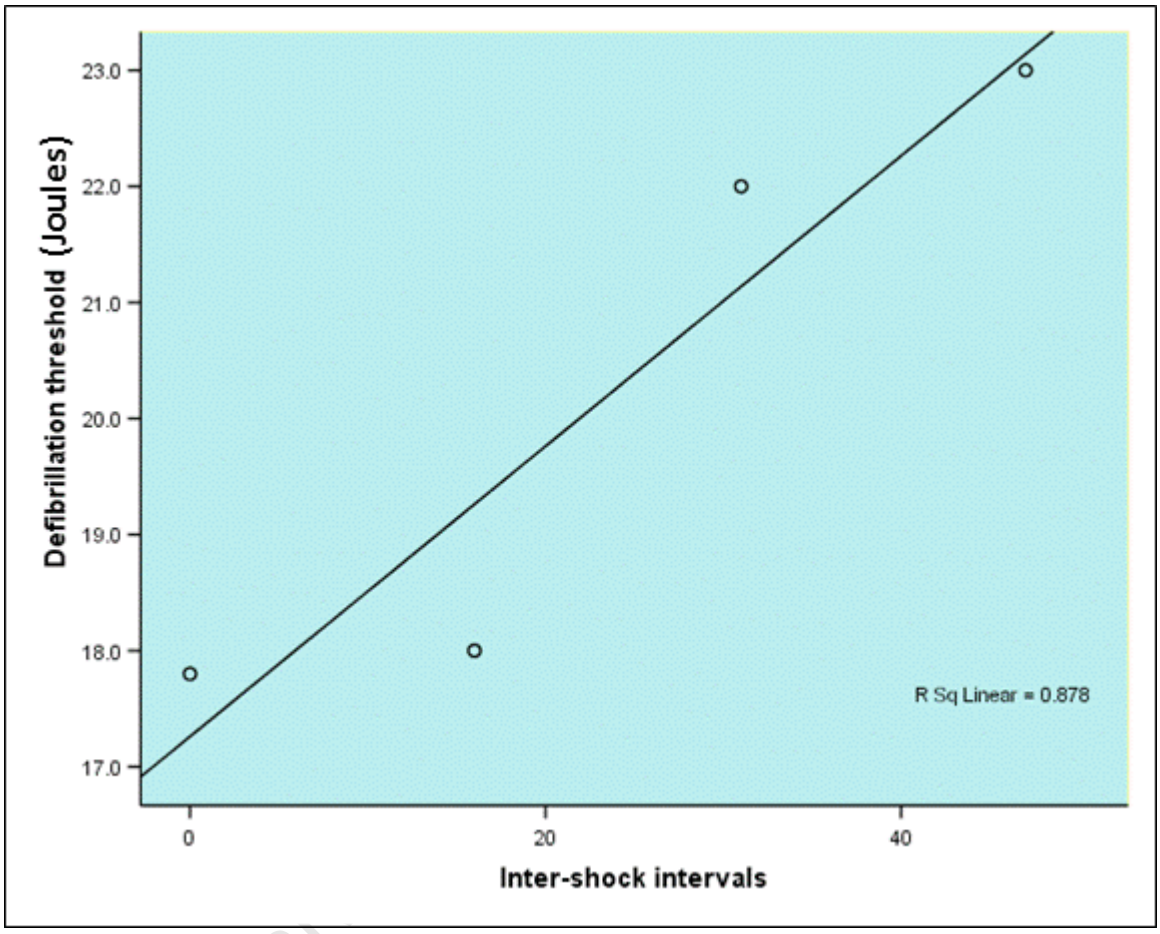

Figure 4.1.8

Linear correlation of the mean DFT for each test group vs. varied ISIs.

Discussion

Previous studies have demonstrated the efficacy of sub-threshold shocks in generating an electrically quiescent period referred to as an ISW[77] The exact mechanism of the ISW is not fully understood. This may represent undetected re-entry or a graded propagated response post defibrillation. This ISW is a variable period and its duration is dependent on the energy delivered[78-80].

The effect of successful and failed defibrillation was studied in isolated normal pig hearts using voltage sensitive dye and dual-camera video imaging by Chattipakorn et al.[76]. Fluorescent signals were derived from the anterior and posterior myocardial walls. A post-shock interval period with no recordable electrical potential differences was noted and termed the **iso-electric window**. The activation of the first post-shock cycle after a failed attempt started 78 ± 32 ms after the shock as determined by optical mapping studies[76].

We postulated that a biphasic shock delivered within this ISW would prevent re-initiation of VF, effecting return to normal sinus rhythm with an overall lower DFT. The preshock that was delivered in the test waveform in this study would have been responsible for brief ISW prior to delivery of the primary biphasic shock. Although the ISW was not measured in this study, the ISIs investigated (16, 31, and 47 ms) were arbitrarily assigned but remained within the minimum measured ISWs determined from prior data[80].

Improved defibrillation efficacy facilitated by delivery of a multiphasic waveform, may be related to intracellular calcium release[81;82].

Supposedly, the preshock then induces a homogenous myocardial cellular charge thus reducing overall defibrillation energy requirements for complete defibrillation by the definitive biphasic waveform.

The alternate hypothesis relates to the **upper limit of vulnerability theory** postulated by Chen et al.[11]**.** This suggests that failed defibrillation energy actually serves to reinitiate VF after negating myocardial fibrillation.

By deduction therefore, sub-threshold shocks are in essence successful in terminating VF, but also have the potential to be pro-arrhythmic. These sub-threshold shocks showed re-initiation of VF after a shorter ISW in the above study.

In this study, the definitive shock was delivered at a critical period after a sub-threshold monophasic discharge. The net effect presumably would have been a reduction in DFTs. Results of this experiment however, show equivalence to the control of a standard biphasic shock and even a trend to DFT increase with increasing ISIs beyond the nominal 16 ms.

Despite these factors, the prototype serial capacitor concept proved feasible, allowing software manipulation of the waveform with relative ease. This software patch (elatermP) was based on a commercially available system in the Alto2 platform (Ela Medical, Sorin Group, France). It is therefore conceivable that additional programmability with multi-sequence defibrillation waveforms for future ICD generations is an option and may afford a therapeutic advantage.

Previous studies have demonstrated the advantage of a “tuned waveform” with a “matched time membrane constant” of myocardial cellular membrane to the defibrillation system thus optimising defibrillation[83].

Standard ICD technology offers waveform programmability to invert polarity of the biphasic truncated exponential decay pattern as well as to alter the pulse wave duration in certain devices. These measures show an advantage in that they may improve DFTs where thresholds are high and no safety margin can be maintained with standard configurations. The secondary advantage is an optimally delivered waveform with matched system and membrane time constants, minimizing local cellular injury and possibly reducing the risk of progression to heart failure post shock delivery[84].

Limitations

A limitation of this study is that the ISI was not actually measured but assumed based on prior studies and therefore the ISIs were arbitrarily chosen for these test permutations. The preshock was standardised but was varied in a 1:2 ratio with the second biphasic capacitor discharge. This, therefore, would have more likely resulted in variability of the ISW for each ISI that was tested.

There is also evidence that triphasic and additional waveforms improve DFTs[85;86]. It is therefore arguable whether the monophasic preshock merely constituted a triphasic waveform rather than a true manipulation of the ISW.

Conclusion

This study validated the use of a serial, single capacitance prototype defibrillator in producing a preshock followed by a definitive biphasic waveform delivered in sequence. The mean defibrillation energy, however, was equivalent between this test waveform and a control consisting of a standard biphasic waveform. The use of larger ISIs between the monophasic preshock and definitive biphasic shock showed a trend to increased DFTs.

Acknowledgements

The concept of a preshock followed by a biphasic shock was conceived by Dr Paul Roberts, my mentor on this project. The Prototype device and software patch was created by Daniel Kroiss and Marcel Lumisan, of R&D, Ela Medical, Sorin Group, France.

I was responsible for designing the methodology and conducting the experiments. I collated and processed all data, and delivered presentations at academic symposia.

The project was supervised by Dr John Morgan and Dr Paul Roberts, my mentors at Southampton General Hospital.

Disclosure

Funding for this project as well as my research fellow's salary was made possible through an unrestricted grant from Ela Medical, Sorin Group,UK.

4.2 An Assessment of the Influence of Polarity of a Monophasic Preshock on Defibrillation Efficacy.

Introduction

Recent data has shown evidence that delivery of a biphasic shock with the RV electrode designated anodal, results in enhanced defibrillation efficacy[45]. This has resulted in a change from the convention of programming the distal RV electrode as cathodal to anodal for a biphasic shock waveform.

In this pilot experiment, I evaluated the optimal polarity of a monophasic preshock in relation to a standard definitive biphasic waveform. In addition, the programmability and efficiency of a prototype serial capacitance device was evaluated as a secondary outcome measure.

Method

Animal Selection and Preparation

Five female Landrace pigs weighing 48.4 ± 9.1 kg were anaesthetised and prepared in the manner previously described in Section 2.

A cut down to the left internal jugular vein was performed and a defibrillation electrode (Medtronic 6931, MN, USA: 2.3 mm 7F, 62 mm RV electrode coil length, surface area = 513 cm^2) was placed under fluoroscopic guidance in the right ventricular apex and an emulator Can was implanted as described in the preceding chapter .

Defibrillation Protocol

The ventricular fibrillation induction and defibrillation binary up/down protocol was maintained as in the preceding experiment in Chapter 4.1 (page 51) for uniformity. The defibrillation protocol entailed **configuration 1,** which was delivery of a monophasic preshock with an active anodal Can electrode for the preshock and 1st phase of the biphasic shock) separated by a 16 ms ISI (defined as optimal for this device in Chapter 4.1). Thereafter, the polarity was reversed to the RV coil as the anode for the 1st phase as well as for the preshock (Table 4.2.1). This waveform inversion was applied for the defined ISI. Testing was randomised initially between each configuration.

Only the RV coil and active Can electrodes were included in the circuit (the SVC coil was excluded) by connecting each externally to the anodal and cathodal poles, respectively, of the prototype defibrillator referred to in 4.1 (Ela Medical, Sorin Group, France).

A custom software patch entitled **elatermP** allowed a sequential dissipation of a selected energy into a preshock and definitive biphasic shock in a 1:2 ratio from the serially arranged capacitors (Figure 4.2.1) as was described previously.

Statistical Analysis

The mean DFT, shock impedance, and VF duration was calculated and represented as mean ± standard deviation. A 2-tailed paired t-test was used to determine statistical significance between configurations (normal vs. inverted preshock polarity. A significant result was regarded as $p < 0.05$.

	Configuration 1		Configuration 2		
	Preshock (polarity)	Biphasic shock	Preshock	Biphasic shock	Inter-shock interval
Polarity settings	C(+)→R(-)	C(+)→R(-)	R(+)→C(-)	C(+)→R(-)	16ms

Table 4.2.1

Polarity configurations and the ISIs achieved through the prototype device.

(C= active Can electrode, R = right ventricular coil electrode).

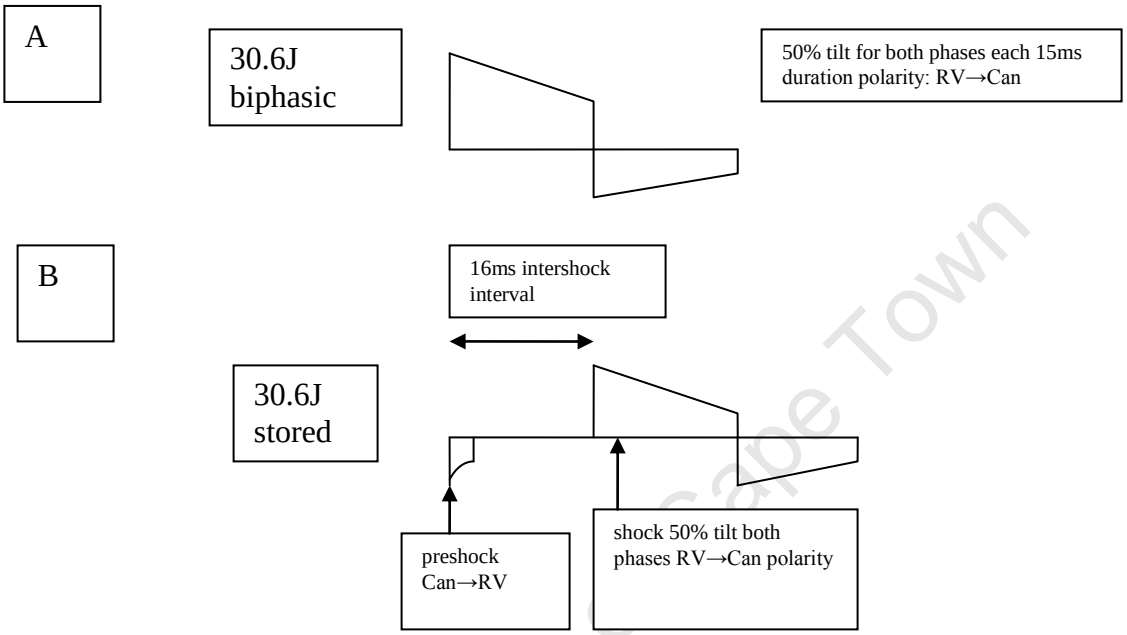

Figure 4.2.1

Control and configuration 2 waveforms:

A. The control shock waveform consisting of a single biphasic shock delivered at normal polarity with phase reversal after 50% decay from the leading edge.

B. The configuration 2 waveform consisting of a pre-shock (reversed polarity) preceding the definitive biphasic shock in a 1:2 energy dissipation of the stored energy.

Results

The distribution of DFTs and median values are shown in Figure 4.2.2.

There was no significant difference in the mean DFT values ($p = 0.1$) between configuration1 (DFT1) and configuration 2 (DFT2).

There was also no difference between the mean shock impedances and VF durations between each configuration ($p = 0.3$ and $p = 0.1$, respectively).

The results of each individual experiment are depicted in Table 4.2.2.

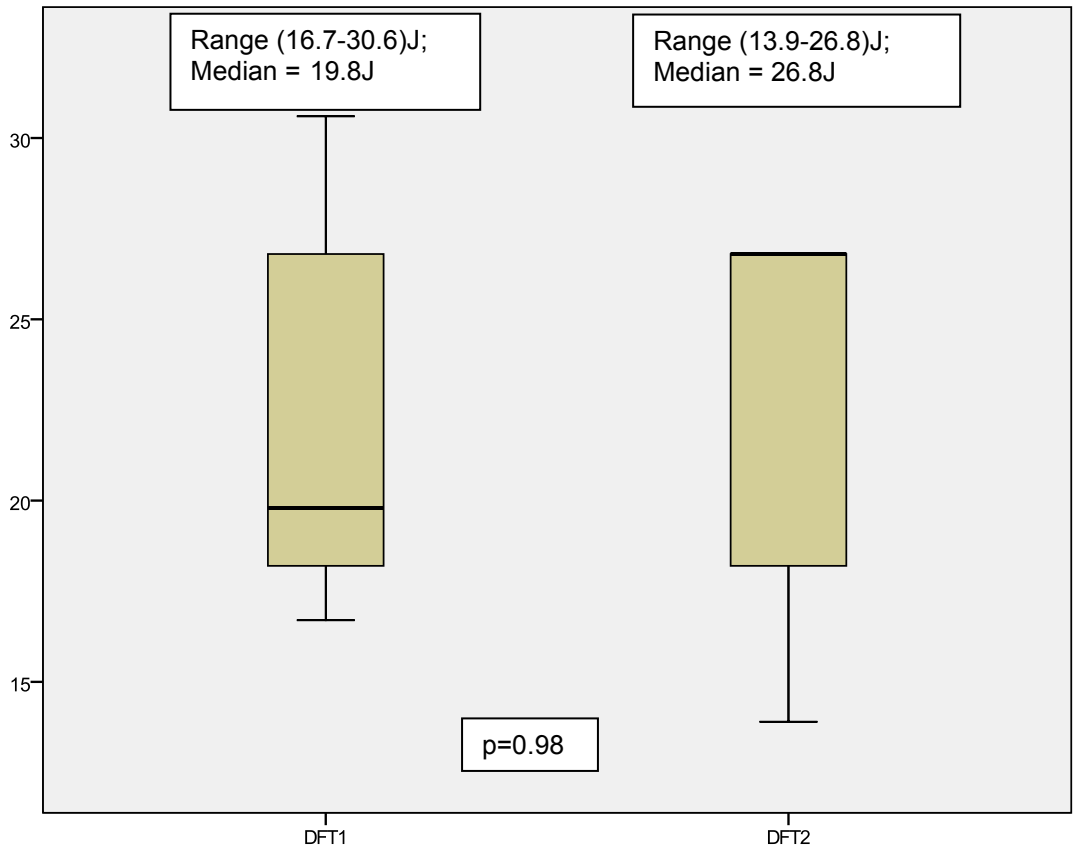

Figure 4.2.2

A plot of the range (50%) of DFTs in configurations 1 (DFT1) and 2 (DFT2). The dark line represents the median while the whiskers show the highest and lowest recorded values.

		DFT 1					DFT2				
Shock polarity				Can>RV	Can>RV				RV>Can	Can>RV		
experiment #		wt (kg)	stored energy(J)	pre	primary	impedance	VF time (s)	stored energy(J)	pre	primary	impedance	VF time (s)
	1	40.0	16.7	4.9	9.8	40.2	18.0	26.8	7.8	15.9	39.2	26.8
	2	37.0	18.2	5.4	10.8	53.3	18.0	18.2	5.4	10.8	53.3	20.0
	3	55.0	30.6	9.0	17.9	56.9	11.1	26.8	7.8	15.9	53.8	17.7
	4	55.0	26.8	7.8	15.9	52.3	11.1	26.8	7.8	15.9	53.8	17.8
	5	55.0	19.8	5.8	11.8	52.1	15.1	13.9	4.1	8.1	47.6	12.4
Mean		48.4	22.4	6.6	13.2	51.0	14.7	22.5	6.6	13.3	49.5	18.9
std dev		9.1	6.0	1.7	3.5	6.3	3.5	6.1	1.7	3.7	6.3	5.2

Table 4.2.2

Summary of defibrillation results by group and weight.

Discussion

In the preceding chapter, I demonstrated the feasibility of producing a monophasic preshock followed by a biphasic waveform. This sequential waveform was produced by a prototype serial capacitance defibrillator. The outcome, however, was equivalent to that of a standard 50% tilt biphasic waveform. An optimal ISI of 16 ms was established from this preliminary work.

Recent evidence suggests that delivery of the first phase of the shock waveform should have the RV electrode assigned as anodal resulting in an implosion of colliding wavefronts at the RV electrode rather than an expansion which may be pro-arrhythmic[87].

In this study, I investigated the ability to deliver a monophasic preshock through a prototype serial capacitance device with alternate polarity settings and the effect of this polarity setting on defibrillation efficacy. In this pilot study, no statistical difference was demonstrable between preshock deliveries with a distal cathodal RV electrode vs. anodal polarity.

The exception being that of experiment 5 which revealed a 5.9J reduction in DFT with configuration 2 but this may also have been influenced by a reduced VF duration and shock impedance rather than purely the result of a polarity change. The overall effect of polarity inversion of the monophasic preshock did not significantly alter defibrillation efficacy.

The theoretical benefits of an RV anode are related to the virtual electrode effect of inducing a positive charge on neighbouring myocytes. This then results in imploding wavefronts rather than expanding electrical energy during the delivery of a shock[45]. Despite this benefit, this polarity may potentially cause greater acute cellular membrane injury. This effect is called electroporation and has been previously defined in this work. It is however a transient phenomenon as the second phase of a biphasic shock results in "repair" of the cellular damage. However, an anodal monophasic preshock may be responsible for greater cellular membrane injury.

Limitations

The obvious limitation in this experiment is the small sample size. However, this was a pilot experiment to determine whether the polarity of the preshock has any obvious influence on DFT. The random nature of the DFTs obtained in these five experiments also reflects the probabilistic nature of defibrillation, regardless of the sample size of this experiment.

Conclusion

Delivery of a monophasic preshock, delivered with distal anodal polarity as opposed to a RV cathodal electrode, did not consistently improve defibrillation efficacy. Preshock polarity reversal offers no further benefit to defibrillation outcome.

Acknowledgements

The concept of a preshock followed by a biphasic shock was conceived by Dr Paul Roberts, my mentor on this project. The Prototype device and software patch was created by Daniel Kroiss of the Research and Development department at Ela Medical, Sorin Group, France and Marcel Lumisan, Head of R&D, Ela Medical, Sorin Group, France.

I conceived the idea to vary the polarity of the preshock after establishing an optimal ISI. I was responsible for the methodology and execution of the experiments.

The project was supervised by Dr John Morgan and Dr Paul Roberts, my mentors at Southampton General Hospital.

Disclosure

Funding for this project as well as my research fellow's salary was made possible through an unrestricted grant from Ela Medical, Sorin Group, UK.

5. An Investigation of Multi-Site Right Ventricular Endocardial Electrode Placement on Measures of Defibrillation Outcome.

Introduction

In a clinical setting, elevated defibrillation thresholds may be influenced by factors in the substrate or in the defibrillator system. These may be improved by repositioning leads, upgrading to higher energy devices, or altering the shock waveform or defibrillation vector. The use of additional defibrillator electrodes implanted at extracardiac locations, e.g. subclavian vein, SVC, pulmonary artery, coronary venous system, have also been shown to enhance defibrillation, presumably by increasing the electrode surface area exposed to defibrillation as is explained by the critical mass hypothesis[10].

My colleague, Dr John Paisey, examined the use of defibrillation incorporating electrodes in the pulmonary artery and middle cardiac vein (unpublished data from his thesis entitled “Defibrillation, the Coronary Venous System and the Passive Electrode Affect”, Southampton University School of Medicine, July 2004). It has not been shown whether just increasing the number of endocardial electrodes at a conventional site (i.e. the right ventricle) will be advantageous.

Methods

Eight female Landrace pigs weighing 21.4 ± 1.2 kg were prepared in the manner previously described (section 4.1, page 46).

Placement of Defibrillation Electrodes

Dissection was then performed with a cut down to an internal jugular vein using the previously mentioned technique (page 46) with the modification described below:

Using a double ligature technique with ties proximally and a loose tie distally, an incision was made into the ventral surface of the vein allowing insertion of two identical, dual coil 2.3 mm (7 F, 62 mm RV electrode coil length, surface area = 513 cm^2) active fixation defibrillator leads (Medtronic 6949, MN, USA) via the same vein. These were positioned at the RVA and RV outflow tract (RVOT) using fluoroscopic navigation (Figure 5.1). Placement sites were randomised for defibrillation testing. Fluoroscopy was used after each shock to confirm lead positions.

Both leads were coupled using a Y-type DF-1 adapter (model 6835, Guidant, Inc., St. Paul, MN, USA) during the multi-electrode defibrillation strategy described below. The control configuration consisted of a single lead deployed at the RVA plugged directly into the DF-1 port of the ICD.

A standard ICD (model 7274, Medtronic, Inc., MN, USA), with plugged atrial and SVC ports was implanted into a subcutaneous left precordial pocket to resemble a clinical implantation.

Defibrillation Protocol Design:

The configuration of ICD (+) > single RVA lead (-) served as the **control** defibrillation vector. Ventricular fibrillation (VF) was induced by administering 5 seconds of 50 Hz burst pacing or with a 1J T wave shock. The DFT was determined using a binary method with a three-stage reversal (Figure 5.2).

The shock waveform was non programmable with a 50% / 50% tilt phase duration 2.8 ms / 2.7 ms in the ICD and therefore standardised for this experiment.

Rescue shocks were delivered using maximal discharge from the ICD or via a transthoracic biphasic shock from an external defibrillator.

In the test configuration, a second identical active fixation defibrillator lead (model 6949, Medtronic, Inc., MN, USA) was then employed in the defibrillation circuit. Both defibrillator leads were coupled using a Y-adapter as mentioned above. Thus both RV electrodes on the leads had the same polarity (-). The second electrode position was randomised between either of the RVA or the RVOT. The defibrillation vectors employed were ICD (+) > RVA+RVA (-) and ICD (+) > RVA+RVOT (-) respectively (Figure 5.1).

Defibrillation tests were repeated for both these test configurations. The distal electrodes were cathodal in all shock configurations used. The order of testing was randomised. A 31J (maximal device output) shock was regarded as a failed defibrillation attempt. The average of the two lowest energies used to achieve defibrillation was regarded as the DFT.

The lead positions were rechecked after delivery of each shock with fluoroscopy to identify possible dislodgement before the next VF induction and defibrillation.

Statistical Analysis

A Kolmogorov-Smirnov test revealed non-parametric data distribution.

The data for each individual lead configuration was compared using a Wilcoxon signed-ranks test. A Spearman correlation was also performed on the measures of defibrillation outcome (ie. defibrillation energy, impedances, and VF duration) for these groups.

A

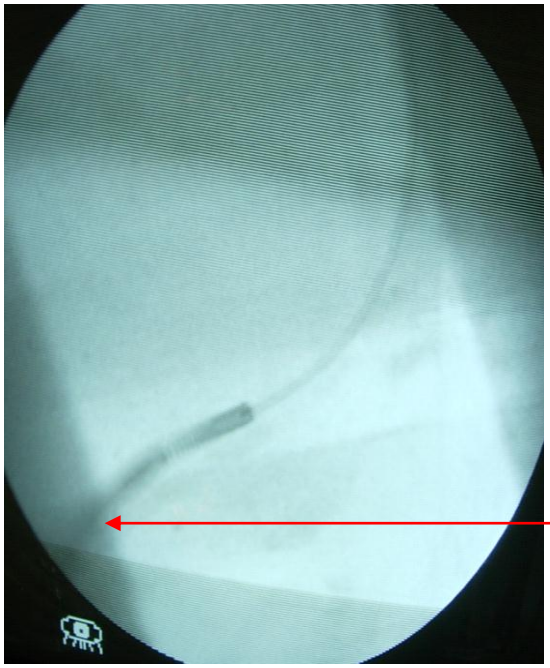

Single defibrillator lead at the RV apex

B

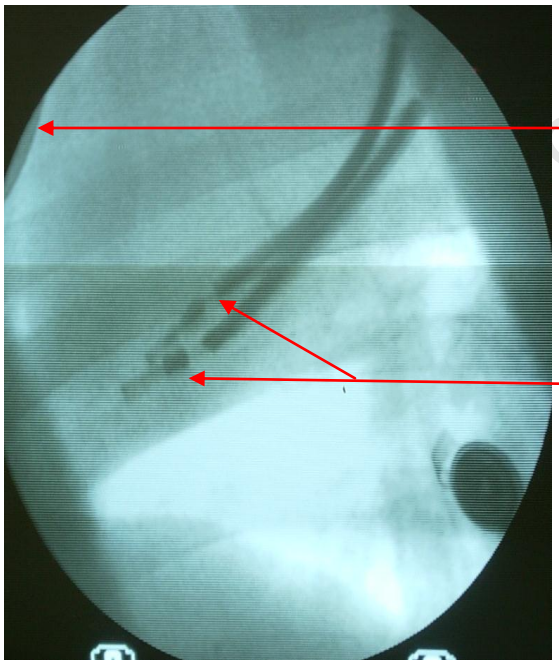

ICD placed in a left precordial subcutaneous pocket

Two active fixation 7F defibrillator leads placed at the RV apex

Figure 5.1

Refer to legend on page 84.

C

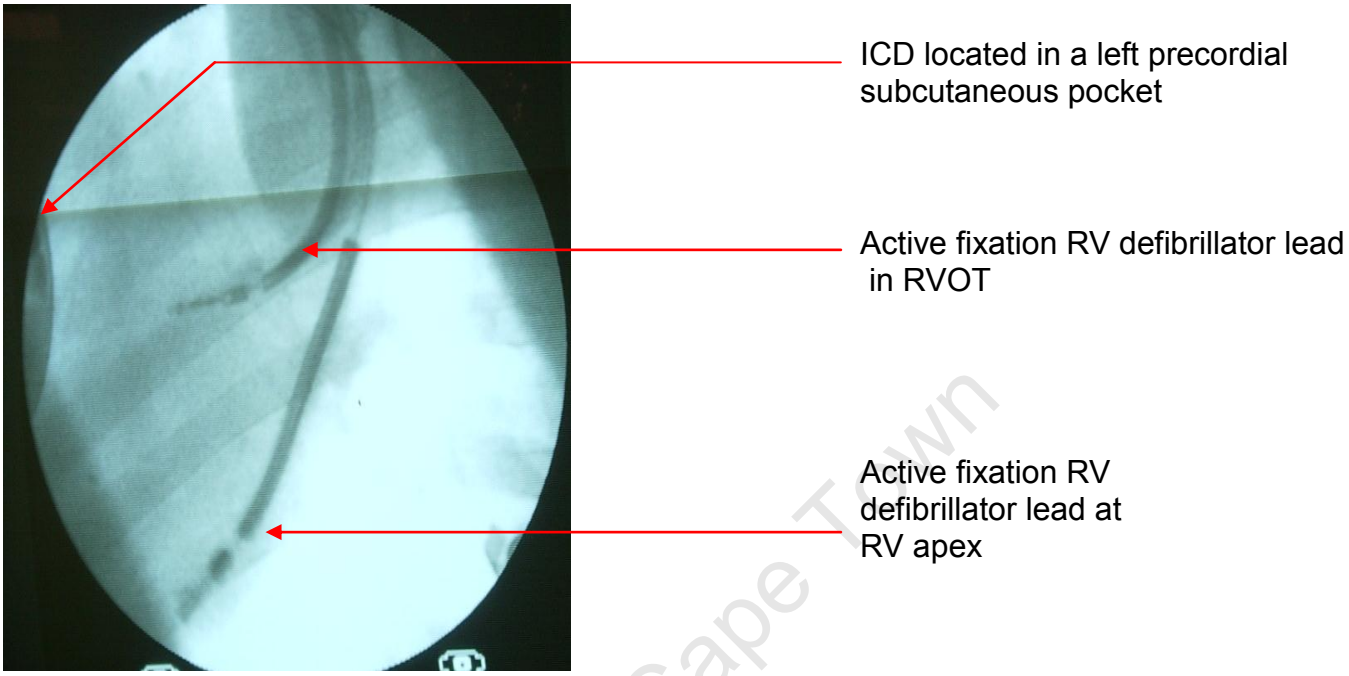

Figure 5.1

Fluoroscopic images of RV electrode positions:

A. Single RV electrode at RV apex

B. Two RV electrodes coupled at the RV apical location both cathodal

C. RV electrodes separated to RVOT and RV apex but both coupled together as a cathode using a DF-1 adapter at the ICD port.

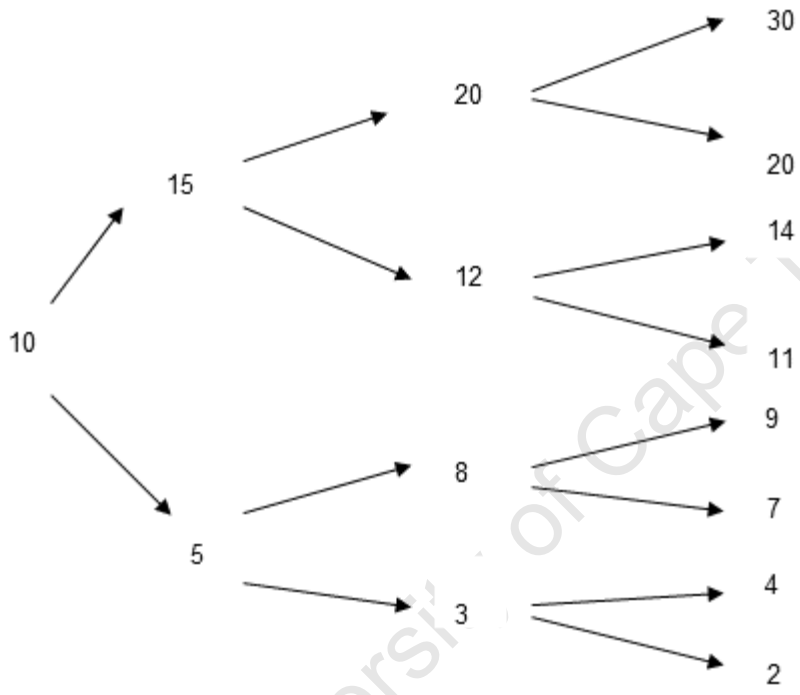

Figure 5.2

The Binary DFT search protocol.

Results:

The study was conducted in 8 anaesthetised female pigs (21.5 ± 1.2 kg). Lead positioning at both the RVA and RVOT were guided by R wave amplitude and pacing thresholds.

Mean R waves recorded at the RVA were 8.3 ± 2.3 mV in the control experiment.

For the second electrode the mean R waves measured were 7.9 ± 0.05 mV at the RVA and 8.3 ± 5.7 mV at the RVOT (p = NS). Pacing thresholds for endocardial RV sites were regarded as acceptable if they ranged between 0.5–2.0V at 0.5 ms as these served as a surrogate marker for electrode-myocardial apposition.

The results from the use of a second electrode in the RV at either location (RVA+RVA / RVA+RVOT) were combined. Both these combinations are collectively referred to here as the multi-electrode strategy (MES). The lowest defibrillation energy for either of the electrode combinations was recorded as the DFT for the MES.

The accompanying impedances were also recorded for this group.

A maximum of 18 shocks were delivered in each animal studied taking into account rescue shock deliveries as well. Mean VF durations were 9.7 ± 3.4 sec and 9.9 ± 3.0 sec (p = NS) for the control and MES.

The MES (RVA+RVA / RVA+RVOT), achieved a reduction in shock impedance (mean reduction 13%, range 5–28%; p < 0.01) against control (single RVA electrode) when taking into account the lowest DFT yielded at either location (Figures 5.3 and 5.4).

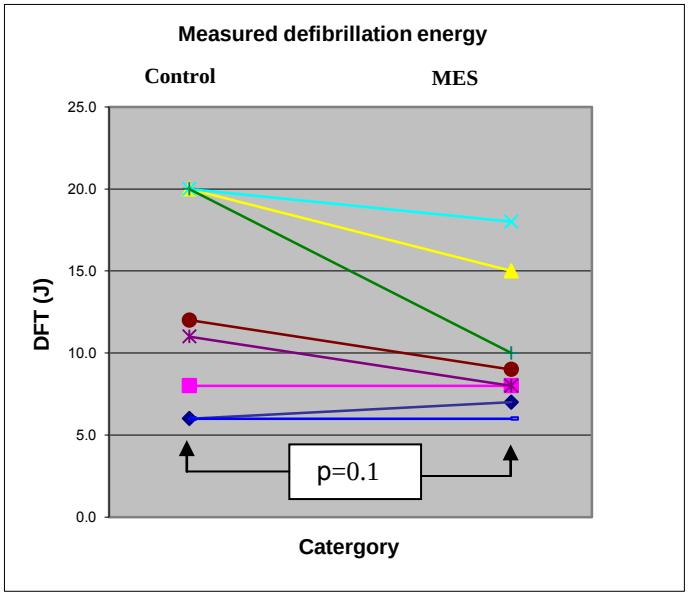

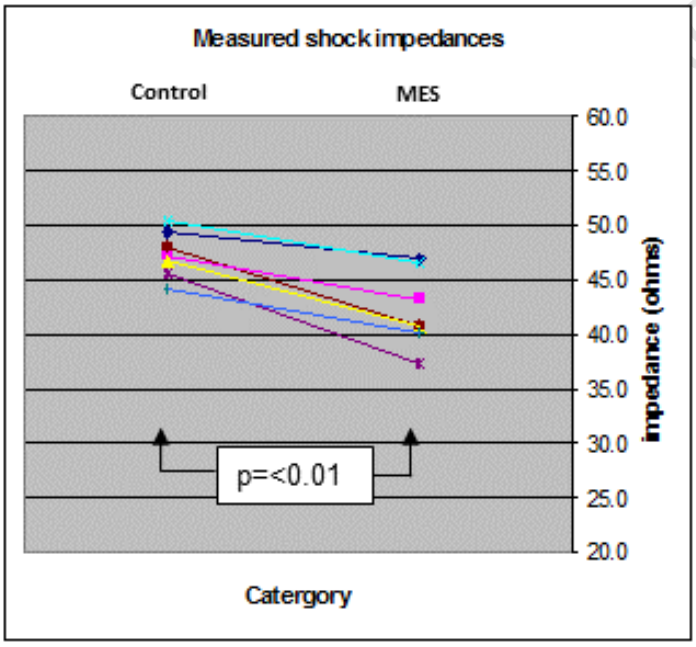

Figure 5.3

Measured mean impedances and DFTs in control vs. MES strategies.

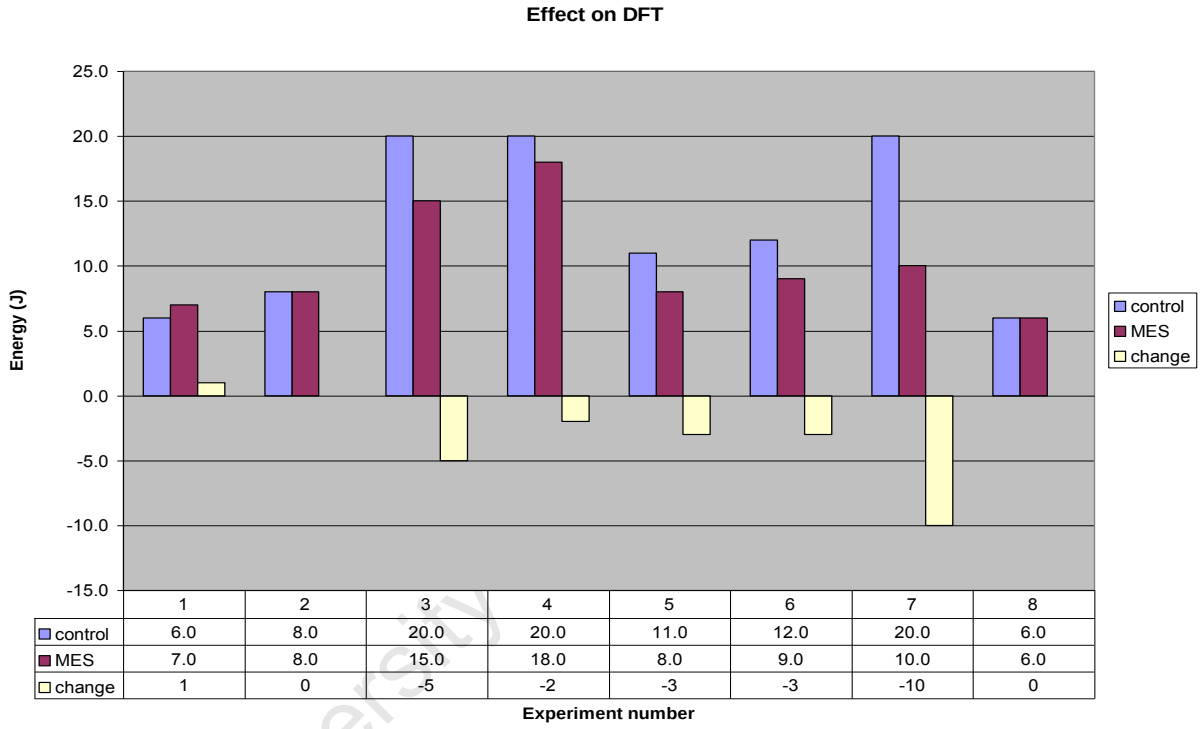

	1	2	3	4	5	6	7	8
control	6.0	8.0	20.0	20.0	11.0	12.0	20.0	6.0
MES	7.0	8.0	15.0	18.0	8.0	9.0	10.0	6.0
change	1	0	-5	-2	-3	-3	-10	0

Figure 5.4

Effect on DFTs of an additional RV electrode in RVA or RVOT locations (MES). The change in DFT energy recorded with the MES is also represented in the yellow bars.

In terms of defibrillation energy requirements, there was an average 25% (range 3–50%; p = 0.1) reduction in DFTs obtained in 5/8 (62%) cases (second electrode locations: RVOT n = 3; RVA n = 2) and equivalent thresholds in 2/8 (25%) subjects (Table 5.1).

There was an increase in DFT energy in one case in the MES and this increase measured 3 J for the RVA+RVA configuration and 1 J for the RVOT+RVA combination. There were also no significant differences in DFTS or impedances between each of the two electrode configurations (RVA+RVA vs RVOT+RVA) ($p > 0.05$) but a positive linear correlation was demonstrated between these sites for both parameters (Figure 5.5).

When comparing the control group against the combined test sets (i.e. the MES), a significant correlation between DFTs and impedances was noted ($p< 0.01$ and $p < 0.01$, respectively) (Table 5.2).

Correlations of DFTs in the control and MES groups against animal weight were also evaluated as an increase in body mass index has previously been shown to reduce defibrillation efficacy[88]. A smaller increase in DFTs was observed in the MES with corresponding increasing weight in the pigs as compared to the control (i.e. a single RV electrode) (Figure 5.6). Therefore, the use of 2 electrodes seems to result in a reduced sensitivity of the defibrillation system to variations in weight and its influence on DFTs.

Electrode configurations

Experiment	Control	RVA+RVA	RVOT+RVA
DFTs (J)			
1	7.0	9.0	7.0
2	8.0	9.0	8.0
3	20.0	20.0	15.0
4	20.0	18.0	30.0
5	11.0	8.0	14.0
6	12.0	16.0	9.0
7	20.0	20.0	10.0
8	7.0	10.0	7.0
Impedances (Ω)			
1	44.8	40.0	35.6
2	49.5	45.0	47.0
3	47.3	43.3	43.3
4	46.8	40.8	33.5
5	50.3	46.5	47.5
6	45.5	36.4	37.3
7	48.0	39.0	40.8
8	44.3	39.0	40.2

Table 5.1

Combined data from individual electrode configurations.

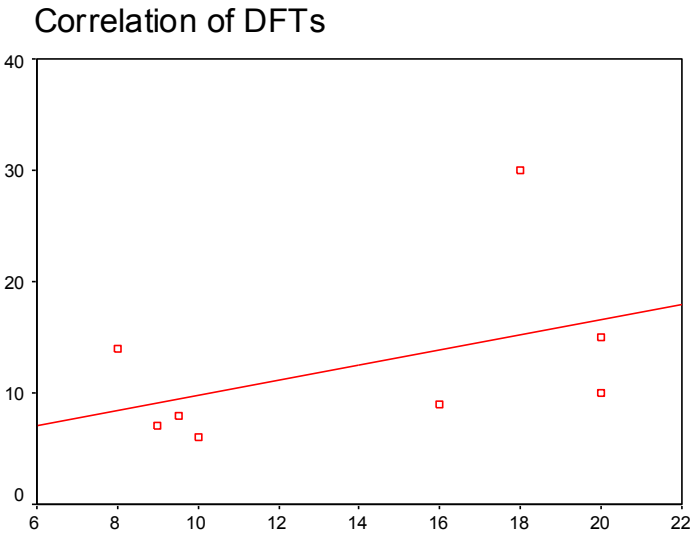

r_s = +0.455, N = 8, p = 0.257

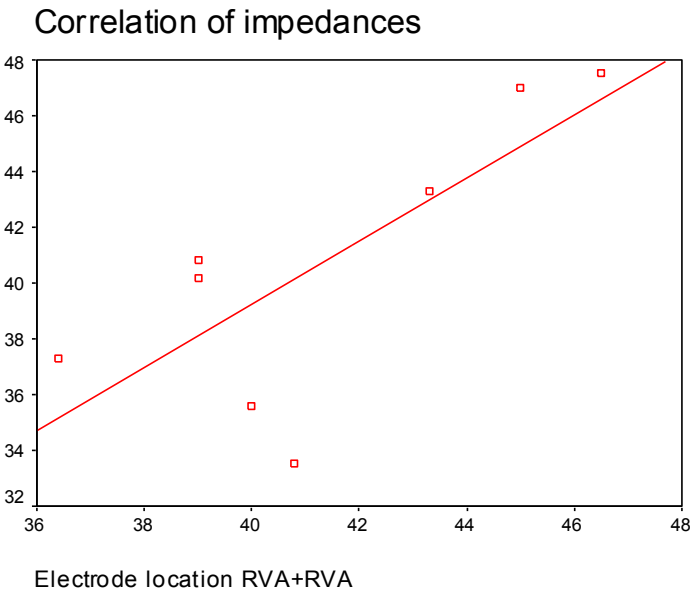

r_s = +0.611, N = 8, p = 0.108

Figure 5.5

Correlation of DFTs and impedances between RVA and RVOT locations (MES)

	Control		Multi-electrode strategy (MES)	
Experiment	**DFT (J)**	**Impedances (Ω)**	**DFT (J)**	**Impedances (Ω)**
1	7.0	44.8	7.0	35.60
2	8.0	49.5	8.0	47.00
3	20.0	47.3	15.0	43.30
4	20.0	46.8	18.0	40.80
5	11.0	50.3	8.0	46.50
6	12.0	45.5	9.0	37.30
7	20.0	48.0	10.0	40.80
8	7.0	44.3	7.0	40.20

Table 5.2

Measurements constituting the MES compared to control data.

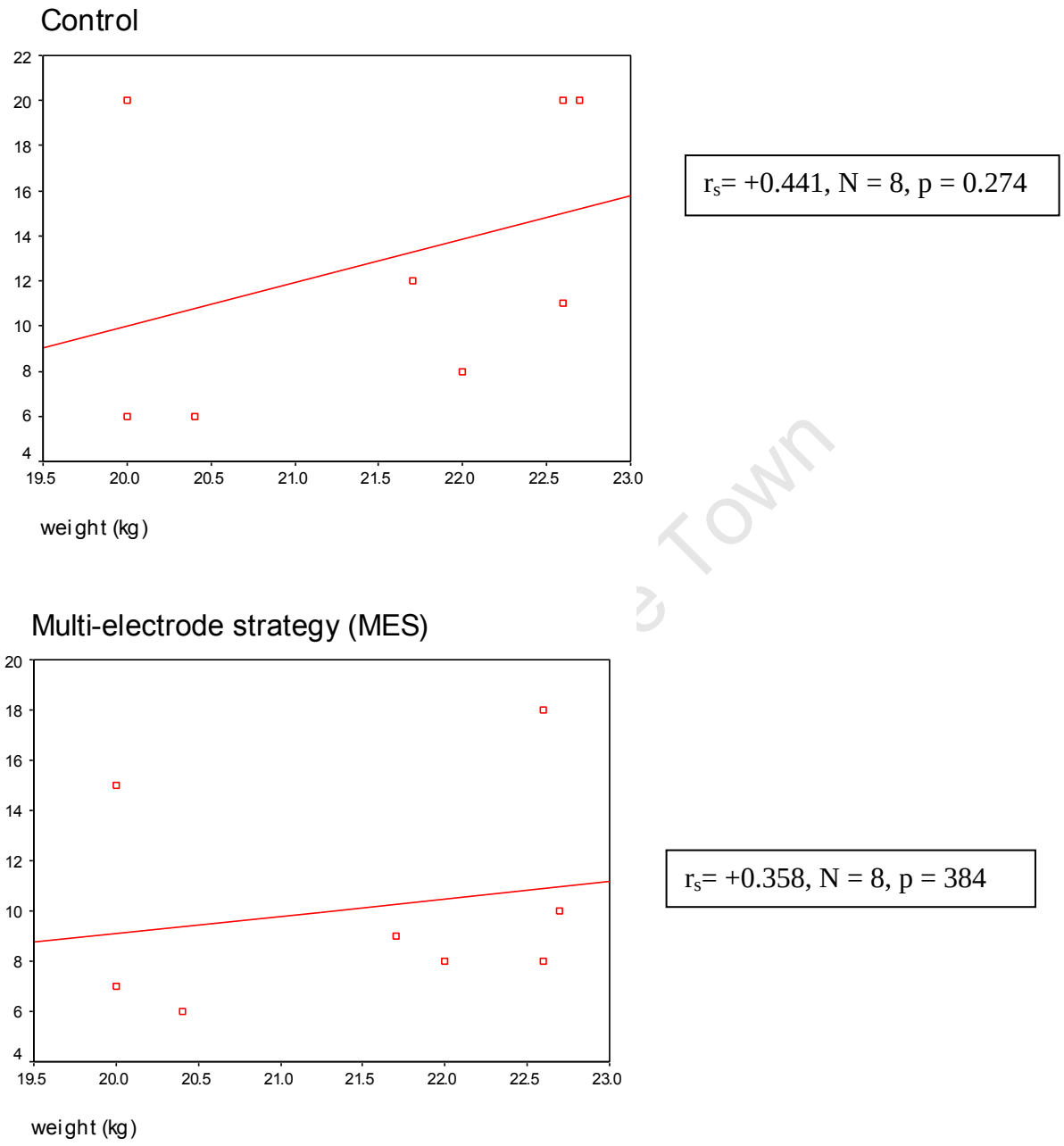

Figure 5.6

DFTs correlated against weight variation for control and MES in each pig.

Discussion

The implantation of two defibrillation electrodes within the RV at either an RVA or RVOT location resulted in reduction in shock impedances but this phenomenon was not consistently accompanied by a decrease in overall DFTs.

Even though the surface of the cathode was doubled, the change in impedance was statistically significant but not proportionate. This means that the coil surface is not the only contributor to improved current flow and defibrillation energy delivery to myocardium. Singer and colleagues, using a combination of endocardial electrodes at the RVOT and RVA and a cutaneous apical patch, also showed a non-significant trend to DFT reduction in dogs[89]. They postulated that the wider endocardial coil separation enhances voltage gradient and current dissipation to the fibrillating myocardium.

The critical mass hypothesis postulated by Zipes et al. suggests that successful defibrillation is dependent on exposure of a specific amount of fibrillating myocardium to shock delivery[90]. The data arising from this study is supported by this concept but it further postulates that changes in defibrillation pathways (i.e., vectoral alteration posed by multi-site electrode defibrillation within the RV) also has an effect on lowering DFTs.

It therefore seems intuitive that by just increasing the myocardial exposure to twice the number of electrodes, a similar benefit may be obtained. This was not the observation in terms of DFTs in this study.

However, a significant decrease in defibrillation impedances during MES shocks was noted. This reflects optimal endocardial defibrillator lead design technology where a maximal electrode surface area is obtained from the coiled nature of the defibrillation electrode around the body of the lead maximising energy delivery to the myocardium.

Defibrillation efficacy has not been shown to be impaired by the placement of a defibrillator lead in the RVOT in a clinical context[91].

In this study, defibrillation efficacy as well as sensing and pacing parameters from the RVA and RVOT were equivalent.

Lead positioning in the RVOT posed minimal technical challenge. This however may have been facilitated by the 7F lead design of the defibrillator leads used (Medtronic Inc. 6949 dual coil defibrillation leads, Medtronic Inc. MN, USA).

The 2.3 mm diameter defibrillator leads used here, theoretically provide less obstruction to blood flow and disruption to the tricuspid valve function, making this strategy a reasonable consideration in a clinical setting.

Currently, the 6949 model lead used has been withdrawn due to an unacceptably high fracture rate.[92] This has been attributed to long-term stress and fatigue on the pace/sense wire within this multi-lumen lead.

There has also been an association of a greater incidence of lead fractures in patients with higher cardiac ejection fractions. This may be explained by

increased torque and stress at the lead tip-myocardial interface with more vigorous cardiac contraction[93]. Alternative 7F defibrillator lead technology is available from other manufacturers.

An active Can electrode to RV coil vector was used with the SVC excluded from the circuit. It proved difficult to maintain an optimal intra-thoracic placement of the SVC coil in the small thorax of the pig hence this electrode was omitted. Furthermore, the use of a dual coil lead instead of a single RV coil has not been shown to offer a dramatic advantage in terms of defibrillation efficacy[26]. Nonetheless, it has become common clinical practice to implant dual coil leads. There may also be an advantage when attempting an extraction of a single coil lead, as there would potentially be fewer adhesions around an SVC electrode.

The distal ventricular electrodes were cathodal for all configurations tested, as this study was conducted prior to change in current conventional shock programming. This polarity has recently been shown to be less efficient prompting motivation for the distal ventricular coil to be designated as anodal during the first phase of a biphasic shock[45]. A cathodal ventricular electrode results in marginal activation, generation of further VF wavefronts and greater destructive electroporation of surrounding myocytes. By doubling the number of cathodal ventricular electrodes in this study, this deleterious effect potentially could have been compounded. Polarity, however, is a programmable option in ICDs and this can be easily adjusted to optimize defibrillation efficacy in the clinical setting. For the purposes of this study and data interpretation, the shock waveform was kept constant for both the control and test configurations.

Limitations

The limited sample size in this pilot study may have resulted in insufficient power to show statistical differences in defibrillation thresholds in the MES and control groups, although a trend to a reduction in DFTs was noted. The placement of the RVOT electrode was also limited by access to the high RV septum in the pig. The porcine heart occupies a more central position in the chest and a straighter longitudinal cardiac axis than is seen in the human heart[94]. This impeded accurate fluoroscopic placement of a second lead onto the RVOT septum. In addition, the circular structure of the pig's chest wall varies from humans in that the antero-posterior diameter of the chest wall in man is smaller compared to the transverse diameter. The ICD precordial position is therefore an inaccurate comparison to the pectoral position in patients.

Insertion of a second defibrillator lead into the RV is a feasible option given the ease that this can be accomplished surgically. Other interventions, such as insertion of subcutaneous arrays and a lead in the azygous vein, may pose a greater challenge[21;95].

Conclusion

The use of an MES comprising two RV defibrillator electrodes coupled together at RVA and RVOT locations resulted in equivalent DFTs overall. There was a consistent and significant reduction in shock impedances in the MES strategy. However, a trend to DFT reduction was noted in 88% of the MES cases. Thus, a double RV lead strategy may be a consideration in individual patients presenting with compromised DFTs in order to avoid other complex surgical interventions such as subcutaneous array placement.

Acknowledgements

The concept of combining endocardial RV electrodes was conceived by my colleague, Dr John Paisey. I devised the protocol and conducted all experiments.

The project was supervised by Dr John Morgan and Dr Paul Roberts, my mentors, at Southampton General Hospital.

Disclosure

My research fellow's salary was derived from an unrestricted grant provided by Ela Medical, Sorin Group, UK. Additional devices and leads were supplied by Medtronic, UK.

6. Transthoracic Defibrillation Studies

6.1 Comparison of Endocardial and Subcutaneous Defibrillation in a Porcine Model.

Introduction

Transthoracic defibrillation (TDF) is a useful strategy in a clinical setting as an adjunct to impaired defibrillation or where there is limited venous access[96]. Alternatively, it may be the primary option in children or in congenitally and surgically altered cardiac anatomy when intravenous leads are best kept to a minimum or avoided altogether[97]. Extra-cardiac defibrillation thresholds are, however, higher than in an endocardial system[98]. This has not been quantified and the influence of weight with TDF has not been previously documented. We compared defibrillation thresholds (DFTs) from endocardial (EDF) vs TDF in a porcine model in the context of variations in animal weight.

Methods

Animal Selection and Preparation

This experiment was conducted in 9 juvenile female Landrace pigs weighing 20.9 ± 0.7 kg.

The animals were pre-medicated and anaesthetised according to the method previously described in Section 2. A cut down to the left internal jugular vein was performed and a 2.3 mm (7F) ventricular defibrillation lead (model 6949, coil length 6.2 cm, surface area = 513 mm^2) was inserted. The electrode was transvenously positioned at the RVA under fluoroscopic guidance. Adequacy of the electrode position was assessed using pacing thresholds and R wave sensing parameters. An R wave electrogram amplitude of ≥ 5mV and a pacing threshold of < 1 V @ 0.5 ms were accepted.

A subcutaneous single finger array (SQA = Medtronic 6996, coil length = 25 cm, surface area = 500 mm^2) was positioned around the left chest wall directly posterior to the middle of the cardiac silhouette on fluoroscopy, relative to the major myocardial bulk.

The array was inserted using a tunnelling tool on which a split-able sheath was mounted. The tool was burrowed from the left precordial pocket fashioned to house an ICD, around the left chest wall to lie posterior to the cardiac silhouette and opposite the vertebral bodies on fluoroscopy. Once this position was

attained, the radio-opaque tunnelling tool was withdrawn and the SQA was advanced through the sheath.

The sheath was then withdrawn and split over the lead leaving the array in place. The final SQA position was confirmed on fluoroscopy before being connected to the ICD.

A standard dual chamber ICD with capped atrial and SVC ports (Medtronic Inc., Marquis DR 7274, surface area = 66 cm^2) was used in the experiment.

The ICD was implanted into a low precordial subcutaneous pocket overlying the cardiac apex (Figure 6.1.1A and 6.1.1B).

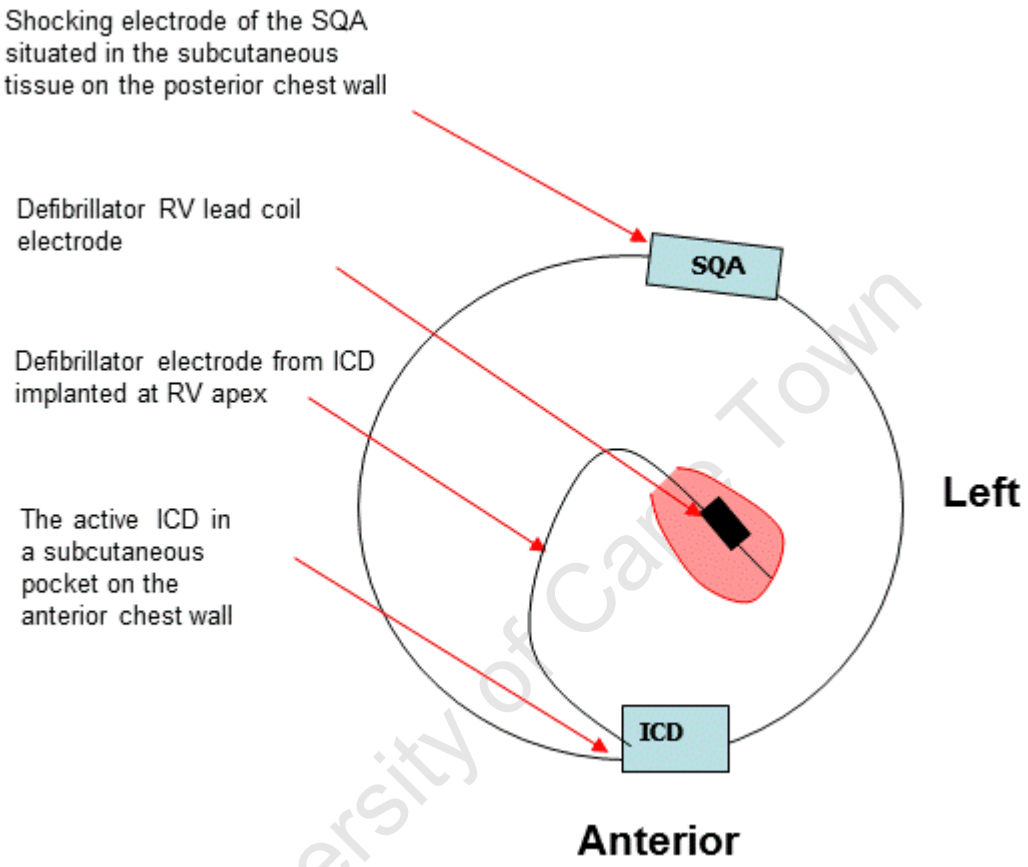

Figure 6.1.1A

A coronal view of ICD and SQA placement:

Showing the position of the ICD in a low precordial subcutaneous pocket with a single finger subcutaneous array placed subcutaneously around the left chest wall of the pig.

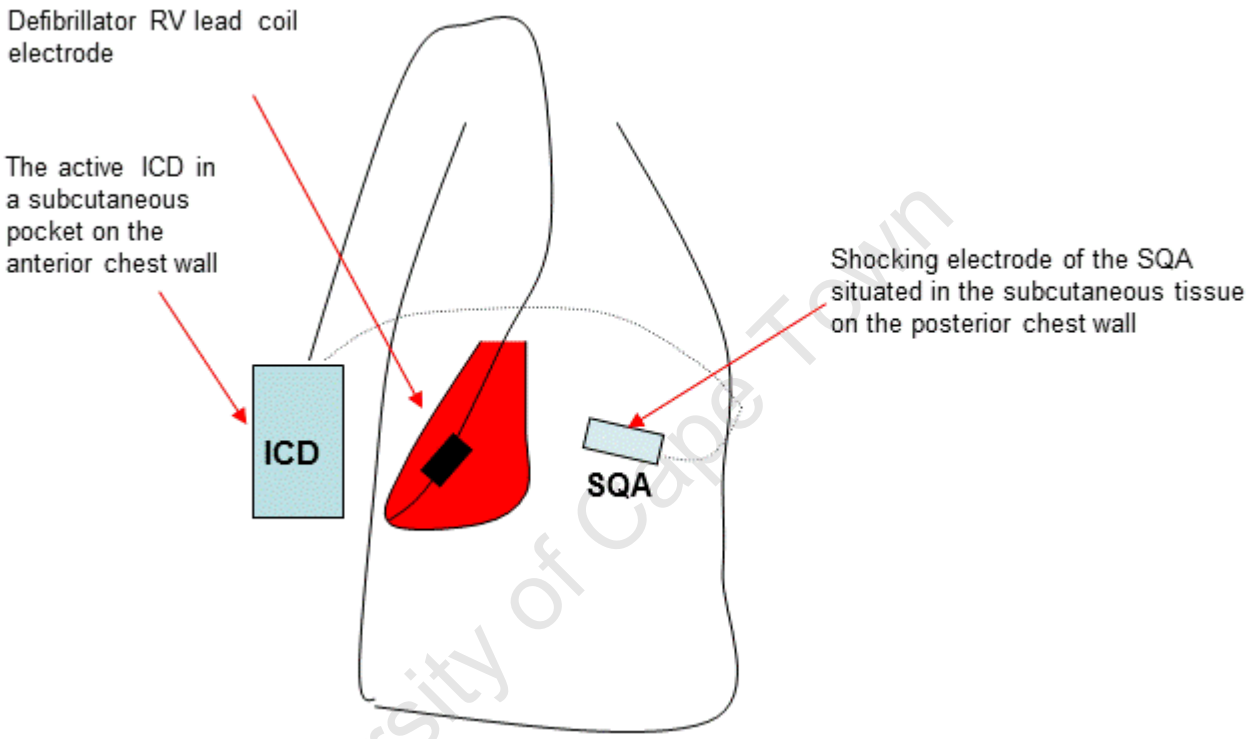

Figure 6.1.1B

A sagittal view of ICD and SQA placement:

Showing the location of the ICD and SQA in relation to the myocardial mass.

Defibrillation Protocol

Group 1 of the experiment entailed determining the EDF threshold. The distal RV coil was connected to the DF-1(-) port of the implanted ICD and the same 3-reversal binary up/down algorithm (Figure 6.1.2) was used to obtain a DFT in an ICD (+) > distal coil (-) shock configuration for both EDF and TDF.
For group 2, this distal RV defibrillator coil was disconnected; however, the pace/sense component of the endocardial defibrillator lead was left in place for VF induction and sensing functions through the ICD. Instead, the posteriorly located, distal SQA (cathode) was inserted into the DF-1(-) port. The defibrillation protocol above was repeated. A 30J shock was regarded as an impaired/high DFT since a 10J safety margin from the maximum output of the implanted device (30 J) could not be assured. The order of testing between the 2 groups was randomised.

VF induction was performed either by a 50Hz burst pacing for 5 seconds duration or with a 1J T wave shock delivered through the implanted ICD as previously described.

Rescue shocks were delivered for failed defibrillation as a 30J endocardial delivery from the device or alternatively a 200J biphasic external thoracic shock. A 3-minute interval between each induction and defibrillation was observed or until haemodynamic stability was regained.

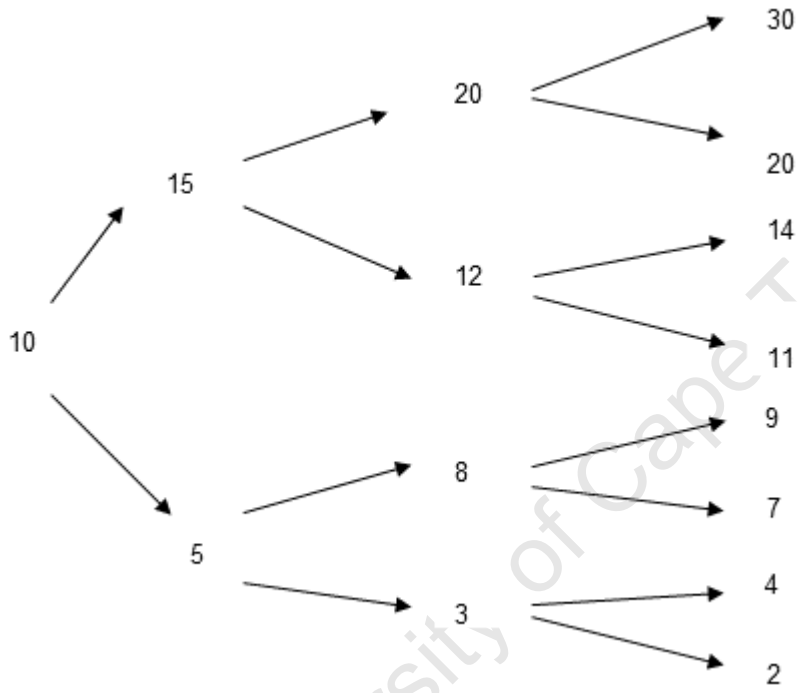

Figure 6.1.2

The Binary up/down defibrillation search.

This schematic depicts the protocol employed for defibrillation testing and is identical to that used in chapter 5 (figure 5.2 on page 85) .

Statistical Analysis

All data were collated into an Excel spreadsheet and then imported into SPSS statistical package for further analyses. The mean ± standard deviation and range were used to represent the defibrillation parameters.

A one-sample Kolmogorov-Smirnov test was applied to the data confirming a normal distribution of the DFT results.

A paired t-test was used to determine statistical significance between the groups and a Pearson's correlation was performed to demonstrate relationships in the data. A $p < 0.05$ was regarded as significant.

Results

A mean DFT of 12.1 ± 5.2 (range 6.0–20.0) joules (J) and 22.8 ± 6.9 (range14–30) J was demonstrated for EDF vs. TDF ($p < 0.01$).

An impaired/high DFT of ≥ 30 J was identified in 3/9 (33%) pigs in the TDF group and none in the EDF group.

A summary of the DFTs for groups 1 and 2 is represented against weight in a linear graph in Figure 6.1.3.

The weight of the animals was correlated against the DFT for EDF (group 1) and TDF (group 2). This correlation was significant for both EDF and TDF with measured values of $r = 0.695$, $N = 9$, $p = 0.04$ and $r = 0.756$, $N = 9$, $p = 0.02$ for each of the groups respectively (Figure 6.1.4). A Pearson correlation, performed to compare the DFT results in both groups, is illustrated in Figure 6.1.5. This, however, did not demonstrate significance but there is an appreciable linear relationship between both groups with increasing weight except for an outlying point in Experiment 5 (Figure 6.1.3).

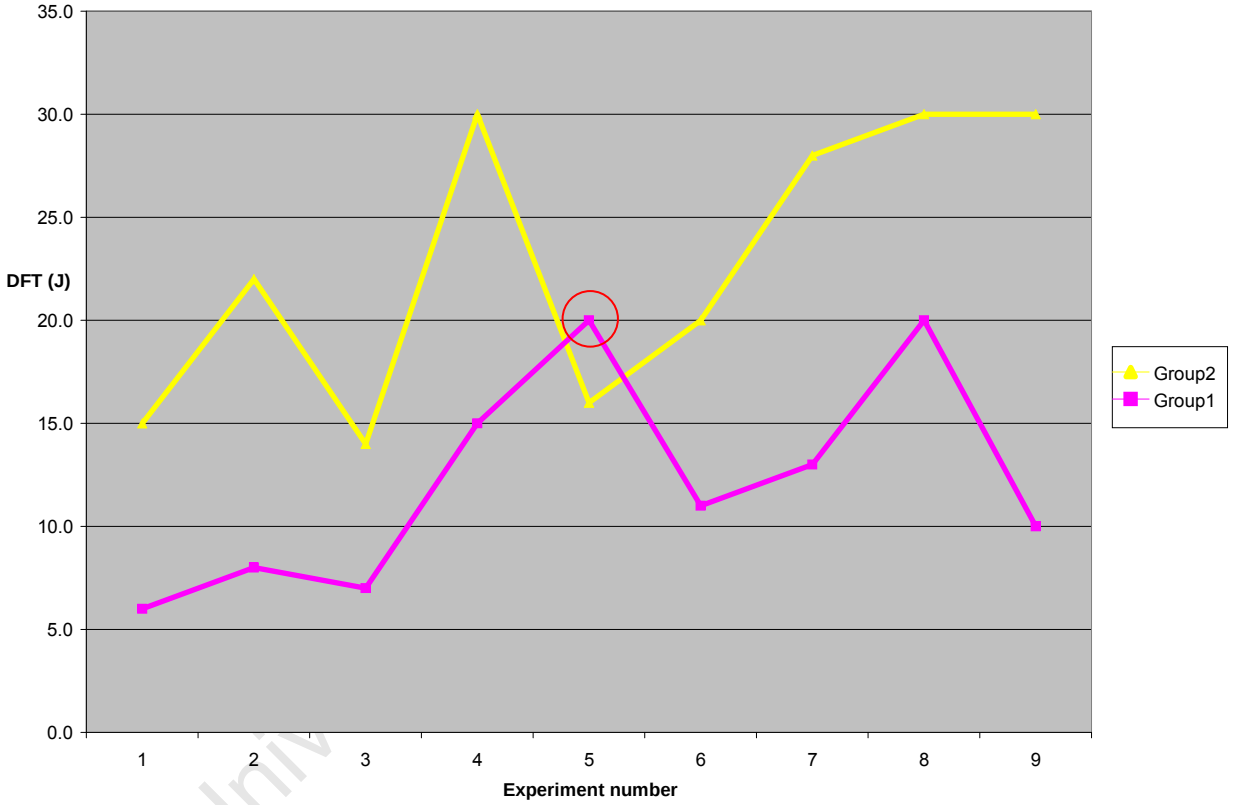

Figure 6.1.3

A linear graph summarising DFTs in groups 1 (EDF) and 2 (TDF).

An outlying point contributed by experiment 5 is ringed.

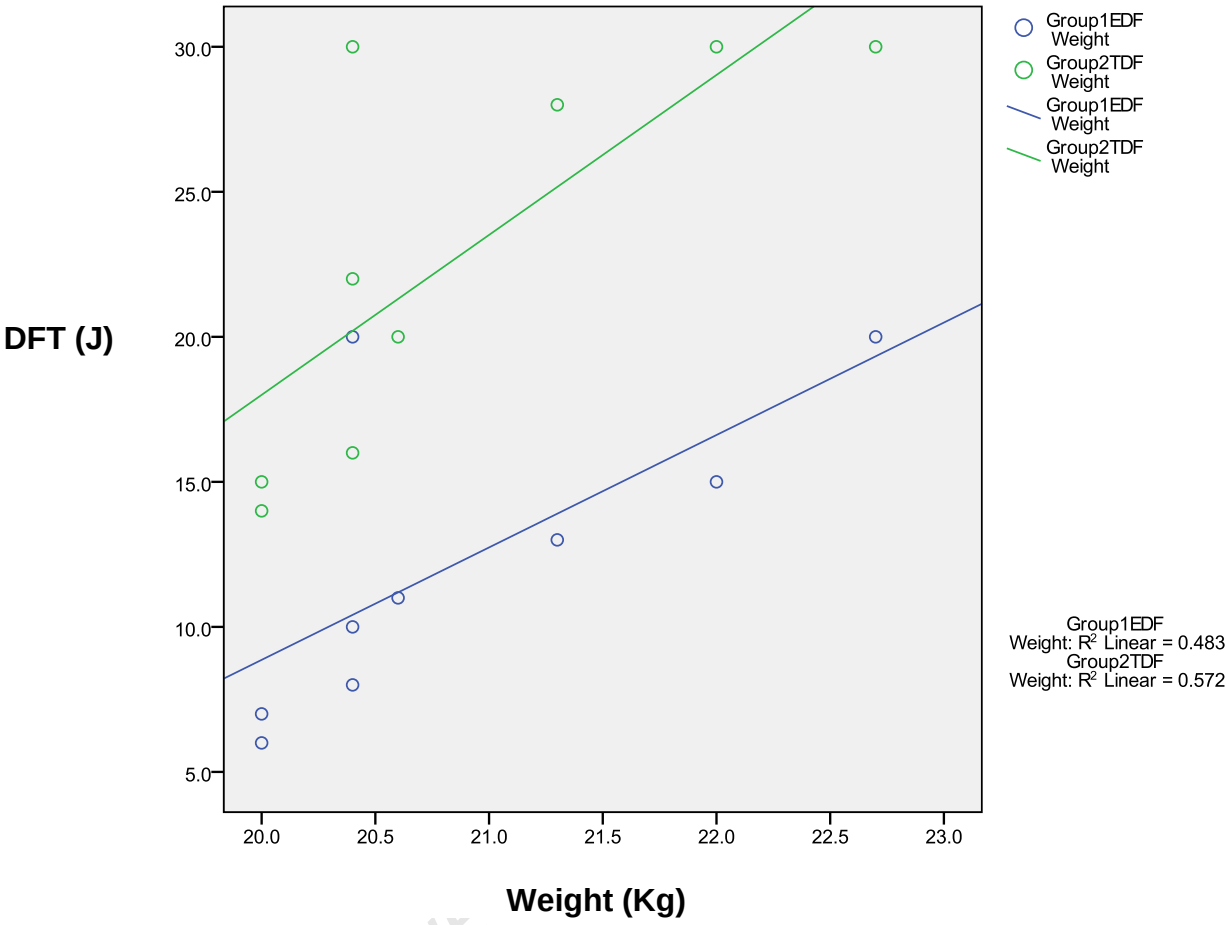

Figure 6.1.4

Correlation of EDF and TDF with bodyweight.

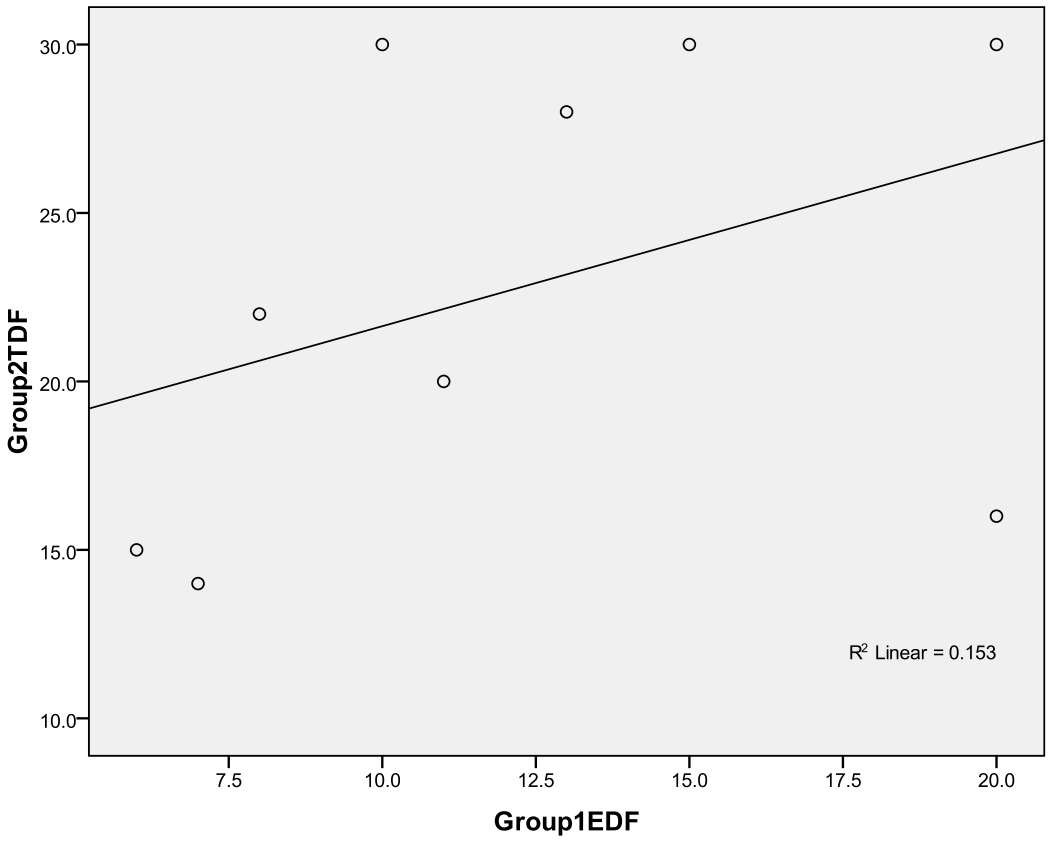

Figure 6.1.5

Correlation of DFTs from groups 1 (EDF) and 2 (TDF).

Discussion

Transthoracic defibrillation in combination with endocardial electrodes is an effective strategy to enhance defibrillation efficacy[96].

This may not be preferred as a sole strategy in a clinical setting because of the high defibrillation energies required. However, it may be a consideration in children or adults of low BMI given the evidence from the above results[99].

This investigation demonstrated a statistical difference ($p < 0.05$) of EDF vs TDF DFTs, with the former having a far better defibrillation success rate. Defibrillation testing in a clinical setting typically tries to insure a 10J safety margin from the maximum output of the device in a clinical setting.

Therefore, a DFT of 30 J (the maximum stored energy of the device used in the experiment) was regarded as impaired or a high DFT as 33% of the animals in the TDF group were noted to fall into this category and none in the EDF group.

This observation was made without apparent differences in shock impedance or VF duration ($p = 0.6$ and $p = 0.2$ respectively) between the TDF and EDF groups. A higher shock impedance was expected on the TDF strategy given the intervening tissue and lung volume between the active Can and SQA electrodes, but these differences were marginal [43.6 ± 10.3 ohms (Ω) for TDF vs 42.8 ± 9.8 Ω for EDF, p = NS]. This finding may be partly explained by the limited weight and size of the pigs chosen, but it also reflects the technology and design of the SQAs since they deliver equivalent impedances to the endocardial lead.

The model 6996 single finger array (Medtronic Inc. MN, USA) has a 25 cm coil length with a total surface area of 500 cm^2.

Subcutaneous array lead placement using the tunnelling tool was performed with ease in all cases. This also relates to the fact that the procedure was being undertaken under general anaesthesia. This is not the standard for transvenous ICD implantation in all centres, as conscious sedation poses a cost and convenience advantage. Subcutaneous array placement with conscious sedation may not be comfortable for the patient. However, whenever the clinical setting warrants, e.g. paediatric patients, it is conceivable that general anaesthesia would be preferred.

In this experiment, 33% of the pigs had an impaired/high DFT classified as ≥30J, i.e. the maximum delivered energy of the ICD used. We therefore suggest that higher energy devices are indicated when considering a TDF strategy in clinical practice.

Alternative strategies to deal with high DFTs include the addition of extracardiac electrodes. These measures include the addition of an SVC coil into the azygous vein in patients with high DFTs[95]. Surgical placement of a defibrillator lead into the transverse sinus in the intrapericardial space has been safe and effective in a series of seven children[100]. Inadequate venous access in the case of vein stenosis sometimes dictates the need for alternative lead placements. Minimally-invasive thorascopy-assisted epicardial defibrillator lead placement has also shown to be effective.

Limitations

The obvious limitation in this study is the small sample size of just nine pigs. Furthermore, the distance between the SQA located on the posterior chest wall and the endocardial RV electrode was not recorded. Apart from the increase in animal weight, the increase in chest wall diameter may have been a factor given that the separation between electrodes may have been disproportionately greater in the larger pigs, increasing the interposed tissue within the shock vector and thus contributing to impaired shock efficacy.

The narrow weight variation in the pigs does not parallel the variation we find in clinical subjects. This, however, was intentional to keep a relatively narrow weight range for other concomitant defibrillation studies as animals were reused in experiments in keeping with a prescribed policy of “reduction” in animal usage. Nevertheless, it highlights the sensitivity of TDF to weight variations.

Conclusion

As expected, a TDF strategy was less efficient than EDF in this porcine model. Despite a narrow weight variation, an impaired or high DFT result was observed in 67% of TDF attempts and a positive correlation with weight in both groups. The TDF strategy was more sensitive than EDF to minor variations in animal weight, suggesting that high energy ICDs should be favoured for a TDF. Despite the variation in DFTs, there was little change in impedance values between TDF and EDF.

6.2 The Influence of Combined Subcutaneous Arrays on Defibrillation Outcome.

Introduction

Although the addition of an SQA may enhance endocardial defibrillation efficacy, a stand-alone TDF is characterised by higher DFTs than endocardial electrode placement as was demonstrated in the preceding section[98;101]. The optimum SQA electrode configuration and polarity for TDF is not known.

In this study, the single SQA was compared with a combination of 2 SQAs located at 2 positions on the dorsal surface of the pig. This was performed to determine the influence of surface area and vectoral variation on a purely TDF configuration.

Methods

Animal Selection and Preparation

This study was conducted in 6 closed chest female Landrace pigs.

A cut down was performed to the left internal jugular vein and a 7F dual coil defibrillator lead (model 6949, coil length 6.2 cm, surface area = 513 mm^2, Medtronic Inc, MN, USA) was inserted and advanced under direct fluoroscopy to the ventricular apex.

A single finger SQA (25 cm coil, Model 6996 Medtronic Inc.) was tunnelled along the thorax, along an intercostal space to lie posterior to the cardiac silhouette on fluoroscopy (refer to the method previously described in section 6.1 page 100–101). The SQA was cathodal (-) in the shock configuration.

The ICD Can electrode (Medtronic 7274 dual chamber device with plugged atrial and SVC port) was implanted into a low precordial, subcutaneous pocket on the chest wall overlying the major ventricular mass as previously stated in 6.1 (page 114). A second identical SQA was then positioned within 1 cm of the first array; evident on fluoroscopy at position1 (**P1**) and both arrays were coupled with a Y-adapter to the distal unipolar defibrillation port of the device, i.e. both SQAs were designated cathodal.

Thereafter SQAs were then separated by ±10 cm to approximate the upper and lower extents of the cardiac image on fluoroscopy. This entailed the next test configuration regarded here as position **P1+P2** (Figure 6.2.1)

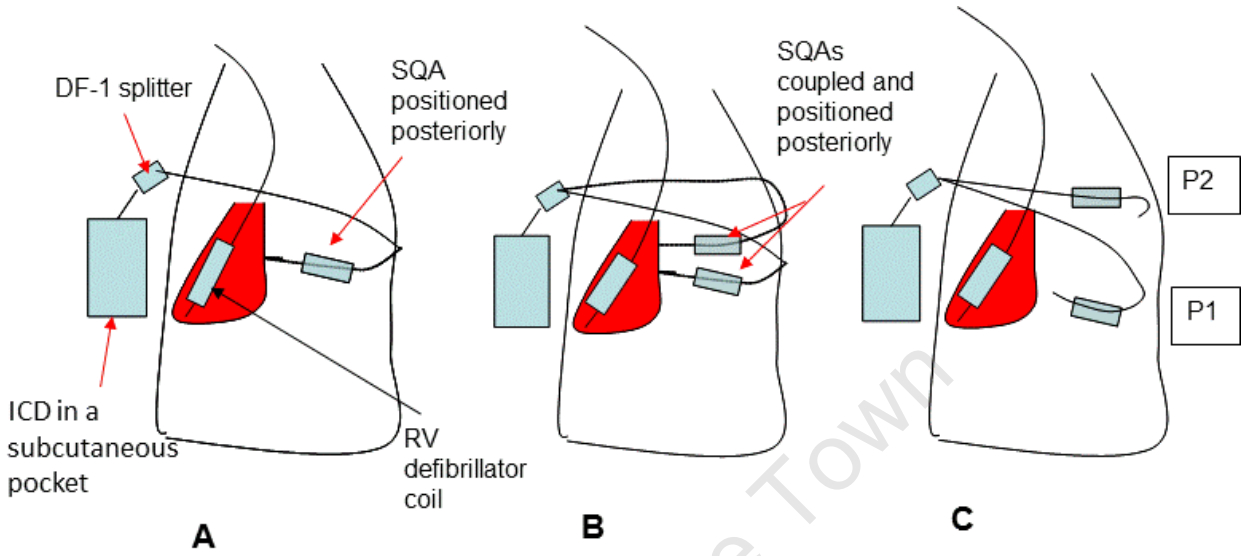

Figure 6.2.1

Cartoon of experimental configurations of SQA positioning

A. Configuration 1 - Sagittal view showing the low precordial Can position with a single SQA positioned posteriorly.

B. Configuration 2- Two identical SQAs combined as cathode in position P1 immediately posterior to the cardiac silhouette on the thorax ± 1 cm apart.

C. Configuration 3 - The second SQA moved ± 10 cm superiorly on the thorax to position 2 (P2) and both SQAs remained coupled together as a cathode.

Defibrillation Protocol

Defibrillation testing was conducted using a Can>SQA shock vector and a 3-reversal up/down binary search (as depicted in Figure 6.1.2 on page 105). The lowest energy obtained was regarded as the DFT for that particular configuration. This was done to reduce the number of VF inductions and shocks in the animal. Ventricular fibrillation was induced by 50Hz burst pacing or T wave shock through an RV apical, endocardial lead connected to a 7274 ICD (Medtronic Inc., MN, USA).

Defibrillation threshold testing was repeated using the method mentioned above. A DFT of ≥ 30 J was regarded as an impaired or high DFT since a 10J safety margin was not attained. A 3-minute rest period was allowed between VF inductions to allow the recovery of the blood pressure and HR to baseline. The order of testing was randomised.

Results

The study was conducted in 6 anaesthetised female pigs weighing 20.8 (range, 20–23) kg. The mean blood pressure recorded was 44.1 (range, 27.4–82.8) mmHg and mean HR 108.2 (range, 96.3–176.8) beats per minute.

This study did not show any significant effect on DFTs by the addition of a second SQA, either at a combined location or with an altered vector arising from SQA separation ($p = 1$, $p = 0.8$, respectively) (Table 6.2.1 and Figure 6.2.2). However there was a trend to lower DFTs with the configuration 3 arrangement of SQAs (p=NS).

Overall impedances, however, were significantly lower with combined SQAs. This is reflective of the increased surface area presented by linking both of these electrodes (Figure 6.2.3)

		Configuration1	Configuration2	Configuration3
DFT	**Mean DFT**	20.7	20.7	20.4
	std dev	6.3	6.1	6.7
Impedance	**Mean Imp**	48.1	42.7	41.0
	std dev	2.4	10.4	7.2
VF duration	**Mean dur**	16.0	12.9	9.7
	std dev	5.7	5.3	2.3

Table 6.2.1

Summary of defibrillation results.

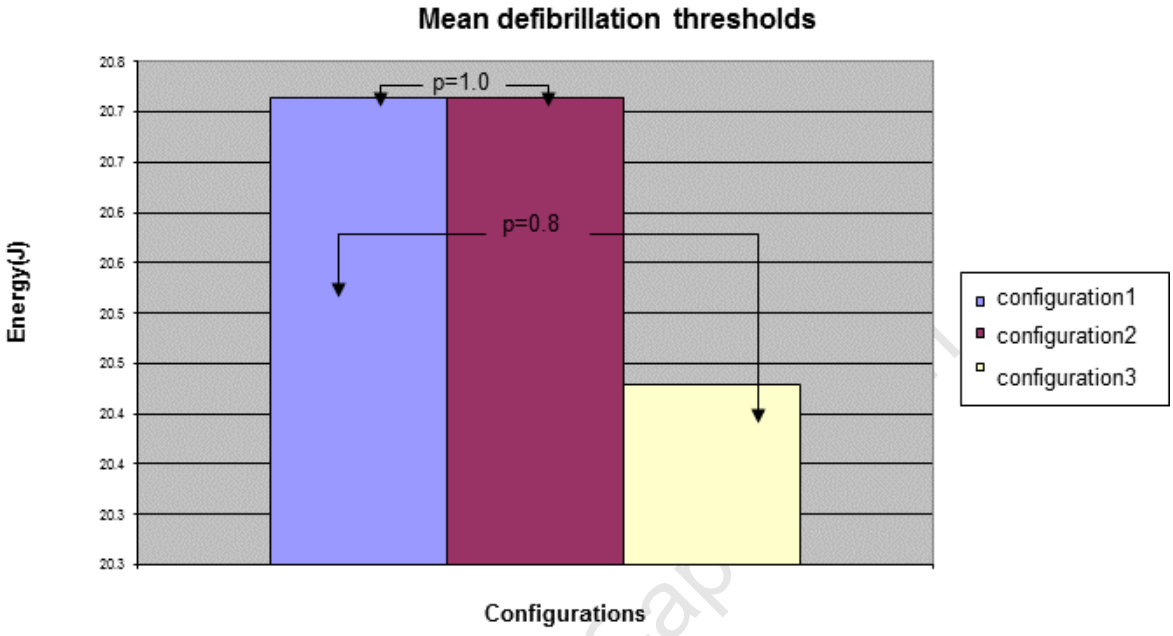

Figure 6.2.2

Comparison of mean DFTs of each configuration.

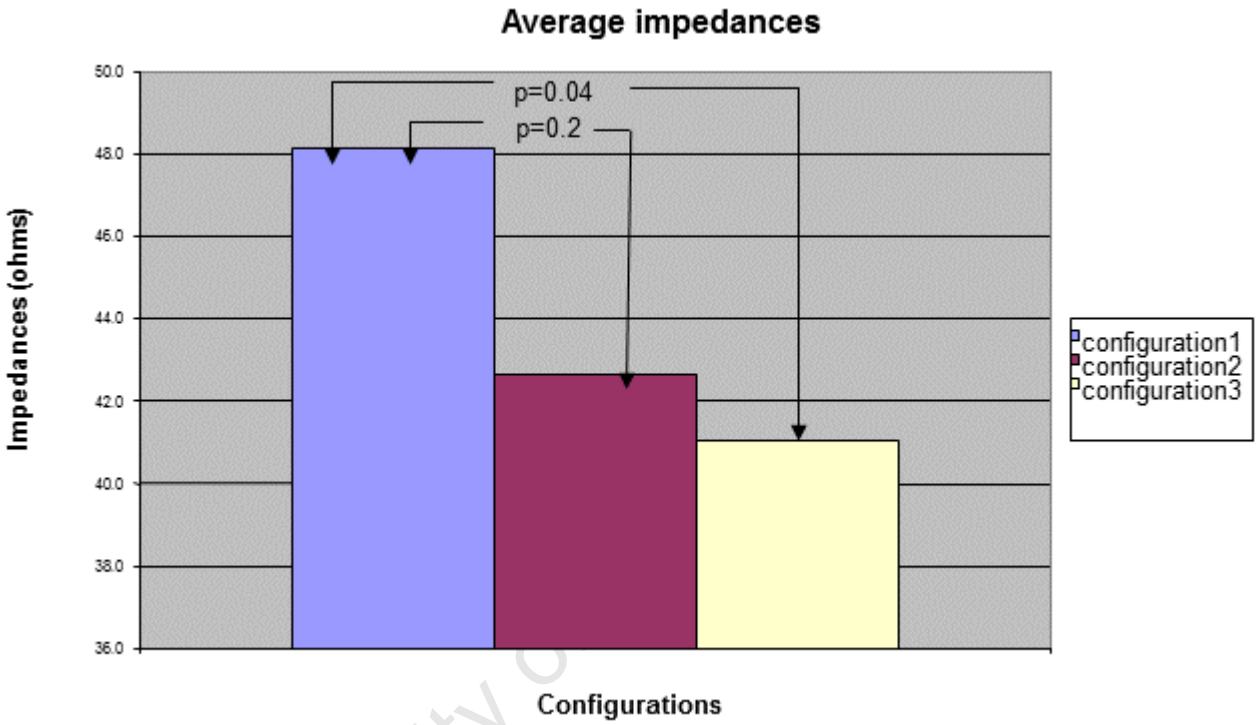

Figure 6.2.3

Comparison of mean impedances of each configuration.

Discussion

Although transvenous defibrillator systems are now the cornerstone of ICD management, they are by no means absolute. The complications related to transvenous systems are also not trivial. Limited venous access related to the age of the patient or anatomical hindrances show the advantage in having extracardiac or subcutaneous ICDs[102;103].

The totally subcutaneous ICD system as proposed by Cameron Health shows promise[104]. There are randomized controlled trials underway that assess the subcutaneous system directly against transvenous systems[105;106]. This system is conceivable for patients who do not require bradytherapies or ATP. The clinical configuration utilizes an axillary ICD placement that can be cumbersome. The configurations explored in this chapter illustrate an effort to maintain a traditional prepectoral Can position for an entirely subcutaneous ICD implantation.

Combining SQAs in a posterior/dorsal location in a TDF did not significantly affect defibrillation efficacy. A further separation in the leads resulted in a marginal 0.1% reduction in the mean DFT (configuration 3). There was a more substantial decrease in defibrillation impedances by adding 2 SQAs.

The reduction in impedance that was observed may imply improved current delivery through the chest wall to the underlying fibrillating myocardium; however, this was not reflected in the DFTs. The vectoral variation created in configuration 3 showed a trend to DFT lowering as compared to the closely set SQA pair seen in configuration 2.

It is unlikely that there was current shunting in configuration 2, as the impedance values in configurations 2 and 3 were comparatively similar. It therefore seems more likely that the DFT change was truly due to the minor vectoral change afforded by electrode separation on the dorsal wall of the animal.

The overall non-superiority of combining electrodes indicates, however, that using multiple SQAs contributes little to enhance TDF.

Long term stresses and tolerance on these subcutaneous leads need to be investigated in a clinical setting. There was relative ease of implantation with use of the tunnelling tool in the animals bearing in mind this was also performed under general anaesthesia.

Limitations

This again was a small study consisting of just six pigs. The overall distance between the SQAs and the heart was not recorded in this study but was unlikely to be altered by just increasing the number of electrodes. This, together with animal weight and chest wall configuration, was influential in determining the DFTs.

Conclusion

In a TDF strategy, the use of a single finger cathodal SQA situated in a dorsal thoracic site with a precordial ICD, was as effective as combining two SQAs in various dorsal locations. A drop in defibrillation impedance was noted with the combination of two arrays but this did not influence the defibrillation threshold.

Acknowledgements

I designed the protocol and conducted this experiment. Roland Bullens, of the Medtronic, Bakken Research Centre in Maastricht, the Netherlands, provided advice on preparation of abstracts and presentation of data at scientific symposia.

The project was supervised by Dr John Morgan and Dr Paul Roberts my mentors at Southampton General Hospital.

Disclosure

My research fellow's salary was derived from an unrestricted grant from Ela Medical, Sorin Group, UK. Additional equipment was supplied by Medtronic, UK.

6.3 The Effect of an Extended Anterior Chest Wall Anodal Electrode in a Transthoracic Defibrillation Model.

Introduction

In the preceding chapter, I examined the influence of an increased cathodal surface area in an antero-posterior TDF format. Recent studies have proposed that a reversed RV anode > ICD Can cathode defibrillation is more effective with endocardial lead placement[45]. In this section, the anodal electrode surface was extended using an experimental 15cm single-finger SQA to enhance the anodal (+) polarity dominance during TDF in order to assess the effect on defibrillation efficacy.

An antero-posterior chest wall electrode configuration consisting of an anteriorly located active Can electrode with a posteriorly implanted single finger SQA has been proven to be effective in anecdotal clinical scenarios[99;107;108].

Here, I investigated the effect of increasing the anterior chest wall subcutaneous electrode area by implanting an experimental, 15cm single-finger array (6996s. Medtronic Inc., MN, USA) at a parasternal location and designated this electrode anodal (+) coupled together with the ICD housing.

Methods

Animal Selection and Preparation

The study was conducted in 6 anaesthetised female Landrace pigs (average weight 20.8 ± 0.7 kg). An ICD was placed in a precordial subcutaneous pocket and connected to a single-finger subcutaneous 25 cm coil electrode (model 6996, Medtronic Inc.), which was tunnelled horizontally around the left chest wall, posterior to the cardiac silhouette on fluoroscopy using the previously described technique (page 100–101). This electrode was not located to a specific interspace, but an attempt was made to have the major myocardial mass located between the anterior chest wall electrodes and this single, posteriorly located SQA using fluoroscopy.

A 15 cm experimental SQA (exSQA = model 6996s, Medtronic Inc.) was then implanted subcutaneously to lie parallel to the right parasternal edge with intervening tissue separating it from the implanted precordial ICD (Can electrode). The shorter lead design allowed easier lead positioning, particularly in the smaller size pigs chosen for the experiment. A standard pace/sense lead was endocardially positioned at the RVA for induction and sensing and back up pacing (method described on page 60). This was connected to the IS-1 pacing port of the ICD.

Defibrillation Protocol

The additional exSQA was connected to the SVC port (+) of the device. The active Can (ICD) and exSQA were therefore coupled together as a combined anterior chest wall anode. A Can > posterior standard SQA (pSQA) was used as the control while the Can + exSQA > pSQA was the test configuration.

Ventricular fibrillation was induced with 50Hz burst pacing or a T wave shock delivered via a right ventricular pace/sense lead implanted transvenously and connected to the device. Defibrillation threshold testing was conducted using a 3-reversal Binary protocol (Figure 6.1.2 on page 105). The average of the two lowest energy achieving defibrillation was regarded as the DFT. The order of DFT testing was randomised between control and test configurations. Rescue shocks were delivered via an external defibrillator using transthoracic paddles.

Results

Placement of the additional parasternal anode-electrode resulted in a significant rise in DFTs from control ($p = 0.04$) (Table 6.3.1, Figure 6.3.1). The mean rise in DFT = 4.7 ± 3.3 J with 66% (4/6) cases in the test group having a defibrillation requirement of ≥ 30 J; i.e., the maximum output of the ICD. A drop in shock impedance was a consistent observation when the additional exSQA was used (mean decrease = 14.6 ± 3.2 Ω; $p = 0.001$, Figure 6.3.2). The longer VF time (average difference = 12.5; range 1.5–30 sec) in the test group reflects the overall VF duration and includes initial failed attempts. The fact that more initial failed shocks were recorded in this group increases the mean VF duration recorded.

	Control	Test
	Can(+) > pSQA	Can + exSQA > pSQA
DFT (J)	21.7 ± 6.4	28.0 ± 4.0
Impedance (Ω)	43.6 ± 10.3	33.2 ± 3.9
VF time (s)	16 ± 5.7	29.9 ± 16

Table 6.3.1

Summary of defibrillation results in control and test groups.

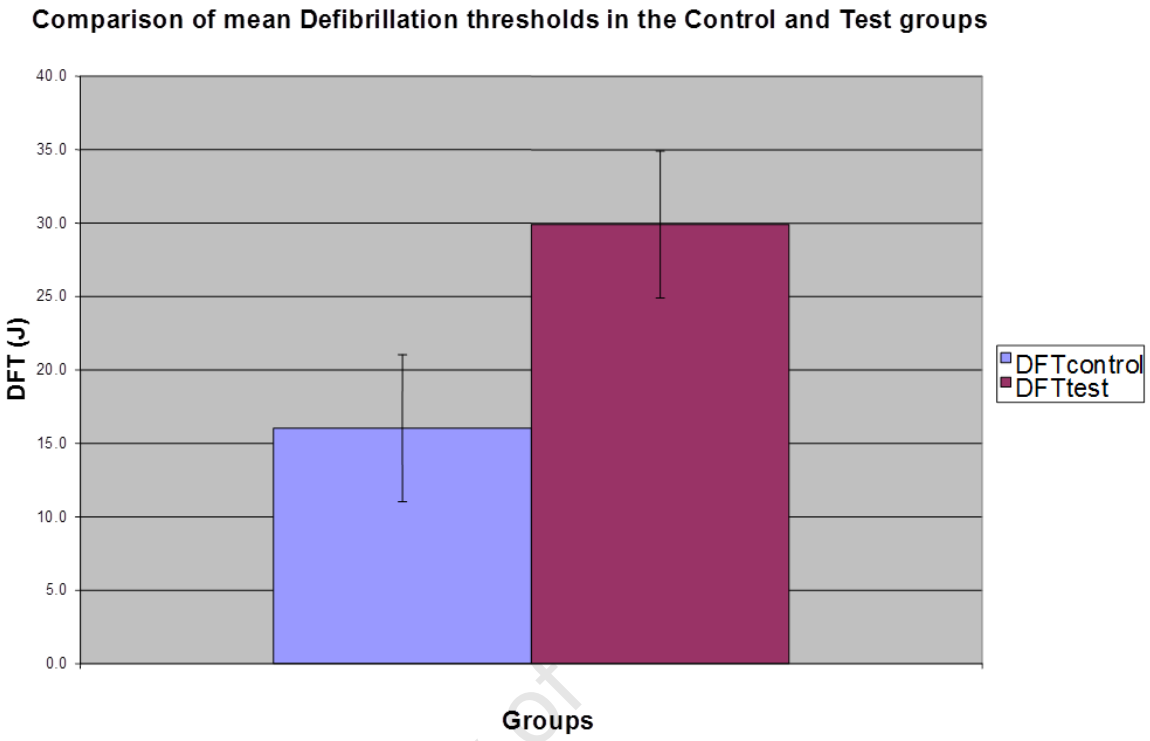

Figure 6.3.1

Comparison of mean DFTs in control and test groups.

Bar graph of the mean DFTs in each group with indicated standard error, $p < 0.05$.

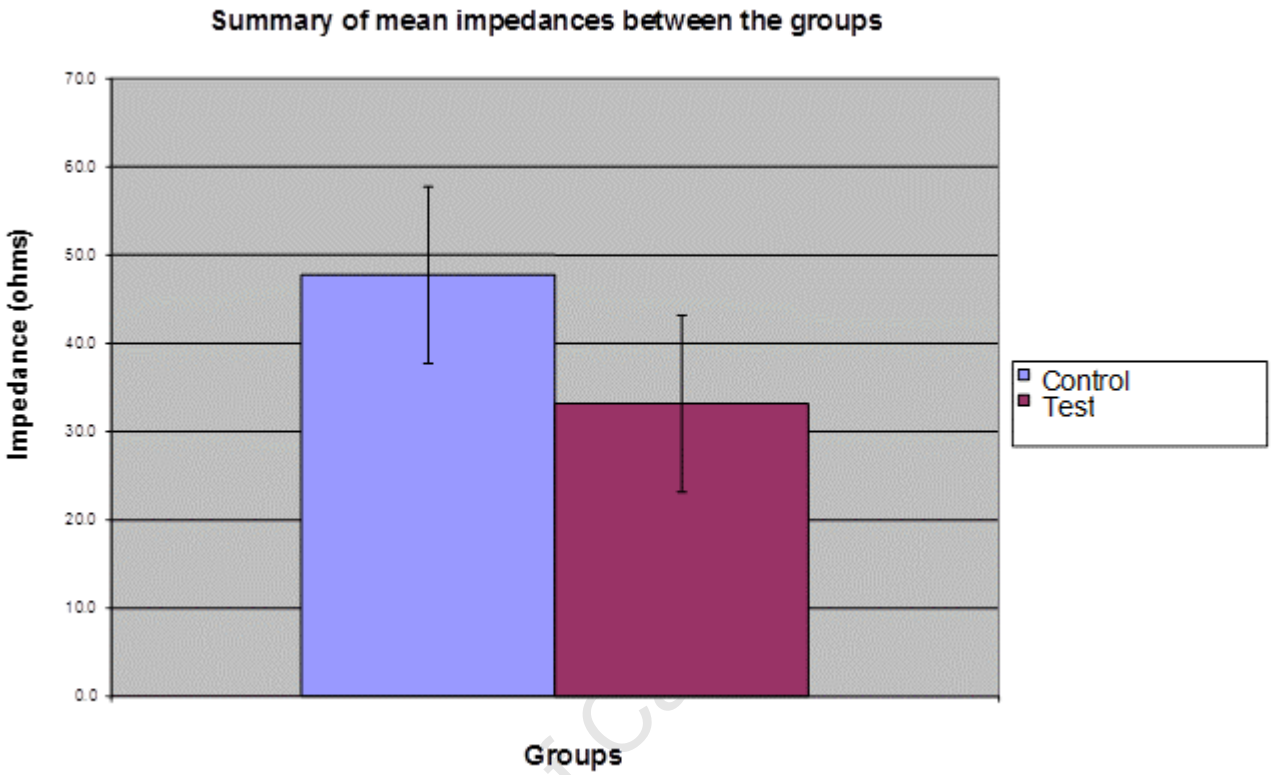

Figure 6.3.2

Summary of mean impedances in control and test groups. Mean impedance difference between test and control groups with indicated standard error, $p < 0.01$.

Discussion

The addition of an experimental 15cm SQA in a left parasternal location resulted in a 29% increase in DFTs compared to a standard antero-posterior transthoracic defibrillation vector.

The reduction in defibrillation impedances may reflect current shunting between the Can and exSQA electrodes. This may also explain the reduced defibrillation efficacy. This phenomenon occurred despite the care exercised to maintain adequate separation between both (Can and exSQA) of these electrodes.

Despite the disappointing defibrillation outcome, the reduced length of the exSQA presented ease of manipulation together with the use of a shorter tunnelling tool. Placement in the parasternal region requires a shorter coil length array which is the same in human subjects, particularly with children in whom TDF would be an option. A 25 cm coil would result in increased tissue manipulation, operative morbidity and possibly redundant coil exposure risking encroachment into the ICD pocket.

A low precordial subcutaneous, ICD pocket has been shown to be advantageous, not only from TDF efficacy perspective, but is also cosmetically more pleasing, particularly in woman as the ICD can be placed beneath breast tissue[109].

Limitations

The need to add an SQA in a clinical setting as an adjunct to endocardial defibrillation is infrequent and this then brings into question the relevance of this study. However, subcutaneous and “leadless” ICDs are increasingly topical, particularly with the increasing use of ICDs in the paediatric population[98;110;111]. The use of shorter SQAs potentially reduces trauma to tissues during implantation. It is then also useful to determine which SQA positions are beneficial, but also to determine configurations that should be avoided, as is highlighted by this experiment.

Conclusion

Addition of a short (15cm) subcutaneous array (exSQA) at a parasternal location increases the anterior anodal electrode surface area but reduces defibrillation efficacy. This may be because of current shunting between the Can and SQA despite their equal polarities and is reflected by a reduction in shock impedance. The clinical implication is therefore not to position additional SQA electrodes on the anterior chest wall in proximity of the Can electrode as this may compromise defibrillation efficacy.

Acknowledgements

I was responsible for the protocol design and execution of this experiment. Roland Bullens at the Medtronic, Bakken Research Centre in Maastricht, the Netherlands provided advice on preparing the protocol and supplied the experimental 6996s SQA under permission from Medtronic. The project was supervised by Dr John Morgan and Dr Paul Roberts my mentors at Southampton General Hospital.

Disclosure

My research fellow's salary was derived from an unrestricted grant from Ela Medical, Sorin Group, UK. Additional equipment was supplied by Medtronic, UK and from the Bakken Research Centre, Medtronic, Maastricht, the Netherlands.

7. A Pilot Project to Assess Defibrillation from an Intrapericardial Location.

Introduction

In a clinical setting, failed defibrillation may present a challenge to adapt the defibrillation circuit to enhance efficacy. In this thesis I have expanded on waveform manipulation and the use of additional endocardial leads, as well as the inclusion of SQAs. Each of these options has yielded marginal benefit beyond conventional techniques. The pericardial space presents an attractive option for lead placement. This region can be accessed using percutaneous methods. It allows direct contact of electrodes with the ventricular epicardium thus minimising the amount of interposed bystander tissue within a shock vector. Percutaneous intrapericardial delivery of a standard ICD lead has been demonstrated anecdotally[112].

This study was a pilot project to assess the feasibility of percutaneous delivery of conventional defibrillation leads designed for transvenous placement into the pericardial space and to assess their performance in terms of defibrillation efficacy. This was compared against endocardial and subcutaneous defibrillation parameters in the same subjects.

Methods

Animal Selection and Preparation

The study was conducted in 4 female pigs of the Landrace variety with a mean weight of 20.6 ± 1.0 kg. Each animal was anaesthetised using methods previously elaborated on (chapter 2 on page 38).

A 18G Tuohy needle attached to a 10cc syringe containing a 1:1 mixture of sterile 0.9% saline and iodine based radio-opaque contrast was advanced under fluoroscopic guidance from the sub-xiphisternum at a 30–45° angle aiming cranially aligned with the longitudinal axis of the sternum (Figure 7.1).

On entering the pericardial space, an injection of the diluted contrast was injected creating a meniscus around the lower cardiac silhouette on fluoroscopy. A flexible J-tip 0.38 inch, 50 cm guide wire was then advanced through the hollow needle into the pericardial space.

Care was taken to loop the guide wire in the pericardium and to insure that it passed freely in all planes, confirming this in an AP and LAO projection. Once this was done, a 7F splitable sheath (Sorin Biomedica, TFX Medical, Annacotty Ind. Estate, Limerick, Ireland) was advanced over the wire. The introducer was then withdrawn and occluded in order to minimise air entry into the pericardium.

A TransveneR SVC unipolar defibrillation electrode (model 6937 Medtronic Inc., coil length 8 cm, 160 mm^2, 2.3 mm tip diameter and 1.8 mm shaft diameter) was inserted to lie posterior to the LV in the posterior pericardial space (PPS)

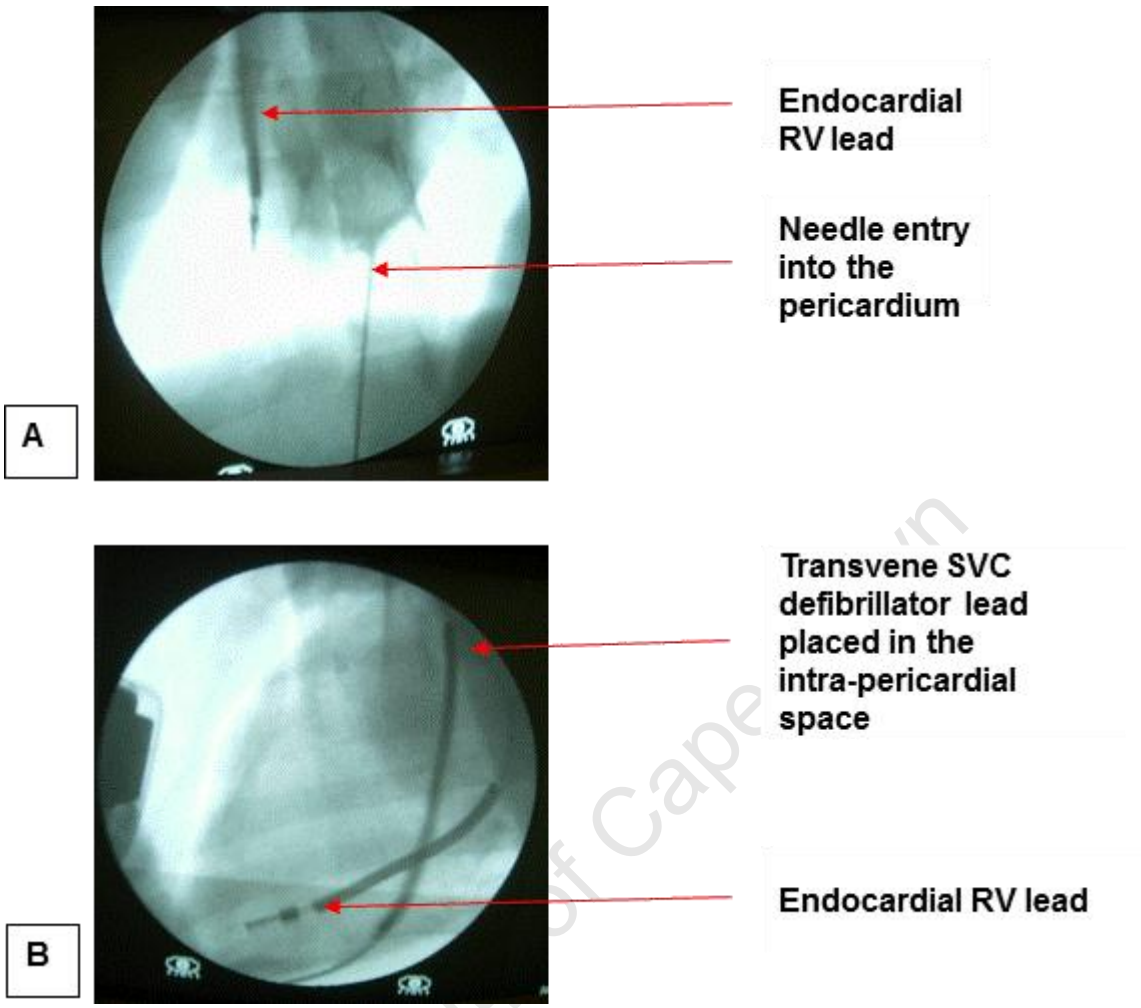

Figure 7.1

AP and LAO projections of entry into the pericardial space.

A. Entry of a bevelled needle from a sub-xiphoid approach with entry into the pericardial space. A meniscus of injected contrast identifies the intra-pericardial space seen in AP projection.

B. A single coil transvene SVC defibrillator coil is then passively inserted through a guide sheath into the posterior pericardial space (PPS). The RV apical electrode is also visible seen in a LAO projection.

The coil orientation was vertical, corresponding to the longitudinal cardiac axis and this was left passively in place for the duration of the experiment. The position was confirmed in antero-posterior and left lateral oblique views and periodically confirmed on fluoroscopy through the experiment. An effort was made to keep the PPS lead position constant but variability was inevitable because of the lack of a fixation mechanism and also as the position was dependent on the access point into the pericardium.

This electrode was connected to the DF-1 distal (-) port of a standard dual chamber ICD (model 7274, Medtronic Inc. with capped SVC and atrial ports, except for experiment 3, where the Gem DR model 7271 was used. The device was implanted into a low precordial subcutaneous pocket directly overlying the cardiac silhouette on fluoroscopy (Figure 7.2).

In addition, a cut down was performed to the left internal jugular vein and a standard single coil defibrillator lead was delivered transvenously to the RV apex. A single finger subcutaneous 25 cm coil electrode (model 6996, Medtronic Inc.) was tunnelled around the left chest wall, posterior to the cardiac silhouette on fluoroscopy (pSQA). These were connected to the ICD in a randomised fashion together with the intra pericardial electrode for DFT testing.

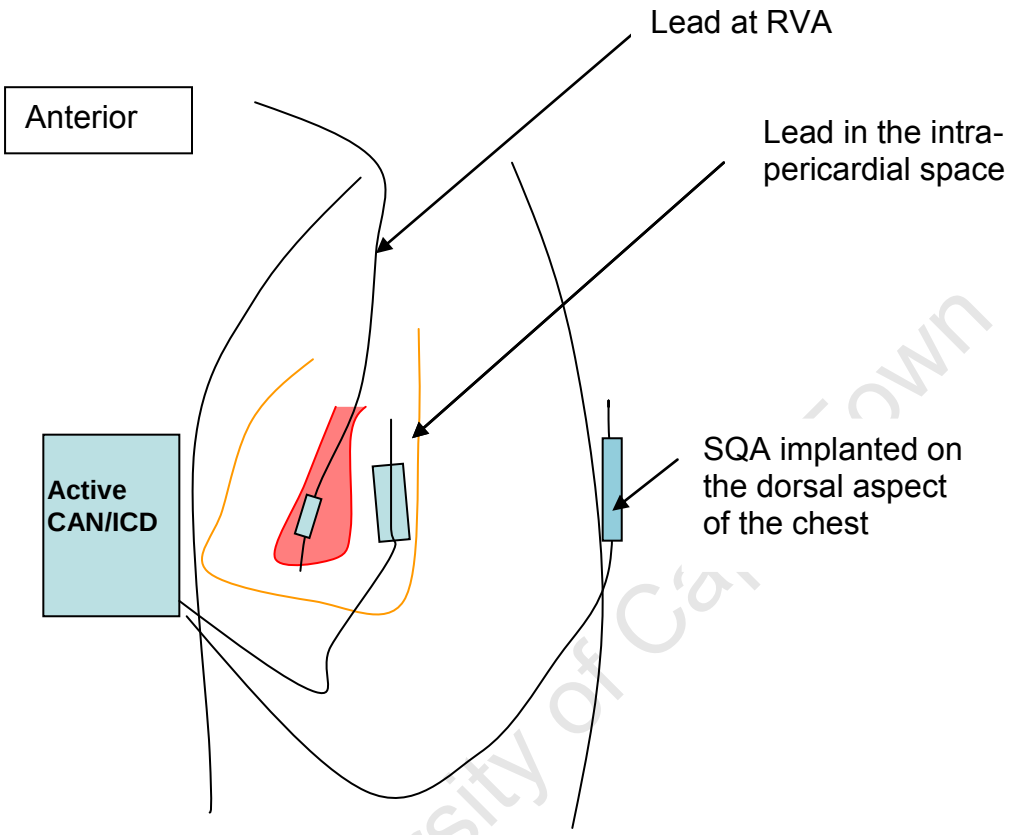

Figure 7.2

Sagittal view of the ICD location.

Reference is given to the intra-pericardial defibrillator electrode, a defibrillator lead at the RVA and the dorsally located SQA.

Defibrillation Protocol

Three defibrillation configurations were compared:

1. CAN > RV apex (endocardial electrode)
2. CAN > posterior subcutaneous array (pSQA)
3. CAN > post pericardial space electrode (PPS)

The order of testing was randomised between each configuration.

Ventricular fibrillation was induced either with 5 seconds of 50Hz burst pacing or with a T wave shock. If both methods failed, the positive and negative terminals of a 9V battery were crossed and direct current was applied through the pace/sense IS-1 component of the endocardial defibrillator lead.

Shocks were delivered in the format outlined above through the implanted ICD. Rescue shocks were delivered at maximum output from the ICD (30J), failing which, a 200J biphasic, transthoracic shock was delivered via an external defibrillator. The lowest average defibrillation energy was regarded as the DFT. Failed defibrillation was regarded as 30 J (maximum device output).

Statistical Analysis

Continuous data is expressed as mean ± SD. Data was collected in Excel spread sheet format and processed with SPSS version 17 software (SPSS Inc., Chicago, Ill.)

Results

This pilot study consisted of 4 pigs with a mean weight of 20.6 kg. Instrumentation and pericardial lead placement times varied between 10-15 minutes. No animals were lost from pericardial access or lead placement or from pericardial tamponade.

Defibrillation outcomes are shown in Figure 7.3. The mean DFT and impedances in RVA, SQA, and PPS were: 9.0 ± 4.1 J, 46.8 ± 2.5 Ω; 20.3 ± 7.3 J, 49.3 ± 1.9 Ω and 16.5 ± 9.6 J, 66.7 ± 29.5 Ω, respectively.

The PPS defibrillation system displayed equivalent DFTs to the endocardial system in experiment 1. However the remaining 3 experiments displayed equivalence to the SQA system which was characterised by higher DFTs. The overall impression was that there was no significant change between the SQA and PPS configurations although a trend to DFT reduction was observed in the latter. There was a 19% reduction in the mean DFT between the SQA configuration and the PPS.

Experiment 3 also displayed a dramatic increase in impedance to >100 Ω, which warrants explanation.

A

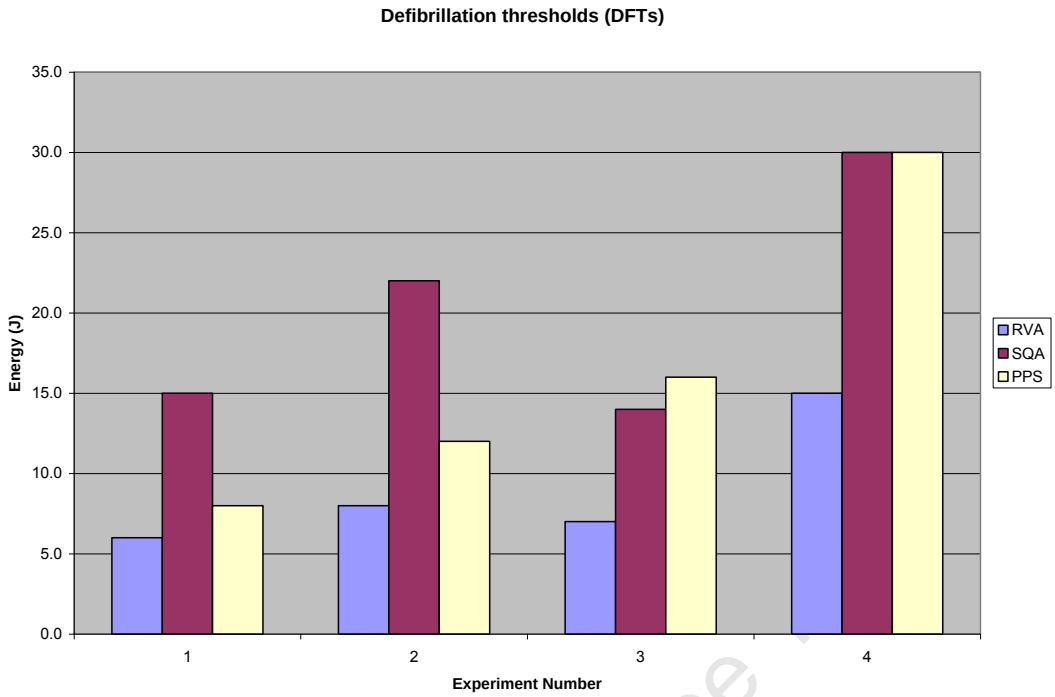

B

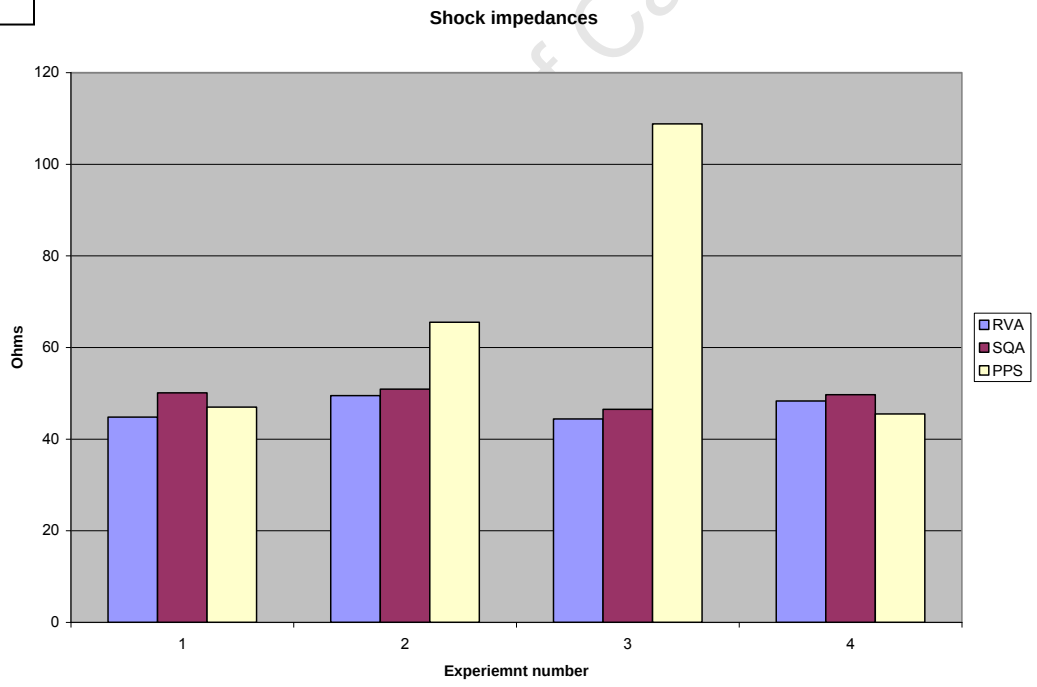

Figure 7.3
Comparison of DFTs and impedance values from RVA, SQA and PPS systems.
A. Bar graph of DFTs in each experiment
B. Corresponding impedance values for each experiment

Discussion

This pilot set of 4 experiments demonstrated the feasibility and safety of percutaneous placement of a defibrillation electrode into the posterior pericardial space. Both the PPS and SQA defibrillation systems displayed higher DFTs than an endocardial system. However, the PPS defibrillation vector showed a trend to greater DFT reduction than the SQA system.

The abrupt rise in impedances in experiment 3 is most likely attributable to air entry into the pericardial space, despite the caution exercised during cannulation and access.

In this set of experiments, a Transvene-SVC electrode, designed for intravascular placement was used. It was easily inserted through a sheath into the pericardial space but was prone to displacement. Hence, periodic fluoroscopy was required to confirm the position of the lead. This would not be reliable in a clinical setting. A recent clinical report by Jacob et al. describe a technique whereby a loop is created in an SQA (Medtronic 6996 lead) in order to minimise movement within the pericardial space[112]. Defibrillation efficacy was also enhanced with this intrapericardial lead configuration in this case report.

Limitations

This is a pilot study that addressed the feasibility of percutaneous delivery of a defibrillator lead to the pericardium and the efficacy of this shock vector. Therefore, no deductions can be made about superiority or equivalence of this

system compared to a subcutaneous or endocardial system. That would require a larger study, as well as a custom-designed percutaneous pericardial delivery system and lead for epicardial fixation in order to be clinically relevant.

Conclusion

Intrapericardial defibrillator electrode placement is feasible using a percutaneous approach. It is also shown to be effective and equivalent in some scenarios to an endocardial strategy, and perhaps superior to the addition of an SQA when used to improve defibrillation efficacy. This approach, however, warrants a custom lead design in order to maintain lead position and stability.

Acknowledgements

I designed the protocol and executed all experiments. Terri Whitman of Medtronic, MN, USA provided assistance in the form of advice on lead placement and methodology. The project was supervised by Dr John Morgan and Dr Paul Roberts my mentors at Southampton General Hospital.

Disclosure

My research fellow's salary was derived from an unrestricted grant from Ela Medical, Sorin Group, UK. Additional equipment was supplied by Medtronic, MN, USA and Medtronic, UK.

8. Clinical Evaluation of Implantable Cardioverter-Defibrillator Derived Electrograms and Anti-Tachycardia Pacing.

8.1. The Pause After Anti-Tachycardia Pacing May be a Useful Tool to Differentiate Supraventricular and Ventricular Tachyarrhythmias in Implantable Cardioverter-Defibrillators.

Introduction

Rapidly conducted atrial fibrillation (AF) or atrial tachycardia (AT) is a frequent cause of inappropriate therapies (ITS) in patients with ICDs[8;113-115].The rate of the conducted SVT may exceed the upper rate at which discriminators and morphology templates are programmed, leading to inappropriate shocks that are usually preceded by an episode of ATP[67;116]. If the ATP is ineffective in terminating the rhythm, the result is in essence a form of manifest entrainment from the RV lead pacing site.

The concept of entrainment has been previously defined as a basic electrophysiological manoeuvre to indicate the proximity of a roving pacing catheter to a macro re-entrant circuit[117;118]. These fundamental principles may be applied to device based electrogram (EGM) interpretation.

Hypothesis

Given the relative proximity of an RV lead, an entrained ventricular tachycardia (from this pacing source), should have a shorter PPI than if the ventricular rate was due to rapidly conducted AF/AT.

Thus, in the case of AF/AT, the pause after pulses of ATP would represent a retrograde penetration of the atrioventricular node (AVN) and His-Purkinje system accounting for a longer interval after ATP before resumption of antegrade conduction of the tachycardia[119].

Methods

This study was a retrospective analysis of all patients implanted with ICDs for combined primary and secondary indications at a single centre. The cohort consisted of 250 patients (46 female). These were of mixed ischaemic and non-ischaemic aetiologies with a mean age of 73 ± 7 years.

All patients received either dual chamber (DR) or biventricular (BiV) ICDs. Patients were excluded if they received single chamber devices or if the atrial ports of the devices were plugged. This was done so that only episodes with a corresponding atrial EGM would be analysed for proof of concept.

Events were adjudicated by two observers. The maximum follow up period was 23 months.

Data Collection

The clinical records of all patients implanted with DR and BiV ICDs, were examined for the period from December 2006 to October 2008. All patient related device therapies that were flagged in a database were then re-examined. These were then classified into appropriate or ITS. All non-physiological events ("noise related events") and oversensing phenomena were excluded from the analysis.

Definitions

The PPI was defined as the first return cycle length after ATP (burst/ramp). The PPI -TCL where the tachycardia cycle length (TCL) was the average ventricular tachycardia cycle length calculated by the device. The mean cycle length (CL) of the tachycardia for analysis was determined as the average of five successive CLs, excluding the first interval after the PPI (to allow for minor CL variation after ATP) (Figure 8.1.1).

The mean CL post ATP was compared to the preceding mean CL of the tachycardia pre ATP to ensure that there was no significant variation in tachycardia (i.e. CL variation > 50 ms) (refer to exclusion criteria listed below).

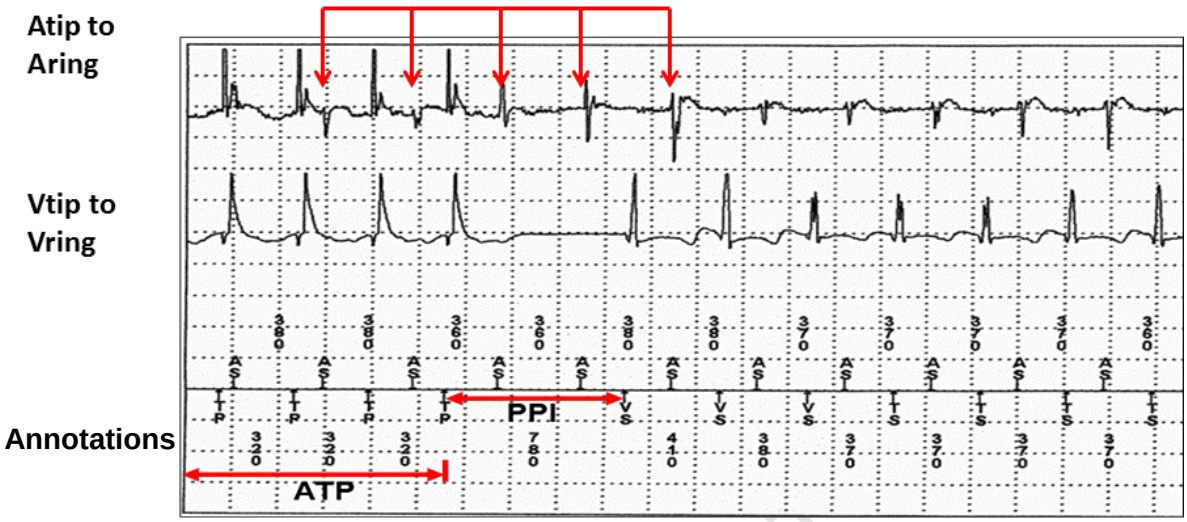

Figure 8.1.1

An illustration of the ATP response in an episode of AT.

The ATP response with PPI and TCL intervals in an episode of AT with a rapidly conducted ventricular rate resulting in inappropriately delivered ATP by a dual chamber device. The arrows in the atrial EGM show that AT cycle length is not advanced by ventricular pacing but "marches" through. The AT is ongoing after the ATP and because of the pause seen after ventricular pacing, a "pseudo AAV" post ATP is seen. In essence, the ventricle was dissociated from the atrium during ATP further confirming that this is AT.

Exclusion Criteria

Exclusion criteria were applied to the remaining data sets to ensure that the delivered ATP did not significantly perturb the ongoing tachycardia to account for the episode as a single ongoing event:

1. The post ATP and pre ATP TCL varied > 50 ms if the preceding tachycardia was stable, e.g. in VT, AT, or pseudo regularisation of rapidly conducted AF.
2. ATP terminated the episode
3. A ventricular paced event occurred at the lower programmed rate immediately after ATP
4. ATP accelerated the preceding tachycardia CL by > 50 ms

All events were evaluated in a standardised manner:

a. The scatter plot (dot-plot), and local and farfield EGMs were viewed collectively to aid diagnosis.
b. Events were evaluated in chronological order (episode) and then sequentially (sequence of ATP) per individual patient.
c. Each episode was categorised as appropriate or inappropriate depending on whether criteria for VT or AF/AT were observed (Table 8.1.1).

Electrogram Criteria	
Ventricular (V) Tachycardia	**Atrial (A) Fibrillation/Atrial Tachycardia**
Onset of tachycardia in ventricle	Onset of tachycardia in atrium
V rate > A rate	A rate > V rate
A and V dissociation	V rate predicted by atrial rate
Stable V-V relation	Number of A events > number of V events
V–A timing with retrograde conduction	Unstable/variable V-V
	Variable V to A timing

Table 8.1.1

Criteria for distinguishing VT from AF/AT using device scatterplots and intracardiac EGMs.

Statistical Analysis

Patient demographics are represented as mean ± standard deviation. Data was analysed and presented using Minitab and SPSS. A t-test was used to assess significance and a $p < 0.05$ was regarded as significant. Receiver operator curves (ROC) were used to determine absolute cut-off values that would differentiate AF/AT from VT.

Results

There were 165 DR and 85 BiV ICDs implanted in the cohort. All Medtronic ICDs Entrust, Virtuoso, and later models were included because of familiarity of the observers with the manufacturer's method of data representation, allowing optimal observer diagnostic capability.

A total of 39 episodes were identified in 20 patients over a mean follow-up period of 23 months. The incidence of delivered therapies was 8% in this population. There were 76 sequences of ATP (burst/ramp) delivered in total within these episodes.

Twenty-eight sequences (37%) were categorised as inappropriately delivered for either AF/AT. This was observed despite all but one patient having advanced discriminators programmed on. All elements of PR logic (Medtronic Inc., MN, USA) were selected except for "other 1:1 SVTs", which is nominally off in these devices.

After applying the exclusion criteria listed above, 51 sequences of ATP (n = 18 AT/AF, n = 33 VT) were available for analysis. The mean PPI was 693 ± 96 ms vs 582 ± 83 ms for VF, $p < 0.01$ and mean PPI-TCL was 330 ± 97 ms vs 179 ± 102ms, $p < 0.01$ for AT/AF and VT, respectively (Figures 8.1.2 and 8.1.3).

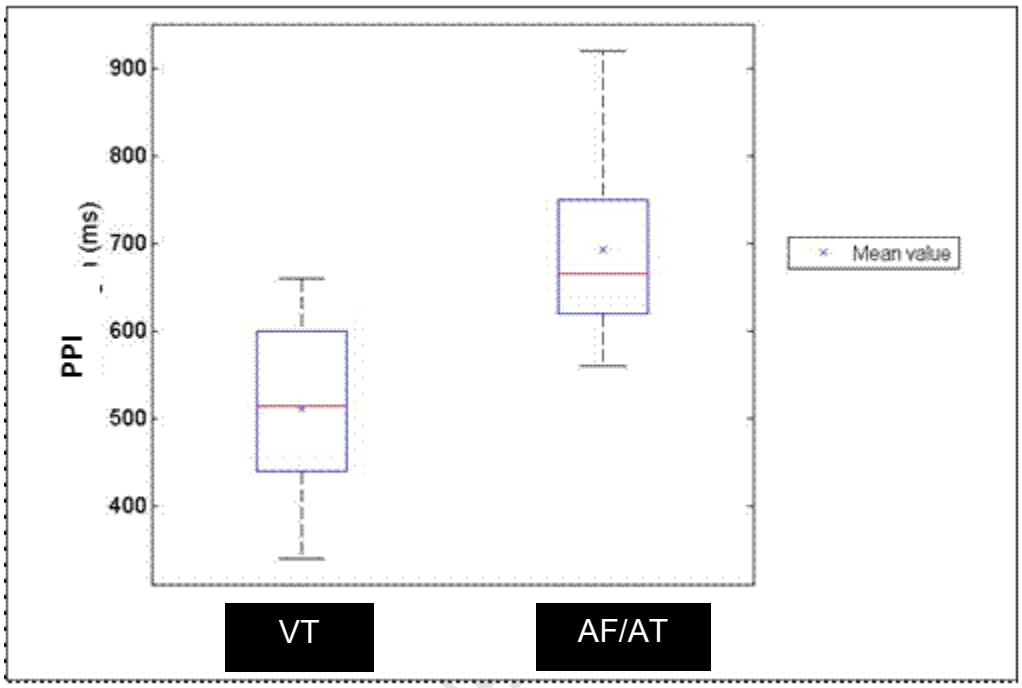

Figure 8.1.2

Distribution of data and means using PPI as a discriminatory tool for AF/AT and VT.

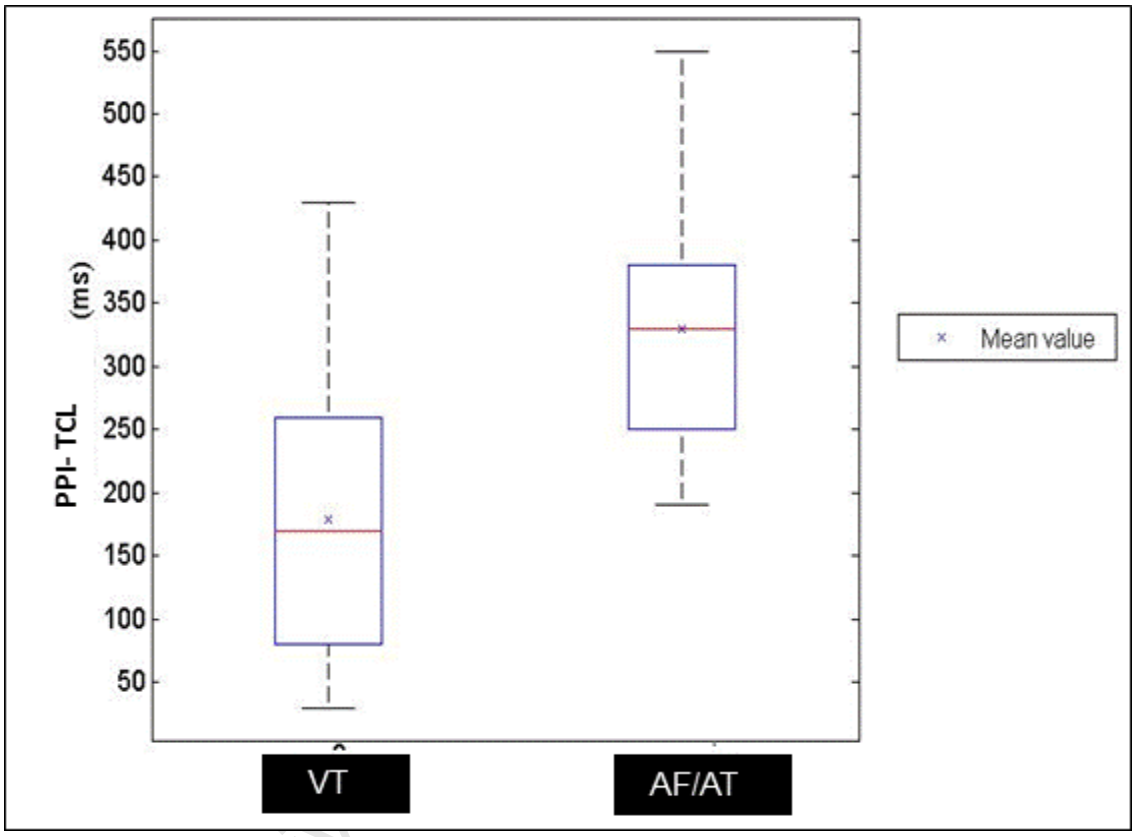

Figure 8.1.3

Distribution of data and means using PPI-TCL as a discriminatory tool for AF/AT and VT.

A ROC curve was applied to both the PPI and PPI-TCL diagnostic criteria to determine an absolute cut-off to that would define VT from conducted AF/AT. Cut-offs of 615 ms, AUC 0.93 (95% CI: 0.84–1.00), $p < 0.01$ for the PPI, and 260 ms, AUC 0.86 (95% CI: 0.74–0.98), $p < 0.01$ for PPI-TCL (Figure 8.1.4) were identified.

When applying these two criteria, a PPI < 615 ms predicted VT, rather than AF/AT with a sensitivity of 77.8% (95% CI: 58.6–97.0%) and a specificity of 87.5% (95% CI: 76.0–99.0%). The positive predictive value (PPV) for AT/AF detection was 77.8% (95%CI 58.6–97%) and the negative predictive value (NPV), i.e. not AT/AF, but VT, was 87.5% (95% CI 76.0–99.0%).

Furthermore, a PPI-TCL with a value < 260 ms was more likely to be VT than AF/AT with a sensitivity of 72.2% (95% CI: 51.5–92.9%) and a specificity of 78.1% (95% CI: 63.8–92.4%). The PPV was 72.2% (95% CI 51.5–92.9%) for AT/AF and the NPV was 78.1% (95%CI 63.8–92.4%), i.e. not AF/AT, but VT detected.

Thus, the predictive value of both parameters had a greater likelihood of diagnosing VT than AF/AT, which is acceptable for a default setting within an ICD where the primary aim is geared towards detecting and treating VT (or VF).

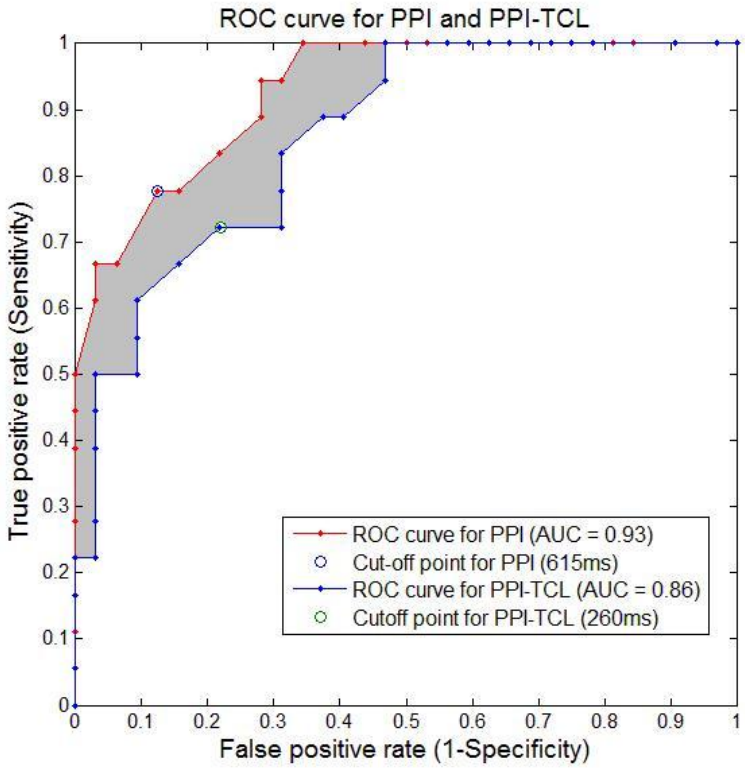

Figure 8.1.4

The ROC curves of PPI and PPI-TCL parameters.

The PPI parameter appears to be more robust with a greater area under the curve (shaded portion).

Discussion

Anti-tachycardia pacing has been shown to successfully terminate VT in over 90% of cases, making this an effective and painless initial therapy in ICDs[67]. As a result, programming strategies usually employ a single sequence of ATP prior to delivery of a shock if the tachycardia is classified as stable despite the cycle length being recorded in a VF detection interval.

If ATP fails to terminate the tachycardia, there is usually an escalation in therapies to defibrillation. Some manufacturers also resort to committed therapies after failure to terminate the episode based on the original diagnostic criteria.

Thus, if there was an incorrect classification of an SVT at the outset, multiple inappropriate shocks may be delivered by the device. This problem is more likely to occur with single chamber ICDs, where the absence of an atrial lead makes diagnosis of VT reliant on rudimentary discriminatory criteria (i.e., rapidity of onset and stability of the tachycardia) and in patients with AF[120].

Some manufacturers also offer a morphology detection algorithm that has been shown to reduce ITS, however, this is also prone to errors in sampling[121].

The above-mentioned study analyses the PPI after a failed episode of ATP until resumption of sensed ventricular intervals by the ICD. Entrainment of a macro re-entrant tachycardia is indicative of the proximity of the pacing electrode to the circuit.

A PPI < 30 ms generally denotes that the pacing stimulus is directly within the macro-re-entrant circuit (Figure 8.1.5). This was not the case for cases with VT (mean PPI of 582 ± 83 ms) or for AF/AT (mean PPI of 693 ± 96 ms), as the site of the re-entrant substrate was very likely to be situated in the left ventricle, particularly for the ischaemic cardiomyopathies. All ICD implants involved lead placement at the right ventricular apex.

Anti-tachycardia pacing was only from the RV electrode in DR ICDs and from both the RV and LV leads in BiV devices. The fact that both ventricles were paced in patients with BiV defibrillators would not affect the principle of using the PPI and PPI-TCL values for VT and AF/AT discrimination.

The ROC curves provide an absolute value where a PPI < 615 ms and a PPI-TCL < 260 ms was more likely to be VT (Figure 8.1.4). However, when reviewing the distribution of all recorded PPI and PPI-TCL values, there were areas of overlap (Figure 8.1.6). The location of the re-entrant substrate possibly in the distant basal-lateral segment of the LV may possibly account for this overlap. The distance from the pacing source in the RV would therefore approximate interval recordings in AT/AF after retrograde invasion of the His-Purkinje system.

A high attrition rate (33%) was recorded for this data in this study. This was because of the strict exclusion criteria that were set in order to maintain the integrity of the measured parameters. These have been defined above.

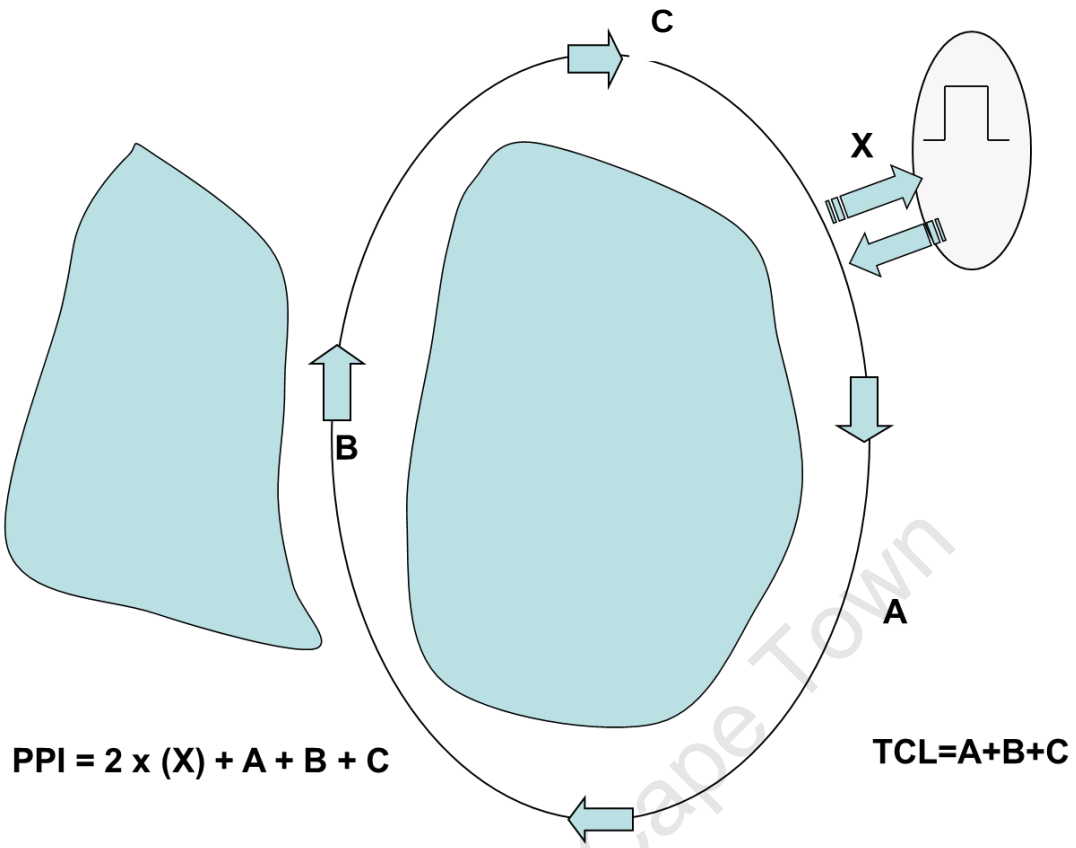

Figure 8.1.5

Representation of entrainment from a pacing site:

Diagrammatic representation of a pacing site at distance X from a macro-re-entrant tachycardia utilizing a critical isthmus. The tachycardia cycle length is a sum of limbs A+B+C.

The post-pacing interval (PPI) would therefore represent 2 x X+ A+B+C as the pacing stimulus would need to penetrate the re-entrant circuit and return to the site of pacing.

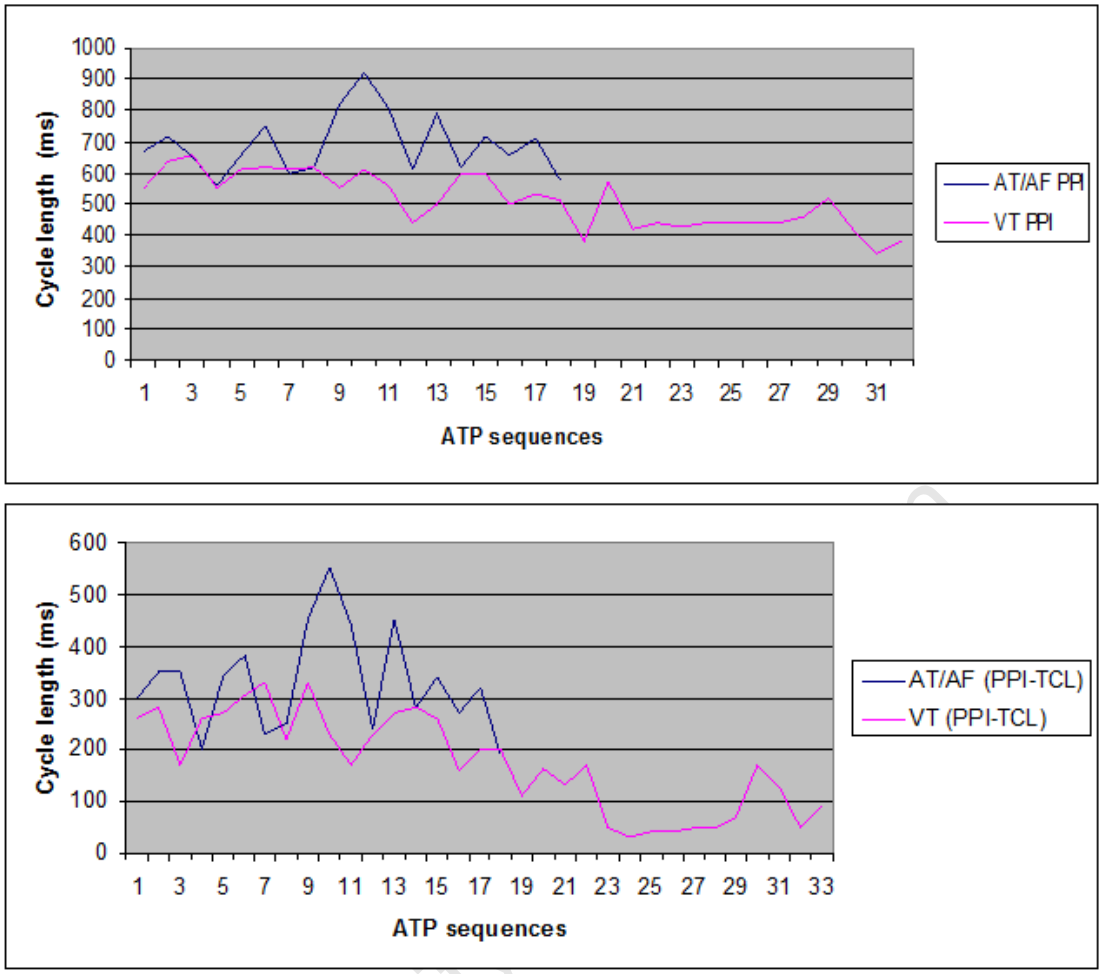

Figure 8.1.6

Simple linear plots of the absolute PPI and PPI-TCL values for AF/AT and VT. These plots show minimal overlap.

In Figure 8.1.7 A and B, an episode of VT is terminated with a resultant pause encroaching within the lower pacing rate of the device. Pacing then continues with the sinus rate being tracked with sequential ventricular pacing in a DDD mode. Termination of VT and resumption of pacing, even for one beat, were regarded as an exclusion from analysis.

Once a tachycardia is classified as VT or VF and therapy is initiated, and if criteria for episode termination are not fulfilled, subsequent therapies may be committed. This phenomenon in some manufacturers may be perpetuated and even escalate therapies for an originally misclassified rhythm disorder.

Rapidly conducted AF (Figure 8.1.8) is detected within the VF zone. Anti-tachycardia pacing in the form of a ramp was unsuccessful in terminating the tachycardia, hence the device proceeds to multiple shocks, which also failed to terminate the AF initially until the fourth shock resolved the AF to a slower AT or sinus tachycardia with conducted ventricular rates below the tachycardia detection interval (TDI). The initial ATP as a ramp, is characterised by long PPI and the PPI-TCL interval in keeping with a tachycardia with a supraventricular origin. This suggests that if these criteria are applied after the initial therapy (ie. ATP) as a downstream" discrimination algorithm, they may indeed abort progression to inappropriate shocks.

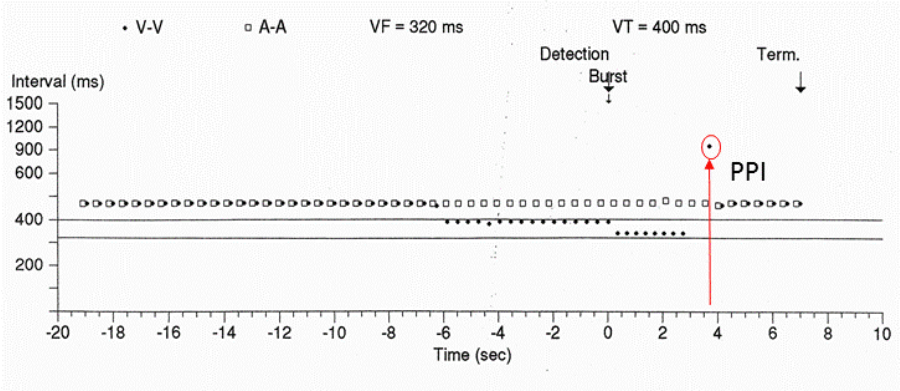

A

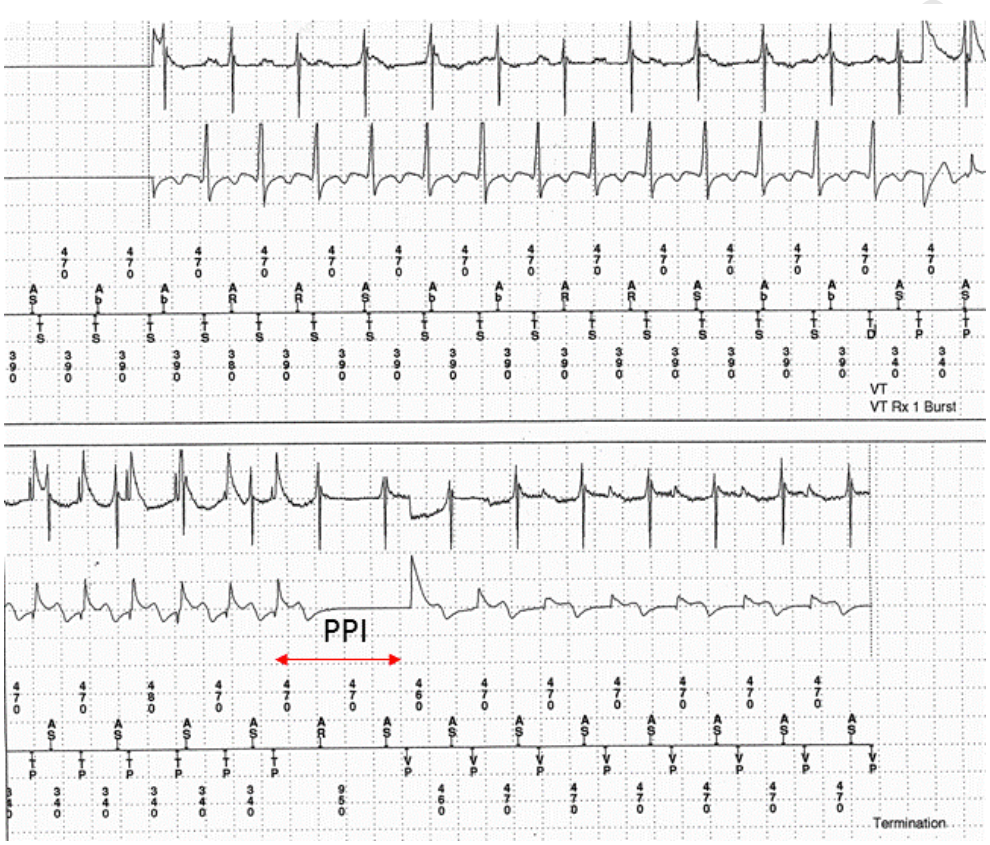

B

Figure 8.1.7

Depiction of VT terminated by an ATP burst yielding a falsely long PPI. Scatterplot (A) and corresponding intracardiac EGM (B) depicting a burst of ATP terminating an episode of VT thus yielding a falsely long PPI.

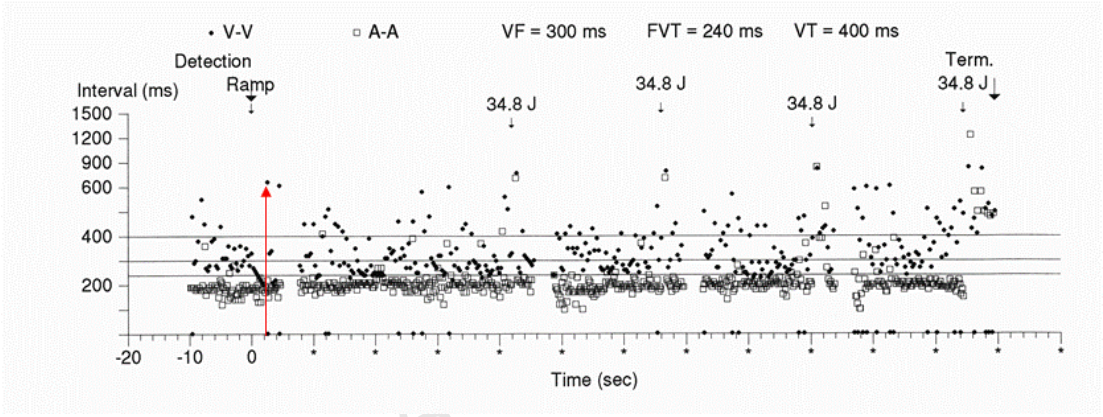

Figure 8.1.8

An episode of rapidly conducted AF into the VT zone resulting in rate determined therapy. The ramp ATP before shocks results in a prolonged PPI of 660 ms (indicated with an arrow) and a PPI (660 ms)–TCL (316 ms average rate) = 314 ms.

At the very least, this concept is fairly intuitive for device specialists when evaluating EGMs in patients presenting with shocks in order to decide if they were in fact appropriate or not.

The next obvious application would be in single chamber devices where the absence of an atrial lead makes these ICDs more prone to result in ITS, and also where it is difficult to interpret the intracardiac EGMs with only ventricular event recordings available. This concept is highlighted in Figure 8.1.9. In this figure, an episode of VT is entrained from ATP in the form of sequential bursts. The PPI intervals after each burst are 380 ms, 400 ms, and 410 ms, with PPI-TCL measurements of 80 ms, 100 ms, and 110 ms. These incremental values are related to shortening of the coupling intervals (nominally 88%, 81%, and 78%) programmed for each burst. On both parameters (PPI < 615 ms and PPI-TCL < 260 ms), criteria are fulfilled to suggest that this, in fact, is true VT and justifies progression to a shock at 22 J, which terminates VT.

The use of the response to ATP in ICDs has been previously studied by Saba and colleagues[122;123]. Their analysis relied on pacing in both the atria and ventricle and they assessed on which chamber the earliest return of tachycardia was recorded in order to differentiate an SVT from VT. Furthermore, it was proposed as a discriminator for 1:1 A to V tachycardias. This study differs, in that discrimination of SVT vs VT is reliant only on a single ventricular lead, making it applicable to single chamber devices as well. It also helps differentiate N:1 tachycardias such as AF/AT from VT and not just 1:1 tachycardias.

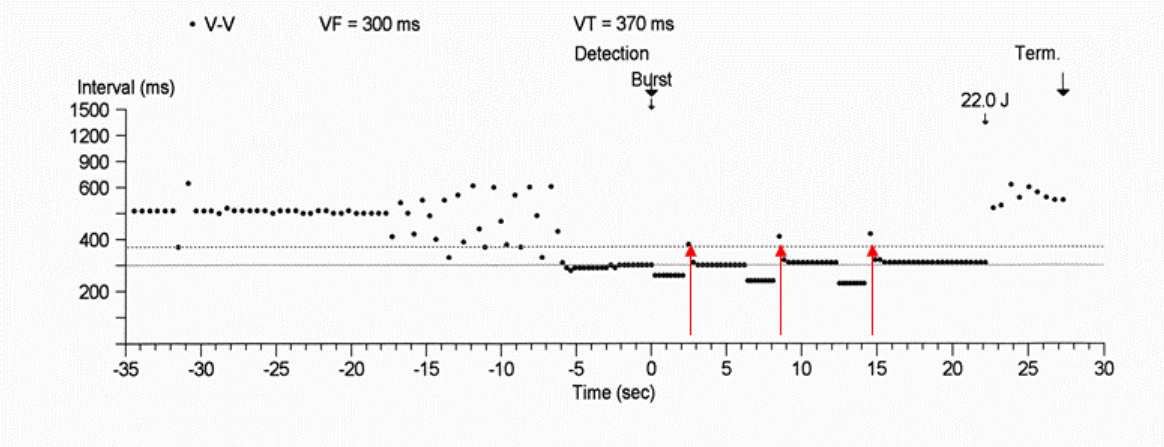

Figure 8.1.9

Scatterplot with only V EGMs in a single chamber device. The chamber of origin of the tachycardia is uncertain, as there is no atrial EGM available. Burst ATP "entrains" VT without termination of the VT. The PPI (indicated) after each burst, is relatively short at 380 ms with a PPI-TCL (380–300) of 80ms making VT the most likely diagnosis and therefore therapy is appropriate.

Limitations

The use of the PPI and PPI-TCL is reliant on the pause that is noted following concealed retrograde penetration of the AVN, specifically in the case of AF/AT. If a retrograde AV block existed, this would be a caveat to interpretation of these parameters. Furthermore, this study is not intended to differentiate re-entrant SVTs viz. AV re-entrant and AV nodal re-entrant tachycardias, which may also account for 1:1 tachycardias and can be difficult to differentiate from VT with retrograde conduction[124;125]. This study evaluated the pause interval post ATP primarily for diagnosis and not the electrogram response. Other studies have shown the diagnostic usefulness of the EGM response post ATP such as a "VAAV" being indicative of underlying AT[126].

Conclusion

The PPI and PPI-TCL difference are established electrophysiological concepts that indicate proximity of a pacing site to the source of a tachycardia. This concept was applied to differentiate VT from AT/AF showing significant differences in the mean values for both these tachycardia sources when identified in DR and BiV ICDs. Although this concept was proven in devices with pre-existing atrial leads, it has potential application as a discriminator in single chamber ICDs with or without morphologic discriminators. It also allows device specialists an additional modality to help interpret difficult ICD derived EGMs when deciding if the delivered therapy was appropriate or not. It has the potential to be incorporated into future device algorithms as a downstream application to re-evaluate the result of the ATP to avoid progression to a shock or committed therapies in the case of ITS for AF/AT. This concept needs further evaluation in a larger prospective study.

Acknowledgements

This project was conceived by my mentor, Dr Damian Redfearn, at the Heart Rhythm Service, Queen's University, Kingston, Ontario, Canada. I drafted the protocol and collected all data. I was also responsible for preparation of the manuscript and presentation of the data at scientific symposia.

Disclosure

This study did not receive funding.

8.2 An Analysis of Inappropriate Therapies in Implantable Cardioverter Defibrillators and Measures to Reduce this Deleterious Effect.

Introduction

Inappropriate therapies from ICDs lead to significant morbidity either from the painful delivery of shocks and from the pro-arrhythmic potential, which includes inappropriately delivered ATP[127]. Prior studies suggest that 15–28% of anti-tachycardia therapies may be inappropriate[113]. Measures to reduce inappropriate shocks, including an empiric ablative strategy, have been shown to reduce the morbidity[128]. It seems intuitive that device specialists should also refine ICD programming to minimise ITS as this is a less invasive option.

These ITS occur more frequently in patients having supraventricular arrhythmias, particularly atrial fibrillation, or in younger patients who achieve higher sinus tachycardia rates[129]. The use of dual chamber devices does improve the algorithmic differentiation of atrial from ventricular arrhythmias but does not completely resolve the problem[130]. I evaluated here the burden of ITS affecting a heterogeneous population of recipients of ICDs with DR or BiV defibrillators with current recommended programming standards.

Methods

This was a single centre retrospective analysis. We examined the overall burden of ITS (ATP/shock) in a cohort of 250 patients implanted with DR and BiV ICDs for both primary and secondary indications over a 23-month follow-up period. Patients without atrial leads were excluded from the analysis. Patients with ITS due to oversensing or detection of non-physiological factors such as “noise” were also excluded from the analysis. This study was therefore streamlined to evaluate the use of ICD programming to discriminate SVTs from VT/VF primarily.

Patients with Medtronic (MN, USA) ICDs: InSynch Sentry, Virtuoso, and later models were included in this study. Events were evaluated by two experienced electrophysiologists.

.

Results

In total, 165 DR and 85 BiV were implanted. Thirty-nine episodes were identified in 20 patients, yielding an event rate of 8% (20/250) over a 23-month period with an average of 1.69 episodes per month (39 episodes/23months) for the whole cohort.

The demographics of patients receiving therapies (ATP and/or shocks) are listed in Table 8.2.1. Of these patients, 4 had devices implanted for a primary indication, while the remaining 16 patients who received therapies had ICDs implanted for a secondary indication. The types of devices were equally distributed with n = 2 DR and n = 2 BiV in the primary indication group and n = 8 DR and n = 8 BiV in the secondary indication group.

All patients (n = 4) implanted for a primary indication had **ITS** for a SVT (AF/AT) while 43% (7/16) of patients implanted for a secondary indication had ITS. The remaining 56% (9/16) in the secondary indication group had an **appropriate therapy** for VT. The overall incidence of ITS delivered was 4% (11/250 patients) in the population (Table 8.2.2).

The records on all patients who received therapies, appropriate or not, were examined. In total, there were 76 sequences of anti-tachycardia pacing (ATP) and 44 shocks delivered. Twenty-six ATP sequences (34%) and 16 (36%) shocks were inappropriate. All but one patient had advanced discriminators (PR logic) turned on.

The supraventricular tachycardias were classified as AT if the atrial EGMs appeared to be regular and as AF if a disorganised and rapid atrial rate (< 200 ms) was recorded. A PSVT (either AVNRT/AVRT) was inferred depending on the response to ATP (VAV vs VAAV response) or termination of SVT without entrainment of the atrium with ATP delivered in the ventricles[126]. The classification and analysis of individual SVT episodes are shown in Table 8.2.3.

No.	Indication	sex	age	Device	Dual/BIV	Episode
1	Secondary	F	78	Virtuoso	Dual	PSVT
2	Secondary	M	76	Virtuoso	Dual	AF
3	Primary	M	62	Virtuoso	Dual	AT
4	Secondary	M	75	Virtuoso	Dual	VT
5	Secondary	F	75	Virtuoso	Dual	VT
6	Secondary	M	82	Virtuoso	Dual	VT
7	Secondary	M	55	Virtuoso	Dual	VT
8	Secondary	M	80	Virtuoso	Dual	VT
9	Secondary	M	73	Virtuoso	Dual	PSVT
10	Primary	M	62	Concerto	BiV	AF
11	Primary	Unknown		Virtuoso	Dual	AF
12	Primary	Unknown		Concerto	BiV	AT
13	Secondary	M	72	InSync Sentry	BiV	AT
14	Secondary	M	72	InSych Sentry	BiV	AF
15	Secondary	F	70	InSynch Sentry	BiV	VT
16	Secondary	F	81	InSynch Sentry	BiV	VT
17	Secondary	M expired	70	InSynch Sentry	BiV	VT
18	Secondary	M expired	73	InSynch Sentry	BiV	AT
19	Secondary	M expired	78	InSyn Sentry	BiV	VT
20	Secondary	M expired	81	InSync Sentry	BiV	AT

Table 8.2.1

Demographic data of patients receiving therapies.

Sequence	ventricular CL	ATP delivered	ATP VT zone 400-370ms	ATP FVT zone 320-240ms	ATP VF zone 320-300ms
1	330	y	Burst		
2	310	y			Burst during charge
3	370	y		Burst	
4	370	y		Burst	
5	370	y		Burst	
6	250	y			Burst during charge
7	350	Y	Burst		
8	340	Y		Burst	
9	350	y		Burst	
10	350	y		Burst	
11	350	y		Burst	
12	350	y		Burst	
13	280	y		Ramp	
14	370	y		Burst	
15	370	y		Burst	
16	370	y		Burst	
17	370	y		Burst	
18	360	y		Burst	
19	360	y		Burst	
20	360	y		Ramp	
21	370	y		Burst	
22	370	y		Burst	
23	380	y	Burst		
24	380	y		Burst	
25	380	y		Ramp	
26	390	y	Burst		

Table 8.2.2

Summary of sequences of ATP delivered inappropriately for SVTs.

Rhythm	atrial CL
PSVT	330
AF	310
AF	370
AF	370
AF	370
AF	250
AT	370
AT	340
AT/PSVT	350
AT/PSVT	350
AT/PSVT	350
AT/PSVT	350
AF	180
AT	190
AT	190
AT	190
AT	190
AT	190
AT	190
AT	190
AT	190
AT	190
AT	190
AT	380
AT	380
AT	380
AF	190

Table 8.2.3

Analysis and classification of SVT episodes eliciting inappropriate therapies.

Discussion

Implantable defibrillators have improved survival in patients at risk of sudden cardiac arrhythmia[131;132]. They have also impacted on the quality of life for patients with heart failure[133]. Despite advances in ICD development and advanced programming, ITS have not been fully overcome. These are also more common in younger individuals because of sinus tachycardia rates approaching the tachycardia detection intervals, as well as in patients with supraventricular arrhythmias, predominantly AF[134]. The delivery of inappropriate shocks has been linked to decreased survival and increased morbidity and measures to reduce this phenomenon are imperative[135].

Advanced discriminators in Medtronic devices (termed “PR logic”) have been demonstrated to have a positive predictive value of 95.2% when therapy is delivered (Medtronic, MN, USA literature on Gem III DR ICD). The study cohort consisted exclusively of patients with Medtronic dual or BiV ICDs. Patients with plugged atrial ports were excluded to allow for all elements of the discriminatory algorithm to be selected. Only one patient did not have additional discrimination parameters engaged, making evaluation of standard programming possible. This would account for the relatively low (4% or 11/250 patients) incidence of ITS in the population studied[136].

The study population entailed a cross section of patients, with a predominance of patients with secondary indications for ICD implantation (80%) while the remaining patients had a primary indication. Only 4 patients implanted with a

primary indication for an ICD received therapies. All of them were delivered inappropriately with EGM analysis revealing underlying AF or AT.

This is keeping with prior data showing a higher incidence of ITS in patients having an ICD for a primary indication[137]. The 16 patients in the secondary indication arm that received therapies had a 43% incidence of ITS, again characterised by inappropriate classification of AF/AT with 1 suspected PSVT.

Anti-tachycardia pacing was the initial therapy in all episodes whether it was classified as VT or a SVT. This regimen was a product of the PainFREE Rx II study protocol[67]. This would allow for at least one burst of ATP even in the VF zone in order to terminate fast VT during a capacitor charge to obviate the need for a shock if the former was ineffective. The categorisation of ITS was therefore based on delivery of ATP rather than shock in this study to increase the detection rate of these episodes. This, however, does not mean that ATP is innocuous. The delivery of rapid ventricular pacing may well be pro-arrhythmic, particularly in the population served given the likelihood of an underlying macro re-entrant substrate[138].

Ultimately, there were 44 shocks delivered with 36% (n = 16) of these delivered for an SVT. However, 6 episodes of ATP succeeded in terminating the SVT. This may be understandable if the ventricle was integral in maintaining the tachycardia or if advancement of the atrium occurred in a case of termination of AT, but this does not explain the cases of AF that were declared terminated.

The latter may presumably have been a consequence of retrograde penetration of the AVN, thus slowing conduction to the ventricle and subsequently reducing the conducted rate to below the tachycardia detection interval (TDI) of the device.

In the case of true VT, ATP successfully terminated VT in 33% (14/28) of cases with 67% (28/42) eventually requiring a shock.

Programming measures that may reduce the risk of an ITS include:

1. Programming a higher TDI in patients with AF/AT or in the case of younger patients receiving ICDs where a higher intrinsic sinus rate may be anticipated.
2. Avoid programming ONSET and STABILITY discriminators as these tend to require fewer detection intervals to evaluate a rhythm, therefore dominating over other more sensitive algorithms thus increasing the chance of ITS.
3. Programming a slower VT detection interval with advanced discriminators so even if an inappropriate shock is delivered it is synchronised to a R wave and thus there is less chance of ventricular arrhythmia induction.
4. If a VT zone is considered, advanced discriminators should be applied to overlap into the VF zone. This is referred to as the “SVT limit” in Medtronic devices and although this was nominally 320 ms in the above-mentioned devices, the current standard is an application of “PR Logic” discrimination up to 260 ms.

Therefore, there may be a place for patient-tailored device programming to minimise the risk of ITS in those at risk of this phenomenon. We do not discount the fact that for the remaining population receiving ICDs, there is merit in an empiric programming regimen[139].

Limitations

The small population size studied makes it difficult to make recommendations on intervention. However, the low incidence of ITS in this cohort validates the effectiveness of the programming measures we adopted in these patients.

Conclusion

The burden of ITS in the population of patients receiving ICDs was 4%, significantly lower than in other studies. This may be a consequence of the presence of atrial leads in all patients and of rationalised programming criteria including having advanced discriminators on. In addition there was a predominance of patients with secondary indications for ICDs as those with primary indications have a higher incidence of ITS.

Acknowledgements

I designed the protocol and conducted this study at the Heart Rhythm Service, Kingston General Hospital, Ontario, Canada.

Disclosure

This study did not receive funding.

9. Conclusion

Implantable defibrillator technology has evolved dramatically and indications have expanded. However, battery longevity, device volume, and the pursuit of painless therapies remain subjects for further investigation.

Defibrillator therapies were evaluated in this work on two levels. Given the need for multiple VF inductions and defibrillations to assess novel, waveform, and vectoral configurations, these studies were conducted in a porcine model. The porcine cardiac structure is similar to man and has been used in prior defibrillation studies, given its resilience to multiple shocks. At the same time however, there are obvious thoracic shape differences, namely a more rounded diameter in the pig vs. the reduced antero-posterior diameter seen in man. In addition, the cardiac longitudinal axis in the pig faces more anteriorly towards the sternal midline as opposed to a left and inferior orientation in humans. These factors undoubtedly contributed to outcomes in these experiments, particularly for subcutaneous defibrillation configurations.

The clinical chapters dealt with the utility of ATP for SVT and VT discrimination as well as evaluated the overall burden of ITS in a typical clinical cohort. These two factors remain topical and challenging despite advances with algorithm development for rhythm discrimination.

In Chapter 4.1. I examined the effect of a preshock delivered endocardially before a standard, definitive biphasic shock from a serial capacitance and single prototype ICD (Ela Medical, Sorin Group, France).

Other studies have looked at delivery of a preshock from epicardial sites and from within the middle cardiac vein. This study was designed to evaluate the prototype device as well as to investigate the effect on DFTs. The monophasic preshock and biphasic shock were delivered with a similar Can(+) > RV(-) polarity at ISIs of 16, 31, and 47 ms.

No significant differences in DFTs were obtained, but equivalent DFTs were noted with the 16 ms ISI, and a trend to increasing DFTs with the higher ISIs. The mechanism by which the subthreshold preshock may influence DFTs was postulated to prolong the ensuing ISW, allowing the biphasic definitive to be delivered into the period of electrical quiescence thus preventing the re-initiation of VF. However, this did not translate into overall DFT reduction. A limitation of this study was that the ISI were arbitrarily programmed into the prototype device and based on prior optical mapping studies that defined the duration of the ISW.

Given the nominal energy delivery contained within the preshock (2.0–9.6 J delivered in a 1:2 ratio with the biphasic shock), the actual ISW after the preshock may have been smaller than previously defined. This was evaluated as a limitation of this study.

Recent data have suggested that the convention of having the RV electrode as cathodal during the first phase of a shock waveform may be deleterious. An anodal configuration allows implosion of colliding defibrillating, high voltage wavefronts in the virtual electrode around the RV lead. The second experiment in Chapter 4.2 therefore dealt with assessing the effect of preshock polarity on

defibrillation efficacy while keeping the optimal ISI evaluated in the preceding chapter fixed at 16 ms.

The prototype defibrillator was again employed to deliver the sequential shock waveform and it allowed manipulation of the preshock waveform polarity through its custom software (elaterm, Ela-Medical, Sorin Group, France). No significant reduction in DFTs occurred with inversion of preshock polarity. This may in part be explained again by the nominal energy delivery from the preshock, which has not affected a critical mass of myocardium in order to influence significant outcome differences. In addition, the duration of the subsequent ISW may not have been influenced by polarity change.

In a clinical setting, patients with high DFTs may have additional electrodes implanted in extracardiac sites but it is not known if just adding an additional RV defibrillator electrode would be beneficial. In Chapter 5, two 7F narrow diameter RV defibrillator leads were placed at an RV apical and at RVOT+RV apical sites to evaluate both these options as the combined MES against the conventional RV apical lead placement strategy. The MES obtained an overall 25% reduction in DFT, but 22% (2/9) of studies yielded equivalent DFTs. The MES strategy is therefore a feasible option when faced with high DFTs. Furthermore, the use of newer generation 7F lead technology allows greater ability to position defibrillator leads onto the RV septum and helps to minimize obstruction to venous flow and tricuspid valve function.

Subcutaneous ICD systems have become topical particularly in the paediatric population. Here, TDF was evaluated against a conventional EDF strategy (Chapter 6.1). Transthoracic defibrillation, using a precordial subcutaneously implanted ICD with a posteriorly located SQA, consistently defibrillated all subjects, and was significantly higher than EDF. Further, TDF was dramatically influenced by marginal increments in the weight of the animals, suggesting that higher energy devices should be a consideration when implanting a subcutaneous ICD system.

The optimal transthoracic lead and ICD position has not been determined and clinical implants have entailed ICD placement in the mid axillary line with an array placed in the parasternal region. The result is aesthetically poor and potentially restrictive to upper arm motion. Chapter 6.2 deals with varying ICD and SQA positions to obtain the optimal TDF configuration. A left precordial ICD Can position with a single SQA array positioned around to the posterior thoracic wall proved as effective as combining two SQAs also in this posterior thoracic location. Minor vectoral variation by separation of the posteriorly placed SQA arrays that widened the shock vector to interpose more cardiac tissue between the precordial ICD and the SQAs did not influence DFT outcomes. This implies than the single SQA and ICD is an adequate subcutaneous system, and minimizes implantation time and the amount of surgical intervention required to place multiple SQAs.

In the preceding chapter, the addition of a posterior SQA, essentially increased the posterior cathode, in Chapter 6.3, the anterior chest wall anode was

extended beyond the ICD Can to add a short experimental15 cm SQA to the right parasternal position, and this was inserted into the SVC port of the ICD. This, however, resulted in a mean rise of 4.7 ± 3.3 J in DFTs, and 4/6 cases had a DFT ≥ 30 J. This impaired DFT may be explained by current shunting between the ICD and the SQA, which also accounts for the significant drop in shock impedances.

The final animal experiment in this manuscript was a pilot project showing the feasibility of percutaneous delivery of an SVC defibrillation electrode into the PPS and then assessing DFTs using a precordial and subcutaneously placed ICD vs. a conventional endocardial RV apical electrode vs. a subcutaneous ICD system with a single subcutaneous ICD placed posteriorly around the chest wall. The electrode placement into the PPS was safely performed but DFTs proved equivalent to the subcutaneous system.

In the clinical chapters, painless ICD therapy namely, ATP was evaluated as a discriminator to differentiate AF/AT from VT. This was evaluated in dual chamber ICDs for proof of concept, but its application is intended for single chamber devices where the absence of atrial electrograms can make rhythm discrimination difficult.

The pause after ATP that fails to terminate or significantly perturb the tachycardia cycle length was then evaluated. The pause after ATP until the return of the sensed tachycardia on the ventricular channel, described as the PPI was evaluated. A cut-off of PPI < 615 ms and the correction factor of PPI and ambient

PPI-TCL difference < 260 ms predicted VT, and higher values suggest AF/AT as the mechanism of arrhythmia.

Inappropriate ICD therapy delivery remains a substantial problem. Analysis of a typical heterogeneous cohort of 250 patients revealed an event rate of 8% of ICD therapies over a 2-year follow-up period. Half of these therapies (4%) were inappropriate for AF/AT. This was significantly lower than other quoted studies, but reflects a selection bias and the fact that physician tailored therapy zone programming was employed in the presence of recognized concomitant SVTs.

10. Future Directions

Myocardial dysfunction increases the risk of sudden cardiac death, but the predominant clinical manifestation is heart failure. Device-based therapy in the form of cardiac resynchronization is used as adjunctive management in eligible patients and is frequently coupled with ICD therapy.

Defibrillation from an electrode within the coronary sinus has shown promise, yielding reduced DFTs. The ICD Can has always been included in these studies

Therefore, it seems reasonable to assume that if the left ventricular pace/sense lead that was being deployed within a coronary sinus branch was capable of incorporating a high voltage defibrillation electrode, it would be conceivable to deliver a shock from the left ventricle as well. Taking this a step further, if the ICD and SVC electrodes were programmed out of the circuit and the shock vector was maintained merely between the RV and LV electrodes, and then bystander non-cardiac tissue from the thorax could be excluded from the shocking circuit.

This may result in lower impedance to the shock and greater current delivery to the ventricular myocardium. This may translate into lower DFTs and possibly minimise pain from the shock by eliminating pain-sensitive structures from the defibrillation circuit.

Thus biventricular defibrillation may therefore be included as a programmable option in new generation ICDs. The LV lead position from effective CRT is typically at the lateral wall of the left ventricle, which is a likely site for macro-re-

entrant substrate in ischaemic aetiologies. This makes ATP from the LV lead effective, as it is delivered closer to the re-entrant circuit. Therefore, delivery of the shock closer to the scar may be more efficacious.

Fibrillating myocardium represents heterogeneous regions of depolarization and repolarisation. The depolarising wavefront from a delivered shock may encounter regions of myocardium that are refractory, making the activation here superfluous. If a sub-threshold high frequency burst of alternating current such as that which is used to induce VF in the ICD is delivered just prior to delivery of the shock, this may serve to homogenise the overall myocardial charge prior to shock delivery this reducing DFTs. This would, however, require specific calibration of the ICD to deliver this discharge from a single device else a serial arrangement of two ICDs with timed delivery would be required to achieve this sequential discharge.

The PPI and PPI-TCL parameters that have been shown to help discriminate AF/AT and VT in the clinical cohort studied here need to be validated in a larger population. It has the potential to be incorporated as a downstream discrimination algorithm post-delivery of ATP. This will help differentiate inappropriate from appropriate ATP delivery and abort progression to a shock, if deemed inappropriate. This potentially will avoid painful discharges and reduce unnecessary battery charges.

Reference List

(1) Kastor JA. Michel Mirowski and the automatic implantable defibrillator. Am J Cardiol 1989; 63(13):977-982.

(2) Tchou PJ. Fixed tilt or programmable pulse widths: are we creatures of habit? Heart Rhythm 2006; 3(5):542-543.

(3) Jung J, Heisel A, Fries R et al. Tolerability of internal low-energy shock strengths currently needed for endocardial atrial cardioversion. Am J Cardiol 1997; 80(11):1489-1490.

(4) Tokano T, Bach D, Chang J et al. Effect of ventricular shock strength on cardiac hemodynamics. J Cardiovasc Electrophysiol 1998; 9(8):791-797.

(5) Morgan SW, Plank G, Biktasheva IV et al. Low Energy Defibrillation in Human Cardiac Tissue: A Simulation Study. Biophys J 2009; 96(4):1364-1373.

(6) Wilkoff BL, Williamson BD, Stern RS et al. Strategic programming of detection and therapy parameters in implantable cardioverter-defibrillators reduces shocks in primary prevention patients: results from the PREPARE (Primary Prevention Parameters Evaluation) study. J Am Coll Cardiol 2008; 52(7):541-550.

(7) Morillo CA, Baranchuk A. Deductive electrophysiology in the modern device technology era: the quest for the prevention of inappropriate ICD shocks. J Cardiovasc Electrophysiol 2005; 16(6):606-607.

(8) Washizuka T, Chinushi M, Tagawa M et al. Inappropriate discharges by fourth generation implantable cardioverter defibrillators in patients with ventricular arrhythmias. Jpn Circ J 2001; 65(11):927-930.

(9) Fye WB. Ventricular fibrillation and defibrillation: historical perspectives with emphasis on the contributions of John MacWilliam, Carl Wiggers, and William Kouwenhoven. Circulation 1985; 71(5):858-865.

(10) Zipes DP JJ. From Cell to Bedside. **Philidelphia,PA.**: **Saunders/Elsevier**, 2009

(11) Chen PS, Shibata N, Dixon EG et al. Comparison of the defibrillation threshold and the upper limit of ventricular vulnerability. Circulation 1986; 73(5):1022-1028.

(12) Walcott GP, Walcott KT, Ideker RE. Mechanisms of defibrillation. Critical points and the upper limit of vulnerability. J Electrocardiol 1995; 28 Suppl:1-6.

(13) Chattipakorn N, Kenknight BH, Rogers JM et al. Locally propagated activation immediately after internal defibrillation. Circulation 1998; 97(14):1401-1410.

(14) Chen PS, Shibata N, Dixon EG et al. Activation during ventricular defibrillation in open-chest dogs. Evidence of complete cessation and regeneration of ventricular fibrillation after unsuccessful shocks. J Clin Invest 1986; 77(3):810-823.

(15) Bourn DW, Gray RA, Trayanova NA. Characterization of the relationship between preshock state and virtual electrode polarization-induced propagated graded responses resulting in arrhythmia induction. Heart Rhythm 2006; 3(5):583-595.

(16) Constantino J, Long Y, Ashihara T et al. Tunnel propagation following defibrillation with ICD shocks: hidden postshock activations in the left ventricular wall underlie isoelectric window. Heart Rhythm 2010; 7(7):953-961.

(17) Morgan JM, Marinskis G. Defibrillation testing at the time of implantable cardioverter defibrillator implantation: results of the European Heart Rhythm Association survey. Europace 2011; 13(4):581-582.

(18) Michowitz Y, Lellouche N, Contractor T et al. Defibrillation threshold testing fails to show clinical benefit during long-term follow-up of patients undergoing cardiac resynchronization therapy defibrillator implantation. Europace 2011; 13(5):683-688.

(19) Verma A, Kaplan AJ, Sarak B et al. Incidence of very high defibrillation thresholds (DFT) and efficacy of subcutaneous (SQ) array insertion during implantable cardioverter defibrillator (ICD) implantation. J Interv Card Electrophysiol 2010; 29(2):127-133.

(20) Gurev V, Maleckar MM, Trayanova NA. Cardiac defibrillation and the role of mechanoelectric feedback in postshock arrhythmogenesis. Ann N Y Acad Sci 2006; 1080:320-333.

(21) Jacob S, Pidlaoan V, Singh J et al. High Defibrillation Threshold: The Science, Signs and Solutions. Indian Pacing Electrophysiol J 2010; 10(1):21-39.

(22) Hohnloser SH, Dorian P, Roberts R et al. Effect of amiodarone and sotalol on ventricular defibrillation threshold: the optimal pharmacological therapy in cardioverter defibrillator patients (OPTIC) trial. Circulation 2006; 114(2):104-109.

(23) Iavelov IS. [Implantable cardioverter defibrillator does not eliminate need for antiarrhythmic drugs in secondary prevention of life threatening ventricular arrhythmias. Results of OPTIC trial]. Kardiologiia 2006; 46(3):74-75.

(24) Deharo JC, Mouliom F, Salamand A et al. [Role of antiarrhythmic drugs in reducing the number of defibrillation shocks]. Arch Mal Coeur Vaiss 2005; 98(2):140-144.

(25) Paisey JR, Yue AM, Bessoule F et al. Passive electrode effect reduces defibrillation threshold in bi-filament middle cardiac vein defibrillation. Europace 2006; 8(2):113-117.

(26) Gold M, Val-Mejias J, Leman RB et al. Optimization of superior vena cava coil position and usage for transvenous defibrillation. Heart Rhythm 2008; 5(3):394-399.

(27) Mouchawar GA, Wolsleger WK, Doan PD et al. Does an SVC electrode further reduce DFT in a hot-can ICD system? Pacing Clin Electrophysiol 1997; 20(1 Pt 2):163-167.

(28) Natarajan S, Henthorn R, Burroughs J et al. "Tuned" defibrillation waveforms outperform 50/50% tilt defibrillation waveforms: a randomized multi-center study. Pacing Clin Electrophysiol 2007; 30 Suppl 1:S139-S142.

(29) Mouchawar G, Kroll M, Val-Mejias JE et al. ICD waveform optimization: a randomized, prospective, pair-sampled multicenter study. Pacing Clin Electrophysiol 2000; 23(11 Pt 2):1992-1995.

(30) Roberts PR, Allen S, Smith DC et al. A systematic evaluation of conventional and novel transvenous pathways for defibrillation. J Interv Card Electrophysiol 1999; 3(3):231-238.

(31) Qi X, Dorian P. Antiarrhythmic drugs and ventricular defibrillation energy requirements. Chin Med J (Engl) 1999; 112(12):1147-1152.

(32) van Welsenes GH, Borleffs CJW, van Rees JB et al. Improvements in 25 Years of Implantable Cardioverter Defibrillator Therapy. Neth Heart J 2011; 19(1):24-30.

(33) Ellenbogen KA, Wood MA. Cardiac Pacing and ICDs. 4 ed. Massachusetts, USA: Blackwell Pulishings Inc., 2011

(34) DiCori A., Bongiorni MG, Zucchelli G et al. Transvenous extraction performance of expanded polytetrafluoroethylene covered ICD leads in comparison to traditional ICD leads in humans. Pacing Clin Electrophysiol 2010; 33(11):1376-1381.

(35) Friedman PA, Rasmussen MJ, Grice S et al. Defibrillation thresholds are increased by right-sided implantation of totally transvenous implantable cardioverter defibrillators. Pacing Clin Electrophysiol 1999; 22(8):1186-1192.

(36) Rinaldi CA, Simon RD, Geelen P et al. A randomized prospective study of single coil versus dual coil defibrillation in patients with ventricular arrhythmias undergoing implantable cardioverter defibrillator therapy. Pacing Clin Electrophysiol 2003; 26(8):1684-1690.

(37) Kidwai BJ, Allen JD, Harbinson MT et al. Waveform optimization for internal atrial defibrillation: effects of waveform rounding, phase duration, and voltage swing. Pacing Clin Electrophysiol 2001; 24(8 Pt 1):1198-1207.

(38) Kidwai BJ, McIntyre A, Anderson J et al. Optimization of transthoracic ventricular defibrillation-biphasic and triphasic shocks, waveform rounding, and synchronized shock delivery. J Electrocardiol 2002; 35(3):235-244.

(39) Swerdlow CD, Fan W, Brewer JE. Charge-burping theory correctly predicts optimal ratios of phase duration for biphasic defibrillation waveforms. Circulation 1996; 94(9):2278-2284.

(40) Denman RA, Umesan C, Martin PT et al. Benefit of millisecond waveform durations for patients with high defibrillation thresholds. Heart Rhythm 2006; 3(5):536-541.

(41) Knisley SB, Hill BC, Ideker RE. Virtual electrode effects in myocardial fibers. Biophys J 1994; 66(3 Pt 1):719-728.

(42) Efimov IR, Cheng YN, Biermann M et al. Transmembrane voltage changes produced by real and virtual electrodes during monophasic defibrillation shock delivered by an implantable electrode. J Cardiovasc Electrophysiol 1997; 8(9):1031-1045.

(43) Fedorov VV, Nikolski VP, Efimov IR. Effect of electroporation on cardiac electrophysiology. Methods Mol Biol 2008; 423:433-448.

(44) Dosdall DJ, Fast VG, Ideker RE. Mechanisms of defibrillation. Annu Rev Biomed Eng 2010; 12:233-258.

(45) Kroll MW, Efimov IR, Tchou PJ. Present understanding of shock polarity for internal defibrillation: the obvious and non-obvious clinical implications. Pacing Clin Electrophysiol 2006; 29(8):885-891.

(46) Liu QM, Bai ZL, Liu ZJ et al. Defibrillation threshold testing: is it necessary during implantable cardioverter-defibrillator implantation? Med Hypotheses 2009; 72(2):147-149.

(47) Swerdlow CD, Russo AM, Degroot PJ. The dilemma of ICD implant testing. Pacing Clin Electrophysiol 2007; 30(5):675-700.

(48) Seidl K, Denman RA, Moulder JC et al. Stepped defibrillation waveform is substantially more efficient than the 50/50% tilt biphasic. Heart Rhythm 2006; 3(12):1406-1411.

(49) Swerdlow CD, Ahern T, Kass RM et al. Upper limit of vulnerability is a good estimator of shock strength associated with 90% probability of successful defibrillation in humans with transvenous implantable cardioverter-defibrillators. J Am Coll Cardiol 1996; 27(5):1112-1118.

(50) Chen PS, Swerdlow CD, Hwang C et al. Current concepts of ventricular defibrillation. J Cardiovasc Electrophysiol 1998; 9(5):553-562.

(51) KIM SC, VASANJI A, Efimov IR et al. Spatial Distribution and Extent of Electroporation by Strong Internal Shock in Intact Structurally Normal and Chronically Infarcted Rabbit Hearts. J Cardiovasc Electrophysiol 2008; 19(10):1080-1089.

(52) Mowrey KA, Efimov IR, Cheng Y. Membrane Time Constant During Internal Defibrillation Strength Shocks in Intact Heart: Effects of Na+ and Ca2+ Channel Blockers. J Cardiovasc Electrophysiol 2009; 20(1):85-92.

(53) Antzelevitch C, Yan GX, Shimizu W. Transmural dispersion of repolarization and arrhythmogenicity: the Brugada syndrome versus the long QT syndrome. J Electrocardiol 1999; 32 Suppl:158-165.

(54) Antzelevitch C. The Role of Spatial Dispersion of Repolarization in Inherited and Acquired Sudden Cardiac Death Syndromes. Am J Physiol Heart Circ Physiol 2007; 293(4):H2024-H2038.

(55) Matiukas A, Pertsov AM, Kothari P et al. Optical Mapping of Electrical Heterogeneities in the Heart During Global Ischemia. Conf Proc IEEE Eng Med Biol Soc 2009; 2009:6321-6324.

(56) Karch SB, Billingham ME. Morphologic effects of defibrillation: a preliminary report. Crit Care Med 1984; 12(10):920-921.

(57) Ehsani A, Ewy GA, Sobel BE. Effects of electrical countershock on serum creatine phosphokinase (CPK) isoenzyme activity. Am J Cardiol 1976; 37(1):12-18.

(58) Kleiman RB, Callans DJ, Hook BG et al. Effectiveness of noninvasive programmed stimulation for initiating ventricular tachyarrhythmias in patients with third-generation implantable cardioverter defibrillators. Pacing Clin Electrophysiol 1994; 17(9):1462-1468.

(59) Swerdlow CD, Shehata M, Chen PS. Using the upper limit of vulnerability to assess defibrillation efficacy at implantation of ICDs. Pacing Clin Electrophysiol 2007; 30(2):258-270.

(60) Oseroff O, Retyk E, Bochoeyer A. Subanalyses of secondary prevention implantable cardioverter-defibrillator trials: antiarrhythmics versus implantable defibrillators (AVID), Canadian Implantable Defibrillator Study (CIDS), and Cardiac Arrest Study Hamburg (CASH). Curr Opin Cardiol 2004; 19(1):26-30.

(61) Connolly SJ, Hallstrom AP, Cappato R et al. Meta-analysis of the implantable cardioverter defibrillator secondary prevention trials. AVID, CASH and CIDS studies. Antiarrhythmics vs Implantable Defibrillator study. Cardiac Arrest Study Hamburg . Canadian Implantable Defibrillator Study. Eur Heart J 2000; 21(24):2071-2078.

(62) Bocker D, Breithardt G. Evaluating AVID, CASH, CIDS, CABG-patch and MADIT: are they concordant? J Interv Card Electrophysiol 2000; 4 Suppl 1:103-108.

(63) Franqui-Rivera H, Sotomonte JC. Implantable cardioverter-defibrillators for primary prevention of sudden cardiac death in patients with left ventricular systolic dysfunction: 14 years after MADIT. P R Health Sci J 2011; 30(2):78-83.

(64) Budde T. AICD treatment in 2004--state of the art. Eur J Med Res 2006; 11(10):432-438.

(65) Blumenthal TD, Burnett TT, Swerdlow CD. Prepulses reduce the pain of cutaneous electrical shocks. Psychosom Med 2001; 63(2):275-281.

(66) Tandri H. ICD Shocks : Not just the Straw That Broke The Camels Back. Heart Rhythm 2010; 7(6):761-762.

(67) Sweeney MO, Wathen MS, Volosin K et al. Appropriate and inappropriate ventricular therapies, quality of life, and mortality among primary and secondary prevention implantable cardioverter defibrillator patients: results from the Pacing Fast VT REduces Shock ThErapies (PainFREE Rx II) trial. Circulation 2005; 111(22):2898-2905.

(68) Gross D. Animal Models in Cardiovascular Research. Boston: Martinus Hijhoff Publishers, 2011

(69) Kenknight BH, Walker RG, Ideker RE. Marked reduction of ventricular defibrillation threshold by application of an auxiliary shock to a catheter electrode in the left posterior coronary vein of dogs. J Cardiovasc Electrophysiol 2000; 11(8):900-906.

(70) Howe BB, Fehn PA, Pensinger RR. Comparative anatomical studies of the coronary arteries of canine and porcine hearts. I. Free ventricular walls. Acta Anat (Basel) 1968; 71(1):13-21.

(71) Bowman TA, Hughes HC. Ventriculoatrial conduction in swine during cardiac pacing: animal model for retrograde conduction. Am Heart J 1984; 108(2):337-341.

(72) Martin DR, Brown CG, Dzwonczyk R. Frequency analysis of the human and swine electrocardiogram during ventricular fibrillation. Resuscitation 1991; 22(1):85-91.

(73) Cox JE, Done SH, Lees P et al. Preliminary studies of the actions of alphaxalone and alphadolone in the pig. Vet Rec 1975; 97(25-26):497-498.

(74) Faulknier BA, Traub DM, Aktas MK et al. Time-dependent risk of Fidelis lead failure. Am J Cardiol 2010; 105(1):95-99.

(75) Kroll MW. A minimal model of the single capacitor biphasic defibrillation waveform. Pacing Clin Electrophysiol 1994; 17(11 Pt 1):1782-1792.

(76) Chattipakorn N, Banville I, Gray RA et al. Mechanism of ventricular defibrillation for near-defibrillation threshold shocks: a whole-heart optical mapping study in swine. Circulation 2001; 104(11):1313-1319.

(77) Chattipakorn N, Fotuhi PC, Chattipakorn SC et al. Three-dimensional mapping of earliest activation after near-threshold ventricular defibrillation shocks. J Cardiovasc Electrophysiol 2003; 14(1):65-69.

(78) Wang NC, Lee MH, Ohara T et al. Optical mapping of ventricular defibrillation in isolated swine right ventricles: demonstration of a postshock isoelectric window after near-threshold defibrillation shocks. Circulation 2001; 104(2):227-233.

(79) Chattipakorn N, Shinlapawittayatorn K, Chattipakorn S. Electrophysiological Mechanisms of Ventricular Fibrillation Induction. Indian Pacing Electrophysiol J 2005; 5(1):43-50.

(80) Trayanova N. Drawing the curtain on the isoelectric window? Heart Rhythm 2007; 4(6):766-767.

(81) Hwang GS, Tang L, Joung B et al. Superiority of biphasic over monophasic defibrillation shocks is attributable to less intracellular calcium transient heterogeneity. J Am Coll Cardiol 2008; 52(10):828-835.

(82) Tang L, Hwang GS, Hayashi H et al. Intracellular calcium dynamics at the core of endocardial stationary spiral waves in Langendorff-perfused rabbit hearts. Am J Physiol Heart Circ Physiol 2008; 295(1):H297-H304.

(83) Kroll MW, Swerdlow CD. Optimizing defibrillation waveforms for ICDs. J Interv Card Electrophysiol 2007; 18(3):247-263.

(84) Tereshchenko LG, Faddis MN, Fetics BJ et al. Transient Local Injury Current in Right Ventricular Electrogram after ICD Shock Predicts Heart Failure Progression. J Am Coll Cardiol 2009; 54(9):822-828.

(85) Zhang Y, Ramabadran RS, Boddicker KA et al. Triphasic waveforms are superior to biphasic waveforms for transthoracic defibrillation: experimental studies. J Am Coll Cardiol 2003; 42(3):568-575.

(86) Zhang Y, Rhee B, Davies LR et al. Quadriphasic waveforms are superior to triphasic waveforms for transthoracic defibrillation in a cardiac arrest swine model with high impedance. Resuscitation 2006; 68(2):251-258.

(87) Dosdall DJ, Sweeney JD. Extended charge banking model of dual path shocks for implantable cardioverter defibrillators. Biomed Eng Online 2008; 7:22.

(88) Kistler PM, Sanders P, Morton JB et al. Effect of body mass index on defibrillation thresholds for internal cardioversion in patients with atrial fibrillation. Am J Cardiol 2004; 94(3):370-372.

(89) Singer I, Goldsmith J, Maldonado C. Transseptal defibrillation is superior for transvenous defibrillation. Pacing Clin Electrophysiol 1995; 18(1 Pt 2):229-232.

(90) Zipes DP. Electrophysiological mechanisms involved in ventricular fibrillation. Circulation 1975; 52(6 Suppl):III120-III130.

(91) Crossley GH, Boyce K, Roelke M et al. A prospective randomized trial of defibrillation thresholds from the right ventricular outflow tract and the right ventricular apex. Pacing Clin Electrophysiol 2009; 32(2):166-171.

(92) Beukema R, Misier AR, Delnoy P et al. Characteristics of Sprint Fidelis lead failure. Neth Heart J 2010; 18(1):12-17.

(93) Ha AC, Vezi BZ, Keren A et al. Predictors of fracture risk of a small caliber implantable cardioverter defibrillator lead. Pacing Clin Electrophysiol 2010; 33(4):437-443.

(94) Crick SJ, Shepherd MN, Ho SY et al. Anatomy of the pig heart: comparisons with normal human cardiac structure. J Anat 1998; 193(Pt 1):105-119.

(95) Kommuri NV, Kollepara SLS, Saulitis E et al. Azygos Vein Lead Implantation For High Defibrillation Thresholds In Implantable Cardioverter Defibrillator Placement. Indian Pacing Electrophysiol J 2010; 10(1):49-54.

(96) Kall JG, Kopp D, Lonchyna V et al. Implantation of a subcutaneous lead array in combination with a transvenous defibrillation electrode via a single infraclavicular incision. Pacing Clin Electrophysiol 1995; 18(3 Pt 1):482-485.

(97) Berul CI, Triedman JK, Forbess J et al. Minimally invasive cardioverter defibrillator implantation for children: an animal model and pediatric case report. Pacing Clin Electrophysiol 2001; 24(12):1789-1794.

(98) Bardy GH, Smith WM, Hood MA et al. An entirely subcutaneous implantable cardioverter-defibrillator. N Engl J Med 2010; 363(1):36-44.

(99) Madan N, Gaynor JW, Tanel R et al. Single-finger subcutaneous defibrillation lead and "active can": a novel minimally invasive defibrillation configuration for implantable cardioverter-defibrillator implantation in a young child. J Thorac Cardiovasc Surg 2003; 126(5):1657-1659.

(100) Hsia TY, Bradley SM, LaPage MJ et al. Novel minimally invasive, intrapericardial implantable cardioverter defibrillator coil system: a useful approach to arrhythmia therapy in children. Ann Thorac Surg 2009; 87(4):1234-1238.

(101) Burke MC. The infinite value in subcutaneous defibrillation. Heart Rhythm 2010; 7(5):699-700.

(102) Lupo PP, Pelissero G, Ali H et al. Development of an entirely subcutaneous implantable cardioverter-defibrillator. Prog Cardiovasc Dis 2012; 54(6):493-497.

(103) Rowley CP, Lobodzinski SS, Gold MR. The Subcutaneous Defibrillator. Curr Treat Options Cardiovasc Med 2012.

(104) Jarman JW, Lascelles K, Wong T et al. Clinical experience of entirely subcutaneous implantable cardioverter-defibrillators in children and adults: cause for caution. Eur Heart J 2012; 33(11):1351-1359.

(105) Pedersen SS, Lambiase P, Boersma LV et al. Evaluation oF FactORs ImpacTing CLinical Outcome and Cost EffectiveneSS of the S-ICD: design and rationale of the EFFORTLESS S-ICD Registry. Pacing Clin Electrophysiol 2012; 35(5):574-579.

(106) Olde Nordkamp LR, Knops RE, Bardy GH et al. Rationale and design of the PRAETORIAN trial: a Prospective, RAndomizEd comparison of subcuTaneOus and tRansvenous ImplANtable cardioverter-defibrillator therapy. Am Heart J 2012; 163(5):753-760.

(107) Block M, Hammel D, Bocker D et al. Transvenous-subcutaneous defibrillation leads: effect of transvenous electrode polarity on defibrillation threshold. J Cardiovasc Electrophysiol 1994; 5(11):912-918.

(108) Block M, Hammel D, Borggrefe M et al. [Transvenous subcutaneous implantation technique of the cardioverter/defibrillator]. Herz 1994; 19(5):259-277.

(109) Obeyesekere MN, Kamberi S, Youngs N et al. Long-term performance of submammary defibrillator system. Europace 2010; 12(9):1239-1244.

(110) Michael KA, Veldtman GR, Paisey JR et al. Cardiac defibrillation therapy for at risk patients with systemic right ventricular dysfunction secondary to atrial redirection surgery for dextro-transposition of the great arteries. Europace 2007; 9(5):281-284.

(111) Nery PB, Green MS, Khairy P et al. Implantable Cardioverter-Defibrillator Insertion in Congenital Heart Disease Without Transvenous Access to the Heart. Can J Cardiol 2012.

(112) Jacob S, Lieberman RA. Percutaneous epicardial defibrillation coil implantation: a viable technique to manage refractory defibrillation threshold. Circ Arrhythm Electrophysiol 2010; 3(2):214-217.

(113) Weber M, Bocker D, Bansch D et al. Efficacy and safety of the initial use of stability and onset criteria in implantable cardioverter defibrillators. J Cardiovasc Electrophysiol 1999; 10(2):145-153.

(114) Langley P, Macgowan GA, Murray A. Circadian variation of human ventricular fibrillation dominant frequency. Resuscitation 2010; 81(8):950-955.

(115) Nanthakumar K, Dorian P, Paquette M et al. Is inappropriate implantable defibrillator shock therapy predictable? J Interv Card Electrophysiol 2003; 8(3):215-220.

(116) Toquero J, Alzueta J, Mont L et al. Morphology discrimination criterion wavelet improves rhythm discrimination in single-chamber implantable cardioverter-defibrillators: Spanish Register of morphology discrimination criterion wavelet (REMEDIO). Europace 2009; 11(6):727-733.

(117) Waldo AL. From bedside to bench: entrainment and other stories. Heart Rhythm 2004; 1(1):94-106.

(118) Stevenson WG, Sager PT, Friedman PL. Entrainment techniques for mapping atrial and ventricular tachycardias. J Cardiovasc Electrophysiol 1995; 6(3):201-216.

(119) Li H, Yee R, Thakur RK et al. The effect of variable retrograde penetration on dual AV nodal pathways: observations before and after slow pathway ablation LDD. Pacing Clin Electrophysiol 1997; 20(9 Pt 1):2146-2153.

(120) Nanthakumar K, Paquette M, Newman D et al. Inappropriate therapy from atrial fibrillation and sinus tachycardia in automated implantable cardioverter defibrillators. Am Heart J 2000; 139(5):797-803.

(121) Klein GJ, Gillberg JM, Tang A et al. Improving SVT discrimination in single-chamber ICDs: a new electrogram morphology-based algorithm. J Cardiovasc Electrophysiol 2006; 17(12):1310-1319.

(122) Saba S, Barrington W, Ganz LI. New method for real-time discrimination and management of ventricular and supraventricular tachyarrhythmias applicable to patients with dual-chamber cardioverter-defibrillators. Am J Cardiol 2004; 93(1):111-114.

(123) Saba S, Volosin K, Yee R et al. Combined atrial and ventricular antitachycardia pacing as a novel method of rhythm discrimination: the Dynamic Discrimination Download Study. Circulation 2010; 121(4):487-497.

(124) Knight BP, Ebinger M, Oral H et al. Diagnostic value of tachycardia features and pacing maneuvers during paroxysmal supraventricular tachycardia. J Am Coll Cardiol 2000; 36(2):574-582.

(125) Knight BP, Zivin A, Souza J et al. A technique for the rapid diagnosis of atrial tachycardia in the electrophysiology laboratory. J Am Coll Cardiol 1999; 33(3):775-781.

(126) Ridley DP, Gula LJ, Krahn AD et al. Atrial response to ventricular antitachycardia pacing discriminates mechanism of 1:1 atrioventricular tachycardia. J Cardiovasc Electrophysiol 2005; 16(6):601-605.

(127) Rinaldi CA, Simon RD, Baszko A et al. A 17 year experience of inappropriate shock therapy in patients with implantable cardioverter-defibrillators: are we getting any better? Heart 2004; 90(3):330-331.

(128) Reddy VY, Reynolds MR, Neuzil P et al. Prophylactic catheter ablation for the prevention of defibrillator therapy. N Engl J Med 2007; 357(26):2657-2665.

(129) Jodko L, Kornacewicz-Jach Z, Kazmierczak J et al. Inappropriate cardioverter-defibrillator discharge continues to be a major problem in clinical practice. Cardiol J 2009; 16(5):432-439.

(130) Dorian P, Philippon F, Thibault B et al. Randomized controlled study of detection enhancements versus rate-only detection to prevent inappropriate therapy in a dual-chamber implantable cardioverter-defibrillator. Heart Rhythm 2004; 1(5):540-547.

(131) Birnie DH, Sambell C, Johansen H et al. Use of implantable cardioverter defibrillators in Canadian and US survivors of out-of-hospital cardiac arrest. CMAJ 2007; 177(1):41-46.

(132) Nery PB, D'Mello N, Beanlands R. Screening patients for primary prophylaxis implantable cardioverter defibrillators: insights into current practices. Can J Cardiol 2010; 26(3):e125-e127.

(133) Saksena S, Nagarakanti R. The future of implantable defibrillator and cardiac resynchronization therapy trials. J Interv Card Electrophysiol 2008; 23(1):29-39.

(134) Yang JH, Byeon K, Yim HR et al. Predictors and clinical impact of inappropriate implantable cardioverter-defibrillator shocks in Korean patients. J Korean Med Sci 2012; 27(6):619-624.

(135) Poole JE, Johnson GW, Hellkamp AS et al. Prognostic importance of defibrillator shocks in patients with heart failure. N Engl J Med 2008; 359(10):1009-1017.

(136) Srivatsa UN, Hoppe BL, Narayan S et al. Ventricular arrhythmia discriminator programming and the impact on the incidence of inappropriate therapy in patients with implantable cardiac defibrillators. Indian Pacing Electrophysiol J 2007; 7(2):77-84.

(137) Kreuz J, Balta O, Liliegren N et al. Incidence and characteristics of appropriate and inappropriate therapies in recipients of ICD implanted for primary prevention of sudden cardiac death. Pacing Clin Electrophysiol 2007; 30 Suppl 1:S125-S127.

(138) Sweeney MO, Ruetz LL, Belk P et al. Bradycardia pacing-induced short-long-short sequences at the onset of ventricular tachyarrhythmias: a possible mechanism of proarrhythmia? J Am Coll Cardiol 2007; 50(7):614-622.

(139) Morgan JM, Sterns LD, Hanson JL et al. A trial design for evaluation of empiric programming of implantable cardioverter defibrillators to improve patient management. Curr Control Trials Cardiovasc Med 2004; 5(1):12.